THE UNIVERSITY OF CALGARY

Dynamic muscle force prediction from EMG signals using Artificial Neural Networks

by

Ming Ming Liu

A THESIS

SUBMITTED TO THE FACULTY OF GRADUATE STUDIES IN PARTIAL FULFILMENT OF THE REQUIREMENTS FOR THE DEGREE OF MASTER OF SCIENCE

DEPARTMENT OF ELECTRICAL AND COMPUTER ENGINEERING

CALGARY, ALBERTA

MAY, 1997

0-612-20875-3

Abstract

Electromyographical (EMG) signals have never been used to predict muscle forces of dynamically contracting muscles across subjects. The purpose of this study was to predict dynamic muscle force from processed EMG, knee and ankle angles, and knee and ankle angular velocities in the cat gastrocnemius and soleus during locomotion. Here, we use an artificial neural network (ANN) approach to first derive an EMG-force relationship of skeletal muscle; second, use this relationship to predict individual muscle forces for different dynamic tasks within and across subjects; and third, validate the predicted muscle forces against the corresponding forces which were experimentally recorded. Our within-subject results were better than those published previously, even though we did not incorporate a muscle model or instantaneous contractile conditions into the force predictions. The across-subject results were considered excellent.

We conclude that ANNs represent a powerful tool to capture the essential features of EMG-force relationships of dynamically contracting muscle, and that ANNs might be used to predict muscle forces within and across subjects accurately from the corresponding EMG signals.

Acknowledgements

I am deeply indebted to my supervisor Dr. W. Herzog for his support, encouragement, and motivation throughout the course of this research. I would also like to thank him for critically reviewing the various manuscripts related to this study, for making so many valuable suggestions and numerous corrections for improving the manuscript.

I am also most grateful to my co-supervisor Dr. A. Sesay for his support, for his helpful suggestions and discussions during the course of this study, and for his complete reviews of early versions of the manuscript.

I would like to thank Dr. Anton J. van den Bogert for reviewing the manuscript of this thesis, and for his valuable comments.

I would like to thank Dr. Y.T. Zhang for his kind help at the begining of this study. This study was mainly supported by NSERC of Canada, Sunity International Inc.

Special appreciation goes to my husband Jun and my son Song for being a constant source of encouragement and support.

Table of Contents

List of Tables

List of Figure

Chapter one: Introduction

All movement is dependent on muscular contraction. Probably the most basic property of muscle in humans and animals is its ability to produce force. Knowing the forces in muscles at any instant in time during a specific movement is like having a window to the central nervous system and its organization and control of movement.

Contracting skeletal muscles produce an electrical signal which is known as the electromyogram (EMG). The EMG is associated with the fibre action potentials which precede active force production in muscle. It has been shown that the EMG signal is the spatial and temporal algebraic sum of the individual fibre (motor unit) action potentials, therefore an increase in the number of active motor units or an increase in the average firing rate of motor units is reflected in an increase in the EMG signal. Because of this relation of motor unit activation and EMG, it is intuitively appealing to associate the EMG signal directly with the force produced by a muscle. The ability to predict individual muscle forces accurately from the EMG signal and kinematic information is a challenge for applied research. Problems such as the appropriate use of EMG signals to assess the rehabilitation process of damaged muscles, or the quantitative relationship between the EMG signal and the force of fatiguing muscle, have been of primary interest.

1.1 The structure and function of skeletal muscle

My thesis is aimed at relating the electromyogram (EMG) to skeletal muscle force production, so the basic concepts about the structure and function of skeletal muscle will be introduced first.

Generally, muscles are divided into striated and non-striated muscles. Striated muscles are further subdivided into skeletal and cardiac muscles. Skeletal muscle is composed of thousands of muscle bundles, which are surrounded by a connective tissue sheath called perimysium. Each muscle bundle contains a number of muscle fibres, the individual contractile muscle cell is surrounded by a connective tissue sheath called endomysium. Muscle fibres are made up of myofibrils lying parallel to one another. The systematic arrangement of the myofibrils gives skeletal muscle its typical striated pattern. The repeat unit in this pattern is called a sacomere, which is the basic contractile unit of a muscle.

Skeletal muscle is organized into motor units, which is the basic control unit of skeletal muscle. A motor unit consists of a single motor axon and all muscle fibres it innervates (Figure 1.1). When a motor axon is stimulated strongly enough to cause contraction, all fibres of the motor unit contract simultaneously.

The intramuscular network of connective tissues becomes continous with the dense connective tissue of the tendons at each end of the muscle. These tendons serve to connect the skeletal muscles to the bony skeleton. The muscle fibres themselves do not come into direct contact with the skeleton; thus the tension developed by muscles is borne entirely by their tendinous attachments.

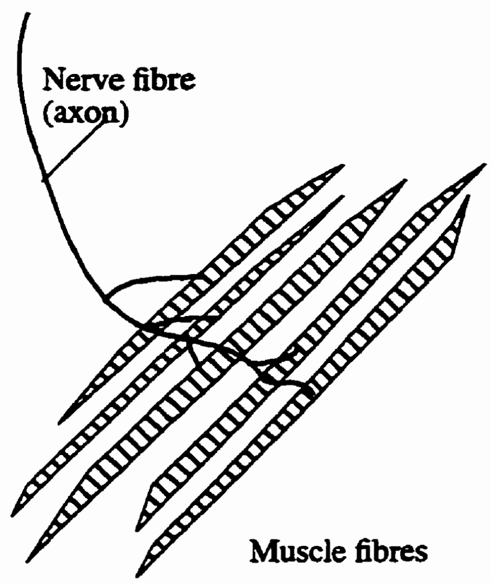

Figure 1.1 Schematic diagram of a motor unit

1.2 The EMG signal

EMG signal of a single muscle fibre At rest, the electrical potential inside a muscle fibre is relative to its outside about -90 mV. Under normal conditions, an action potential of a motor neuron activates all the muscle fibres of a motor unit (Krnjevic and Miledi, 1958a; Paton and Wand, 1967). When an action potential of a motor neuron reaches the presynaptic terminal, a series of chemical reactions takes place that culminate in the release of acetylcholine (ACh). ACh crosses the synaptic cleft, reaches the fibre membrane, and causes a depolarization (action potential) on the muscle fibre which propagates along the muscle fibre causing activation (for review see chapter 2.5 and 3.6, Herzog et al., 1994). If an action potential were measured using an electrode inside the muscle fibre, it would go from about -90 mV (resting potential) to about +40 mV (peak depolarization potential) and back again to the resting value (Figure 1.2).

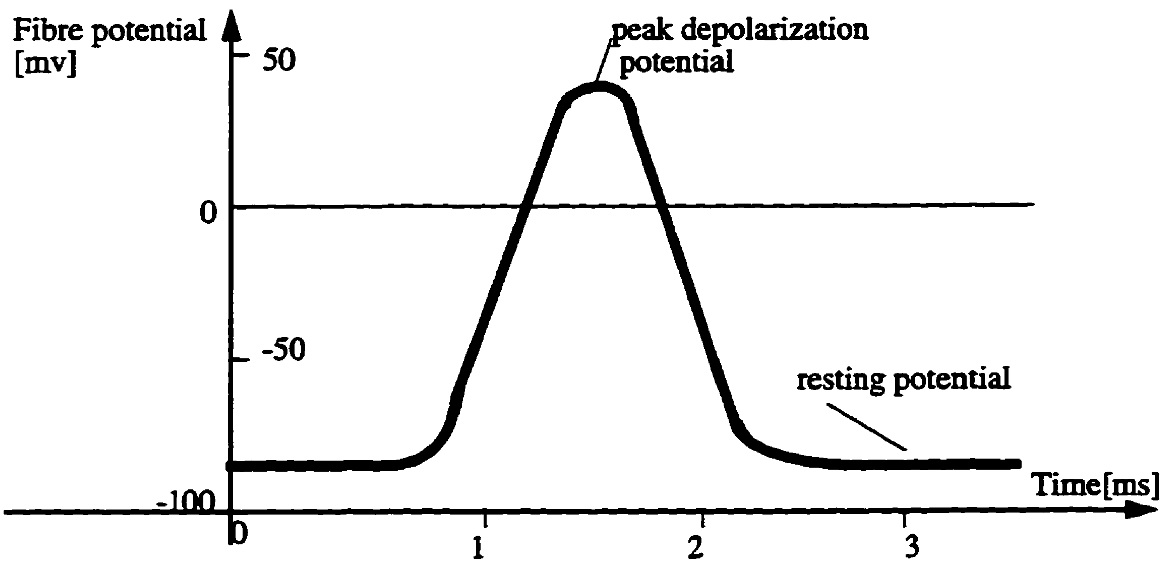

Figure 1.2 The action potential of a muscle fiber

<u>*EMG signal from motor unit*</u> The smallest unit of force control in skeletal muscle is the motor unit. A motor unit is composed of a motor axon and all the fibres it innervates (Figure 1.1). Therefore, activation of a single muscle fibre is not possible in an intact muscle, rather an action

potential in a motor neuron will cause contraction of all fibres in the corresponding motor unit. The EMG signal recorded from the depolarization of a motor unit, called a motor unit action potential (MUAP), is the algebraic sum of the individual fibre action potentials from that motor unit.

EMG signal of a muscle In general, the EMG signal obtained from a contracting muscle is the spatial and temporal algebraic sum of the individual motor unit action potentials.

1.3 The properties of skeletal muscle

The force-length and the force-velocity relation of muscles are two important properties of muscle. They are repeatedly used in biomechanical experiments involving muscles or the musculo-skeletal system. Force-length relations describe the relation between the maximal force a muscle (or fibre, or sarcomere) can exert and its length. Force-length relations are obtained under isometric conditions and for maximal activation. Isometric may refer to the length of the entire muscle, the length of a fibre, or the length of a sarcomere, depending on the system that is studied. Force-velocity relations are defined as the relation that exists between the maximal force of a muscle (or fibre) and its instantaneous rate of change in length. Force-velocity relations are determined for maximal activation conditions of the muscle, and are typically obtained at optimal length of the sarcomeres.

1.4 Studies of dynamic EMG-force relationships in skeletal muscle

Most studies aimed at relating EMG signals to muscle force are performed for isometrically contracting muscle (e.g., Lippold, 1952; Milner-Brown and Stein, 1975; Moritani and deVries, 1978). It has been shown that the relationship between force and processed EMG in isometric contractions is linear (Bouisset and Maton, 1972; Hof and Van den Berg, 1977; Ericson and Hagberg, 1978; Johnson, 1978) or slightly non-linear with the EMG increasing more rapidly than the force (Kramer et al., 1972; Vredenbregt and Rau, 1973; Komi and Viitasalo, 1976).

The force-EMG relationship in dynamic contractions is undoubtedly complex since muscular properties such as the force-length and force-velocity relations may influence the EMG-force relation (e.g., Hof and van den Berg, 1981a,b,c,d; Olney and Winter, 1985). Instantaneous force-length-velocity properties of muscles are hard to measure in vivo. Most of the dynamic experiments have been performed using isokinetic contractions on strength dynamometers. These dynamometers typically enforce a relatively constant angular velocity of joint movement. Only a few studies have attempted to relate EMG and force during normal, unrestrained movements (Hof and van den Berg, 1981a, 1977; Olney and Winter, 1985; Sherif et al., 1983; van den Bogert et al., 1988; Norman et al., 1988; van Ruijven and Weijs, 1990; Savelberg and Herzog, 1995).

Two basic approaches have been used to predict individual muscle force using EMG during dynamic activity. One involves the development of mathematical models based upon biological behaviour, using EMG as an input variable (Hof and van den Berg, 1981a; Olney and Winter, 1985; van den Bogert et al., 1988; Norman et al., 1988; van Ruijven and Weijs, 1990). These methods often employ calibration procedures in which parameter values are adjusted until predicted and observed forces match. A second approach, and that of the present study, is an adaptive filtering approach; a purely mathematical approach linking the EMG to the force signal (Herzog et al., 1994; Savelberg and Herzog; 1995).

The predictions of dynamic muscle force have been limited by the inability to capture the highly non-linear, and temporally distorted relation which appears to exist between muscle force and EMG (Hof and van den Berg, 1981; van den Bogert et al., 1988). Even approaches relying on complex numerical procedures, such as some of the complex adaptive filtering techniques have only met with partial success (Herzog et al., 1994). Recently, artificial neural network (ANN) approaches have been proposed as an alternative tool to pattern recognition and classification problems.

Savelberg and Herzog (1995) used an artificial neural network approach based on a back-propagation algorithm to predict dynamic muscle forces from EMG. In their study, the relationship between EMG plus kinematics and force, as well as the relationship between EMG and force alone were derived for the cat gastrocnemius muscle. Preliminary results indicated that the ANN approach is promising and might be used for general predictions of muscle force from EMG.

In the past two decades, many direct EMG and muscle force measurements have been performed in animal models, particularly in the cat ankle extensors muscle. However these data have not been used systematically to derive the EMG-force relationship for dynamic contractions.

The purpose of this study was to revisit dynamic force predictions from EMG signals using an artificial neural network (ANN) approach. Artificial neural networks are excellent for pattern recognition schemes which involve highly non-linear and temporally distorted signal relations. The ability to generalize results from sample input makes ANNs potentially very powerful for deriving dynamic EMG-force properties for skeletal muscle. In studying the EMG-force relationship of skeletal muscle, we used the cat gastrocnemius and soleus as our experimental model.

The cat gastrocnemius and soleus behave very differently for different speeds and modes of locomotion. Peak forces and EMGs in the gastrocnemius increase in parallel with increasing speeds of locomotion, whereas peak soleus forces remain nearly constant while EMGs increase from still standing to walking to trotting and galloping (Herzog et al., 1993). Using two muscles which behave so differently might be a good test for evaluating the potential of ANN to capture dynamic EMG-force relationships.

1.5 The organization of the thesis

The layout of the thesis is as follows:

In chapter 1, the basic concepts of skeletal muscle and the approaches used in schemes of muscle force predictions from EMG are introduced.

In chapter 2, the basic concepts of the EMG signal and the EMG-force relationship are introduced. Also, a review of previous works aimed at predicting individual muscle forces from EMGs during dynamic activities is presented. A brief description of the experimental methods and the Artificial neural networks [ANN] used in this study, is given in Chapter 3. The force predictions for the cat gastrocnemius and soleus muscles are described in Chapters 4 and 5, respectively. The corresponding discussion is given in Chapter 6.

In chapter 7, an outlook for future work is presented.

Chapter Two: Literature Review

In this part of the thesis, EMG signal recording and processing techniques are described, and the EMG-force relationship is introduced. Also, relevant published works are summarized in this chapter.

2.1 EMG signal recording

For EMG recordings, a *bi-polar electrode configuration* is typically used. In a bi-polar configuration, two recording electrodes are used. The potential recorded by each electrode is compared to a reference electrode, and the difference of the two recording electrodes relative to the reference electrode is amplified (differential amplification). Using a bi-polar recording configuration and differential amplification, noise common to both electrodes is cancelled in the process.

Figure 2.1.a shows a schematic record of an EMG signal from a single muscle fibre measured using an indwelling (inside the muscle fibre), bi-polar electrode configuration. Figures 2.1.b and c (Basmajian and De Luca, 1985) show schematically the generation of an EMG signal from a single motor unit and from a voluntarily contracting muscle, respectively.

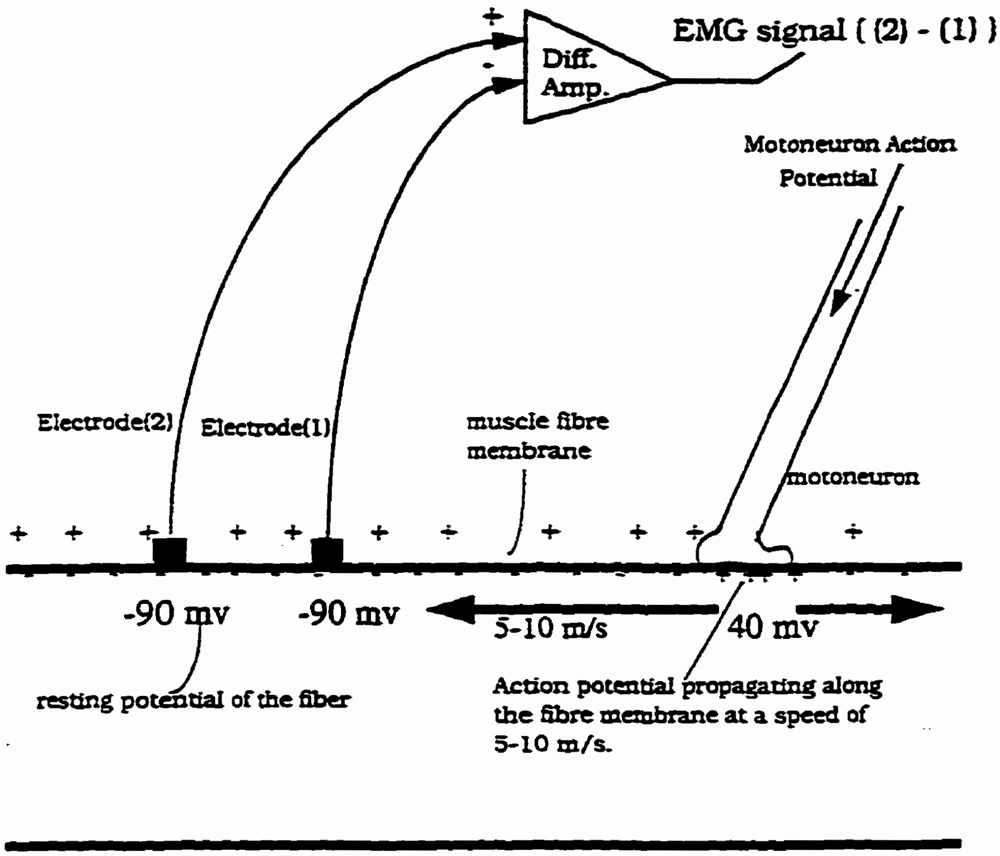

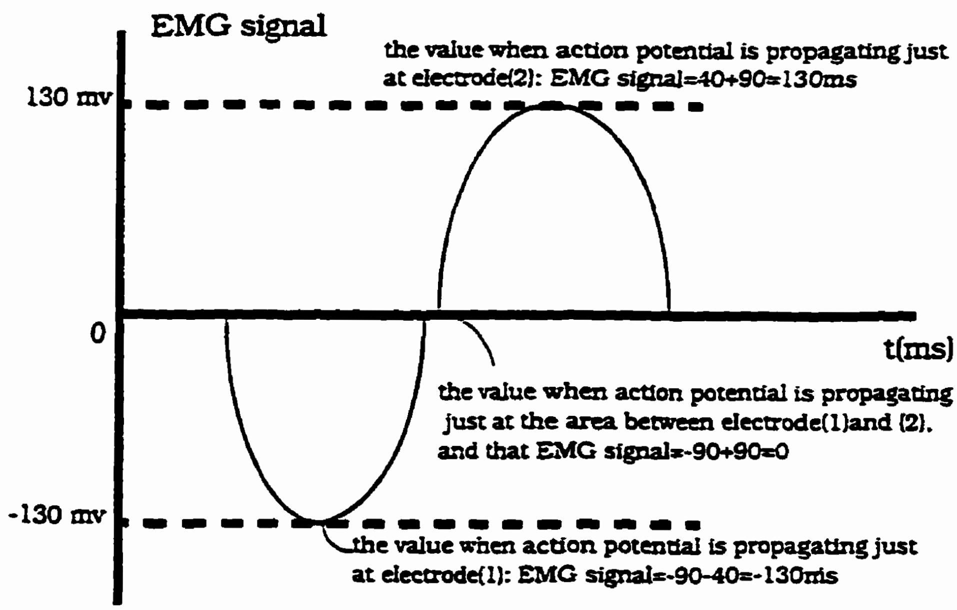

Figure 2.1.a Schematic representation of the recording of EMG signal from a single muscle fibre

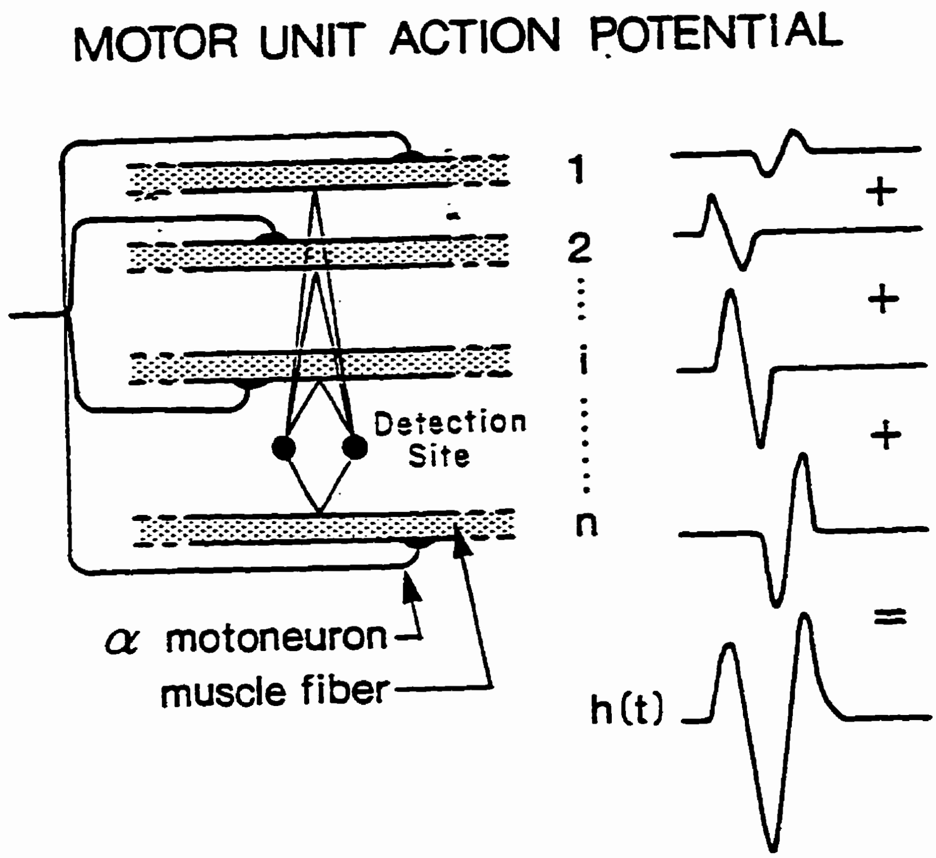

Figure 2.1.b Schematic representation of the generation of the motor unit action potential designated as h(t). The shape and the amplitude of the motor unit action potential are dependent on the geometric arrangement of the active muscle fibres with respect to the electrode site .

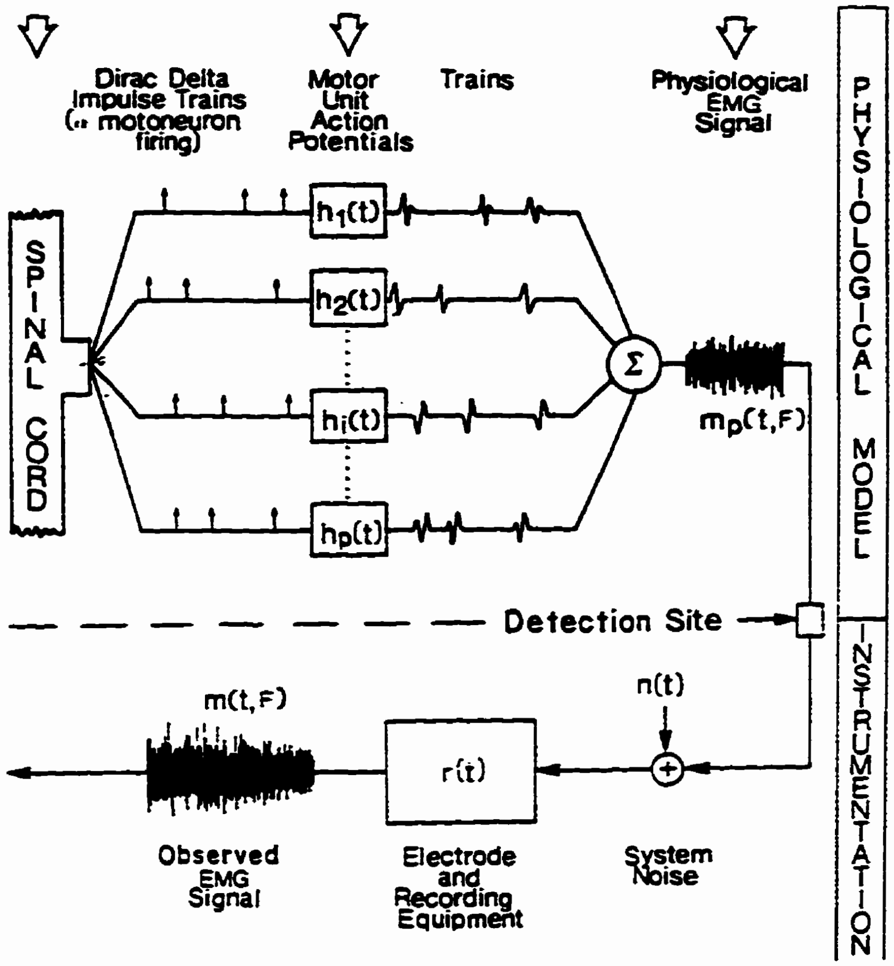

Figure 2.1.c Schematic representation of the EMG signal.

In Figure 2.1.b, the integer n represents the total number of muscle fibres of one motor unit that are sufficiently near the recording electrode for their action potentials to be detected by the electrode. The action potentials associated with each muscle fibre are presented on the right side of Figure 2.1.b. The individual muscle fibre action potentials represent the contribution that each active muscle fibre makes to the signal detected at the electrode site. A depolarization approaching from the right side is reflected as a negative phase in the action potential and vice versa.

The motor unit action potential, designated as h(t) (Figure 2.1.b), is the superposition of the contributions of the individual action potentials.

In Figure 2.1.c, The integer p represents the total number of motor unit action potential trains which contribute to the potential field at the recording site. The superposition at the recording site forms the physiological EMG signal, $m_p(t, F)$. The observable EMG signal ($m(t, F)$) also includes electrical noise ($n(t)$) and the filtering properties of the recording equipment ($r(t)$).

2.2 EMG signal processing

Raw EMG signals resemble white noise with a distribution around the zero point. It is apparent that averaging of the signal will not provide useful information with respect to force production of the muscle. Therefore, EMG signals are typically processed before they are used for muscle force predictions. Processing of the EMG signal can be done in the time or frequency domain. In our study, two methods of processing were used: rectification and smoothing.

The process of rectification involved conversion of the raw signal into a signal of absolute values. Smoothing of the rectified signal was accomplished using second-order Butterworth low pass filter, 5 Hz cut-off frequency.

Figures 2.2.a, b and c show raw EMG signals from the cat gastrocnemius muscle during walking, the corresponding full-wave rectified signals, and the corresponding smoothed signals, respectively.

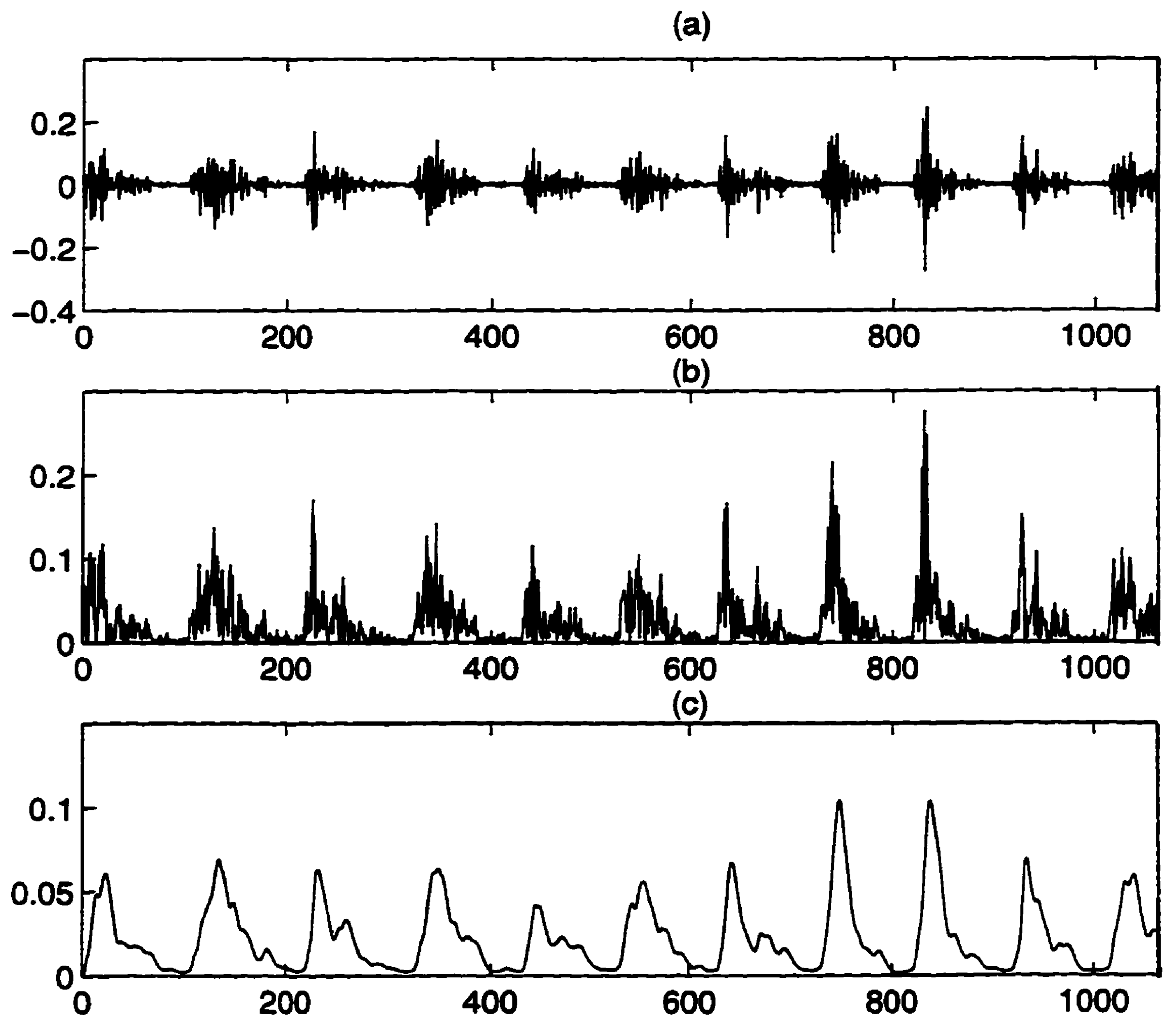

Figure 2.2 Processing of EMG signal: (a) raw, (b) rectified, and (c) rectified+smoothed EMG signal.

2.3 EMG-force relationship

An increase in the firing rate of motor units or an increase in the number of recruited motor units is known to increase the muscular force and the integrated form of the EMG (Basmajian and De luca, 1985). Therefore, there must be a (at least) qualitative relation between the EMG signal and the corresponding muscle force. Figure 2.3 shows the raw EMG signal and the corresponding soleus force for a single step of walking. The goal of this study was to predict muscular force during dynamic contraction from the corresponding EMG signal.

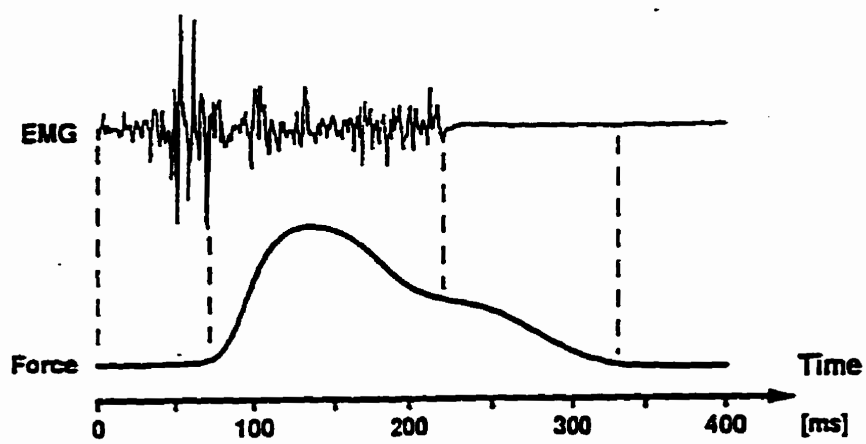

Figure 2.3 Force and EMG signal obtained from a cat soleus muscle

2.4 A brief review of previous models of the EMG-force relationship

In the last decade, only a few studies have attempted to relate EMG and force (moment, torque) during normal movements (Hof and van den Berg, 1981a; Olney and Winter, 1985; Van den Bogert et al., 1988; Ruijven and Weijs, 1990; Savelberg and Herzog, 1994). Most muscle models used for EMG to force predictions were based on the muscle model of Hill (1938, 1949).

The Hill muscle model

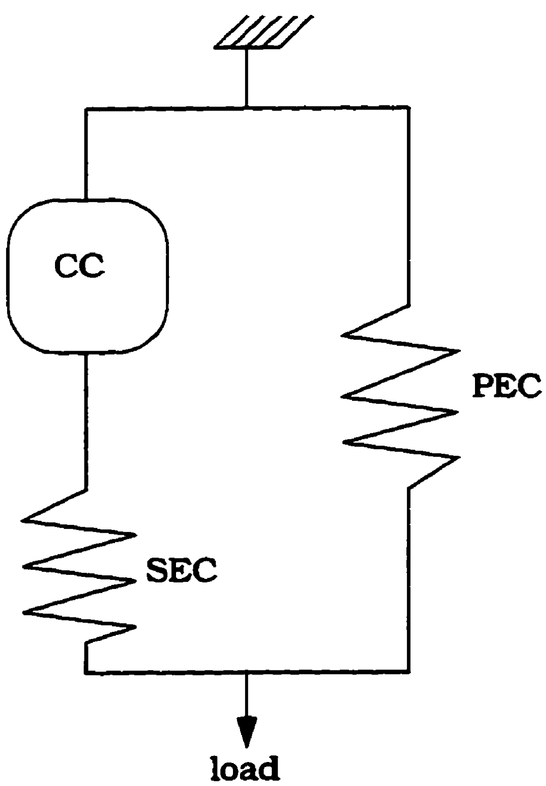

Figure 2.4.1 Schematic diagram of the Hill muscle model

Hill (1938) proposed a muscle model based upon the behaviour of three muscle components: the contractile component (CC), an elastic component placed in series with the contractile component (SEC), and an elastic component located in parallel to the other two elements (PEC) (Figure 2.4.1). The CC and SEC determine the behaviour of the active muscle; the PEC represents the elasticity of the passive muscle. In his model, Hill assumed that the mean rectified EMG is proportional to the so-called active state of the muscle, a property of the CC. Furthermore, the CC is typically assumed to obey a characteristic force-velocity relationship which was described by Hill (1938) based on experiments on entire frog skeletal muscle.

Experimental studies on the dynamic EMG-force relationship

In order to relate EMG to force (torque) for ankle plantarflexors, Hof and van den Berg (1981a-d) used an analogue processor of the EMG signal with an extensive calibration procedure to determine an EMG gain factor, the force-length (torque and joint angle) relationship, and the properties of the series and parallel elastic elements. The EMGs were recorded separately from the gastrocnemius and soleus muscles. Both EMGs were preamplified (100 times) and bandpass filtered with different gain factors for gastrocnemius and soleus. Then, the EMGs were full-wave rectified and smoothed by means of a third order averaging filter with a time constant τ of 25 ms. Hof and van den Berg (1981a-d) incorporated all components of the Hill model into their system (Figure 2.4.2).

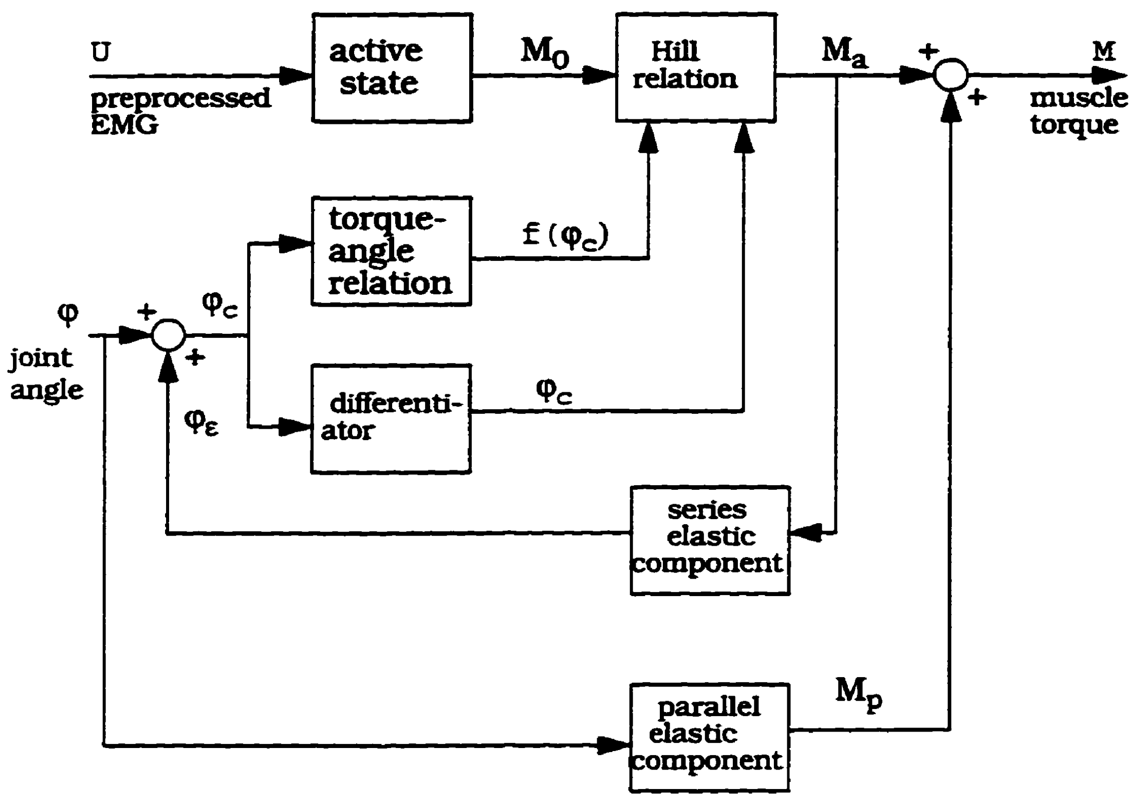

Figure 2.4.2 Block diagram of the Hof's muscle model

The properties of the contractile component were described by an active state function ($M_0(t)$), and the force-length and force-velocity relationship of the muscle of interest. The SEC (φ_e) and the PEC(φ) were represented by purely elastic elements. The torque developed by the CC was a function of three state variables: the active state $M_0(t)$, the CC length(φ_c) and the rate of change in the CC length ($\dot{\varphi}_c$). The isometric force-length relationship was described by the notation: $M_a = M_0 f(\varphi_c)$, where the function $f(\varphi_c)$ is equal to 1 around the optimum muscle length and decreases for smaller and for larger length. The sum of the active states of all motor units is taken to be the active state of the muscle which was derived from the EMG signal. Using this model, they were able to predict reasonably well the ankle joint moments during human walking (Hof *et al.*, 1987). The limitations of this study were that no force predictions of individual muscles could be made, but just some generalized muscle force (the ankle moment) could be calculated. Force predictions, therefore, were not validated against the actual muscle forces, and from a practical point of view, the study was not important because ankle joint moments can be derived quite accurately without EMG input of the muscles by using an inverse system's analysis (e.g. Andrews, 1974).

Sherif et al. (1983) presented an 'intervention model' to associate the force produced by the cat medial gastrocnemius (MG) during unrestrained treadmill locomotion with the corresponding EMG signals. Representative EMGs and muscle forces were recorded from the cat medial gastrocnemius at 0.67 and 2.24 m/s. EMG signals were processed by a differential amplifiers at a band-width of 30-3000 Hz, and force signals were processed by a low pass filter (cutoff at 300 Hz). The EMG and corresponding force were then related using an intervention analysis based on an autoregressive-integrated moving average (ARIMA) model.

Sherif et al. (1983) proposed that the MG myoelectric activity during a single step cycle may be divided into two parts. The primary burst of activity precedes foot contact and produces a major portion of MG force at the tendon by setting muscle stiffness prior to ground contact for "storing" energy in the system. During stance, a second burst (E2 burst) of EMG activity was observed by an almost critically damped second order system, and this burst (the residual term) did not contribute significantly to the total MG force at the tendon. Sherif et al. (1983) proposed that the initial burst of EMG activity in the cat MG was driven by the central nervous system, irrespective of the instantaneous contractile conditions of the muscle. The limitations of this study were that the model used was very complicated and could not be used to make useful predictions of force from EMG during normal movements.

Olney and Winter(1985) developed a biologically deterministic model to calculate instantaneous joint ankle and knee moments during normal walking using processed EMG (rectified and smoothed with a second order low pass filter, cutoff at 1 Hz), kinematic information (e.g., instantaneous joint angle as a correlate of muscle length and angular velocity as a correlate of muscle velocity), and instantaneous joint moments from the participating muscles. The data of the EMG and instantaneous joint moments from two muscles, tibialis anterior and soleus, were used for the prediction of ankle moments. The model assumed that the moment-angle and moment-velocity relationships were linear. The joint angle and angular velocity were assumed to be proportional to muscle length and muscle linear velocity respectively. A linear regression between joint moment and processed EMG was used to determine the static EMG-moment relationship. There were eight parameters used and determined by the calibration procedures and estimation techniques. Using the resultant moment for optimization, the results showed that the predicted moment was proportionally augmented for longer muscle lengths and proportionally reduced for shorter lengths. Further, predicted moments were reduced for shortening contraction and increased for lengthening contraction. The limitations of this study were that muscle forces could not be predicted or validated. Also, in order to obtain acceptable results, model parameters were optimized based on the experimental moments.

van den Bogert et al.(1988) developed and validated a muscle model of the deep digital flexor of the horse. The muscle model was a Hill-type model. It predicted muscle force, F, from the length of the muscle, L, and its activity, $U(t)$. EMG was used as the activation input into the model. The muscle and its tendon were described by a four-element model. The series elastic component, S, represents the tendon (Figure 2.4.3). Tendon force, F_s, is an experimentally determined function of tendon length, $L-x$. The parallel elastic element, P, represents the passive properties of the muscle. Its force, F_p, where $F_p = k(x-x_0)$ when the series elastic element length, x, is larger than the resting length, x_0, and zero otherwise.

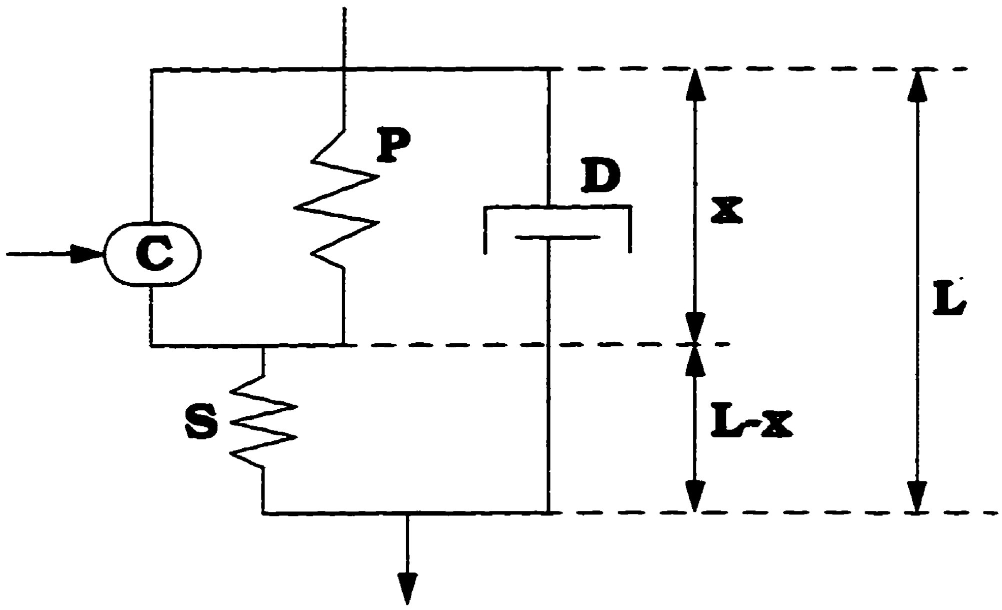

Figure 2.4.3 The muscle model

The force-length relationship, $F_c(x)$, of the contractile element was taken from Hof and van den Berg (1981a). The contractile element force was assumed to be proportional to the active state of the muscle, U(t), with a gain, G. A linear damper, D, was included as a first-order approximation of all velocity-dependent effects.

The state equation for the muscle model is (Figure 2.4.3):

$$F_s(L-x) = F_p(x) + G \bullet U(t) \bullet F_c(x) \qquad \ldots$$

The instantaneous force output of the muscle was found by solving this non-linear equation for x and using $F = F_s(L-x) + D\dot{L}$, where D is the damping coefficient. Therefore, this model was length and velocity-dependent. The parameters used in the muscle model were derived from "irregular" walking trials and the force predictions were made for "normal" walking trials. Force predictions were made for one horse at one speed of locomotion.

Norman et al. (1988) attempted to predict dynamic muscle forces from EMG signals during muscular activity occurring in normal movements. In their model, EMG signal and isometric muscle force were required as model input. Cat soleus forces were measured during treadmill walking. The corresponding raw EMG signals from soleus muscle were digitized (2000 Hz), full wave rectified and smoothed (double-pass Butterworth filter, 2-10 Hz). Soleus forces were predicted by the following equation:

$$F_s = F_{iso} \times \frac{EMG}{EMG_{iso}}$$

where F_s is the instantaneous predicted soleus force, F_{iso} is the measured isometric tendon force when the animal was standing still, EMG is the instantaneous value of the full-wave rectified and smoothed linear envelope of the dynamic EMG, and EMG_{iso} is the average of the EMG signal over two seconds while the cat was standing still (isometric). Norman et al. (1988) validated their model using force measurements obtained for four step cycles in one animal while walking at one speed. No force predictions were made for other speeds of locomotion or across animals. Norman et al. (1988) obtained reasonable force predictions only after optimizing their model based on the dynamic muscle force results.

van Ruijven and Weijs (1990) used eletromyography (EMG), muscle length and speed of contraction to predict muscle forces in jaw muscles of rabbits. The muscle model was a Hill-type model and the properties of the muscle were derived in part by the twitch response of the muscle. The model was tested by predicting the bite forces produced by the jaw muscles during mastication. All input data (muscle length, length change, EMG) and output data (forces) were defined for 13 ms periods. The force of a muscle during a 13 ms interval (F_i) was equal to

$$F_i = F_{max} \bullet (FL_i \bullet FV_i \bullet FQ_i + FP_i)$$

where F_{max} is the maximal tetanic force (30 N/cm^2); FL is a factor describing the force-length properties of the muscle; FV is a factor describing the force-velocity properties of the muscle. FQ is the activation factor which depends on the EMG; FP is a scaling factor for the force in the parallel elastic element. FL_i and FV_i depend on the average length and length change of the sarcomeres during the 13 ms interval, respectively. FQ_i depends on the EMG during the current and the preceding 13 ms interval. The results from their study showed that the accuracy of the prediction was limited; the correlation between the predicted and the measured bite force was only 0.57.

One method that is different from the methods described above is adaptive filtering. Adaptive filtering techniques are not based on Hill-type muscle models; they are mathematical approaches linking EMG and muscle force without concern about the biological properties of the muscle. Adaptive filtering approaches have been chosen to predict dynamic forces from EMG because the characteristics of force and EMG are time-dependent, or non-stationary, during dynamic contractions. Adaptive filtering techniques can account for non-stationarities and have been used successfully in the analysis of a variety of biological signals (Ferrara and Widrow, 1982; Yelderman et al.,1983; Kentie et al., 1981; Chen et al., 1990; Zhang et al., 1991).

Herzog et al.(1994) used an adaptive filtering procedure with the least mean square (LMS) algorithm (for detail see chapter 3.6, Herzog et al., (1994) to estimate force in the cat plantaris from the corresponding EMGs obtained during walking and running. Their results were obtained without prior knowledge of the statistics of the signal and the noise, and without a model of the target muscle. The only assumption made in the force predictions was that the signal components in the primary input (the force signal plus additive noise) and the reference input (full-wave rectified and low pass filtered EMG signal) were correlated with each other, but were uncorrelated with the noise. Using a LMS algorithm, they obtained good estimates of dynamic plantaris force, but the force predictions were of limited accuracy.

Savelberg and Herzog (1995) used an Artificial Neural Network (ANN) approach with the back-propagation algorithm to predict forces from EMG in the cat gastrocnemius during locomotion. ANN, one of the adaptive filtering approaches, is based on biological neural systems. Similar to their biological namesakes, they consist of interconnected cells organized in layers. The essence of an ANN is that information is distributed through connections between cells making up the network. The connections have adjustable weight factors. By adjusting these weights, an ANN is able to learn, that is, to match an input pattern to an output pattern. Depending on the number of layers and the number of cells in each of these layers, the information distributed over the network can mimic complex relationships. Apart from the ability to learn, ANNs, if properly trained, can be used to generalize knowledge. In Savelberg and Herzog's (1995) study, the relationship between EMG plus kinematics and force, as well as the relationship between EMG and force in the cat gastrocnemius were considered. Preliminary results indicated that the ANN approach might be used for general predictions of muscle force from EMG.

We used the Artificial Neural Network approach to predict individual muscles forces from the corresponding EMG signals. The results confirmed that ANNs are a promising technique to predict dynamic forces from EMG signals.

Chapter three: Method

3.1 Animal preparation, force, EMG, and kinematic measurements

Force, EMG, and locomotion kinematics were obtained from soleus and gastrocnemius muscles of three cats walking at nominal speeds of 0.4, 0.8, and 1.2 m/s, and trotting at a speed of 1.8 m/s. The animal preparation, force measurements, EMG recording, and kinematic analysis were described elsewhere (Herzog *et al.*, 1993). Only a brief description of the experimental method is given here for the sake of clarity.

Three outbred, male, adult cats were anesthetized, intubated, and then maintained using 1-1.5% halothane. 'E'-shaped, stainless steel tendon force transducers were surgically implanted onto the separated tendons of the soleus and gastrocnemius muscles under strictly sterile conditions. Bipolar, indweling wire electrodes of Teflon-insulated, multistranded, stainless steel biomedical wire (Bergen, BW9-48) were drawn through the mid-belly of soleus and gastrocnemius using a surgeon's needle (Miltex, MS-140) to record EMG signals. The electrodes were arranged approximately parallel to the muscle fibres and the interelectrode distance ranged from 5 to 7 mm. Leads of all force and EMG devices were drawn subcutaneously to a backpack connector from which all signals were transmitted by cable or telemetry to a computer (PC, 386). Typically, forces and EMG signals were recorded at 2240 Hz.

After implantation of the force and EMG transducers, cats were allowed to recover completely from surgery (five to seven days). Recovery was assessed by visual inspection and by comparison of stance times between implanted and contralateral hindlimbs during locomotion. Cats were enticed to perform locomotor tasks for which they were trained for 4-8 weeks prior to surgery. These tasks consisted of walking at 0.4, 0.8, and 1.2 m/s, and trotting at a speed exceeding 1.4 m/s on a motor-driven treadmill on a level surface.

For each locomotor task, A video camera with its optical axis perpendicular to the plane of motion of the animals and running at 60 Hz was used to monitor locomotion kinematics, and a time code generator on the video image (model 9300, Datum Inc.) was used to synchronize the video and computer records. Synchronization of force and EMG records with video data was obtained using a series of pulses that appeared as spikes on the computer records and as a light-emitting diode on the video. Reflective skin markers placed over the hip, knee, ankle, and metatarsophalangeal joints before data acquisition were digitized from the video records (60 Hz, Motion Analysis, VP310) to obtain ankle and knee joint angles.

All methods were approved by the Animal Ethics Review Committee of the University of Calgary.

3.2 Force, EMG, and kinematic data processing

In this study, force and EMG signals were obtained from the gastrocnemius and soleus of three cats walking at speeds 0.4, 0.8, 1.2 m/s, and trotting at a speed 1.8 m/s. Eight to sixteen step cycles were available for a given cat and speed of locomotion. The EMG data were full-wave rectified, or full-wave rectified and smoothed (second-order Butterworth low pass filter). The full-wave rectified signal retains the information contained in the entire signal; the smoothing eliminates the high-frequency content of the EMG records in order to better relate the EMG signal to the contractile properties of the muscle. For determining the suitable cutoff frequency of the filter used in our study, we predicted forces with the EMG data filtered using a second-order Butterworth low pass filter with cutoff frequencies 2, 5, 15, and 30 Hz. The results indicated that the cutoff frequency of 5 Hz was best in terms of minimizing the difference between the predicted and the actual muscle forces. However, for the sake of comparison, we will show the prediction results in the following chapters using the full-wave rectified and smoothed (second-order Butterworth low pass filter, 5 Hz cutoff frequency) EMG and the full-wave rectified, unsmoothed EMG.

The processed EMG and the corresponding tendon forces were reduced to a nominal sampling frequency of 140 Hz, and the corresponding kinematic data (knee and ankle angles, and knee and ankle angular velocities) were sampled at 140 Hz in order to match all input data for the force predictions perfectly.

3.3 Artificial Neural Network (ANN)

Artificial neural network (ANN) based signal processing methods have been shown to be robust when processing complex, degraded, noisy, and unstable signals (Hassoun et al., 1994). ANNs have unique properties, such as the ability for generalization and learning from experience, and the ability for modifying themselves in accordance with a changing environment.

The field of artificial neural networks is almost five decades old (McCulloch and Pitts, 1943; Hebb, 1949), it has only become widely accepted in research with the recent efforts of Hopfield (1982), Rumelhart *et al.* (1986), and Grossberg (1988). Robotic manipulators have utilized neural networks to replace inverse dynamics algorithms (Kawato *et al.*, 1987), but it is only within the past few years that ANNs have been applied to study real biological systems (Zipser and Andersen, 1988; Massone and Bizzi, 1989; Wells and Vaughan, 1989).

An artificial neural network, as the name implies, comprises a group of neurons which are interconnected and distributed in layers. Networks differ in terms of learning and processing mechanisms, the activation function, the number of layers and neurons, and the distribution of connections. The basic structure of the network used in this study has one input layer, two intermediate hidden layers, and an output layer, illustrated in Figure 3.3.1. The circles in Figure 3.3.1 represent the neurons, and the solid lines represent interneuron connections of varying strengths, known as the synaptic weights. This so-called three-layer neural network has been reported to be sufficient to model problems of

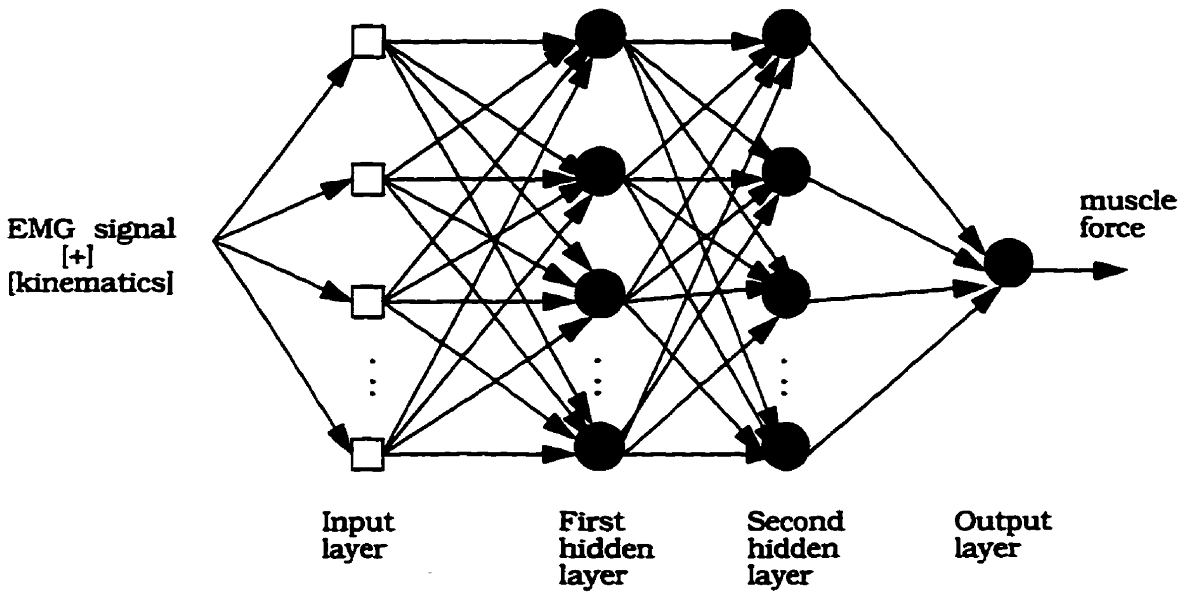

Figure 3.3.1 Architectural graph of a multilayer network

any degree of complexity (Khanna, 1990). We used an error back-propagation algorithm (Rumelhart et al., 1986b) to train the ANN in a supervised manner (Figure 3.3.2). The back-propagation training algorithm is an iterative gradient descent algorithm designed to minimize the mean square error between the actual output of a multilayer perceptron and the desired output. In the back-propagation feedforward algorithm, some of the desired output of the network is assumed to be known a priori. The back-propagation algorithm is composed of two stages: a feedforward step, where neuron output is specified; and a feedback stage, where the connection weights are updated. The two steps are repeated with a training set (EMG-Force examples) until the difference between the network output and the desired values is below a specified value. This procedure is called the learning phase. The goal of the learning phase is to enable the neural network to generalize results so

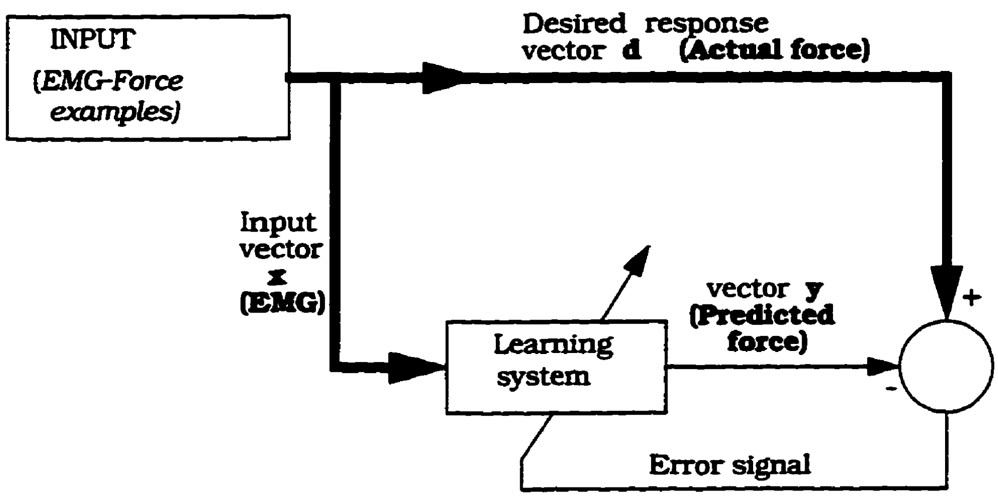

Figure 3.3.2 Block diagram of supervised learning with the *back-propagation* algorithm

that the input-output mapping is excellent even when the input is different from the examples used to train the network.

When an ANN is created, the weights in each neuron are randomly and uniformly initialized using a standard random number generator. In the EMG to Muscle force mapping used here, the input layer had 20 neurons containing EMG information, and an output layer with one neuron, corresponding to the muscle force. The training set in our study was denoted by {[**x**(n), d(n)]; n=1,2,..., N}, with the input vector **x**(n) given to the input layer, and the desired response d(n) represented in the output layer.

In the feedforward step, the output signals of the network were calculated by proceeding forward through the network, layer by layer. Outputs from each middle layer neuron are given by the following activation function:

$$y_j^{(l)}(n) = \frac{1}{1 + \exp(-v_j^{(l)}(n))}$$

where $v_j^{(l)}(n)$ is a simple linear summer for neuron j in layer l:

$$v_j^{(l)}(n) = \sum_{i=1}^{p} w_{ji}^{(l)} y_i^{(l-i)}(n)$$

where $y_i^{(l-i)}(n)$ is the output signal of neuron i in the previous layer $l-1$ at iteration n, and $w_{ji}^{(l)}$ is the synaptic weight of neuron j in layer l that is fed from neuron i in layer $l-1$.

If neuron j is in the first hidden layer (i.e., l=1), set

$$y_j^{(0)}(n) = x_j(n)$$

where $x_j(n)$ is the jth element of the input vector **x**(n). If the neuron is in the output layer (i.e., l=3), then

$$y(n) = y_1^{(3)} = \frac{1}{1 + \exp(-v_1^{(3)}(n))}$$

where

$$v_1^{(3)}(n) = \sum_{i=1}^{q} w_{1i}^{(3)} y_i^{(2)}(n)$$

where q is the number of neurons in the second hidden layer.

Hence, compute the error signal

$$e(n) = d(n) - y(n)$$

where $d(n)$ is the desired response.

In the back-forward step, compute the local gradient, δ of the network by proceeding backward, layer by layer:

$\delta_1^{(3)}(n) = e(n)y(n)[1 - y(n)]$ for the neuron in the output layer,

and

$$\delta_j^{(l)}(n) = y_j^{(l)}(n)\,[1 - y_j^{(l)}(n)]\sum_k \delta_k^{(l+1)}(n)\, w_{kj}^{(l+1)}(n)$$

for neuron j in the hidden layer l.

The synaptic weights of the network in layer l are determined by

$$w_{ji}^{(l)}(n+1) = w_{ji}^{(l)}(n) + \alpha\,[w_{ji}^{(l)}(n) - w_{ji}^{(l)}(n-1)] + \eta\,(n+1)\,\delta_j^{(l)}(n)\, y_i^{(l-1)}(n)$$

where η is the adaptive learning-rate parameter and α is the momentum constant which was set to 0.9 in our study.

The change for η, initialized by 0.2 in the training procedure, is based on the error of the network:

$$\eta\,(n+1) = 0.7 \bullet \eta\,(n) \quad \text{if } e\,(n) > 1.04 \bullet e\,(n-1)$$

and

$$\eta\,(n+1) = 1.05 \bullet \eta\,(n) \quad \text{if } e\,(n) < e\,(n-1)$$

otherwise

$$\eta\,(n+1) = \eta\,(n)\,.$$

In this study, an ANN architecture with one input layer, two hidden layers, and one output layer was used. There is only one neuron in the output layer, 20 or 30 neurons in the input layer, 20 neurons in the first hidden layer, and 10 neurons in the second hidden layer. For the input vector $\mathbf{x}(n)$, $x(n)$ is viewed as the current value of the EMG input, the remaining M (M=19) tap inputs, $x(n-1), \ldots, x(n-M)$, represent past values of the EMG input; however, $x(n-20)$ is viewed as the current value of the kinematics input, the last 9 tap inputs, $x(n-21), \ldots, x(n30)$, represent past values of the kinematics input. When a critical threshold was reached (Haykin, 1994), the two step cycle procedure (the forward-forward step and the corresponding back-forward step) called learning phase, was stopped. In our study, it was repeated about 600-1000 times during the training of the ANN. Our experiments showed that the force prediction can not be improved by increasing arbitrarily the number of the learning phase; learning got worse when the number of the learning steps was greater than 5000.

In this study, the relationship between EMG and force (EMG-force mapping), as well as the relationship between EMG plus kinematics (e.g. knee and ankle angles, knee and ankle angular velocities) and force (EMG^+-force mapping) in the gastrocnemius and soleus were considered during locomotion. The ANN was trained in a supervised mode. The muscle force was the desired response of the network. For the determination of the relationship between EMG and force, the EMG signal was the input to the network; for the relationships between the EMG plus kinematics and force, the input to the network was the EMG signal, the knee and ankle angles, and/or the knee and ankle angular velocities.

3.4 Muscle force prediction

Muscle forces were predicted in three different ways:

(1) For the first prediction scheme, force estimates were made across animals in two ways: (a) the ANN was trained with EMG (with and without kinematics) input from two cats walking/trotting at a given speed of locomotion (0.4, 0.8, and 1.2 m/s); the force predictions were made for the third cat using its EMG for walking/trotting at the same speed as the training was done (inter-subject-A tests), and (b) the ANN was trained with EMG and force input from all available data of two cats walking/trotting; the force predictions were made for the third cat walking/trotting at a given speed of locomotion (inter-subject-B tests). For 'inter-subject-A' predictions, force values were normalized with respect to the peak force of the muscle at a given speed of locomotion. Values of the full-wave rectified, or the full-wave rectified and smoothed EMG signal were normalized with respect to the mean value of the full-wave rectified EMG signal at a given speed of locomotion. For 'inter-subject-B' predictions, force values were normalized with respect to the absolute peak force of the muscle at any of the tested speeds of locomotion in the same cat. Values of the full-wave rectified, or the full-wave rectified and smoothed EMG signal were normalized with respect to the mean value of the full-wave rectified EMG signal for walking at 1.2 m/s in a given cat.

(2) For the second prediction scheme, the ANN was trained with EMG (with and without kinematics) and force input from one cat walking/

trotting at three different speeds of locomotion; the force predictions were made for the fourth speed of locomotion of that same cat (intra-subject tests). Muscle forces and EMG signals were not normalized.

(3) For the third prediction scheme, the ANN was trained with force and EMG (with and without kinematics) input from an increasing number of step cycles of a given cat walking/trotting at one speed of locomotion; the force predictions were made for different steps of the same cat walking at the same speed (intra-session tests). Muscle forces and EMG signals were not normalized.

Evaluation of the force predictions from the EMG signals was made by calculating the coefficients of cross-correlation, and the root mean square (RMS) errors between the predicted and the actual force-time histories. Every result shown in this study was an average value obtained from four independent learning precedures (with the same ANN structure and number of learning steps). Predictions were considered good if the coefficient of cross-correlation was greater than 0.91, RMS error was equal to or smaller than 14% of the corresponding maximum peak force, and the predicted force-time histories did not systematically deviate from the actual force-time histories.

Chapter four: Force Predictions for the Cat Gastrocnemius

4.1 Inter-subject-A tests

Force predictions for the inter-subject-A tests are shown in Tables 1.a. and 1.b. All training examples were from cat 1 and 2, and the force predictions were made for cat 3. The coefficients of cross-correlation for the tests ranged between 0.91-0.96. The corresponding RMS prediction errors are listed in the third and fifth columns of the Table. The input to the tests shown in Table 1.a were the full-wave rectified (the fourth column of the Table) or full-wave rectified and smoothed (the second-third columns of the Table) EMG signal (EMG Model); the input to the tests shown in Table 1.b were the full-wave rectified (the fourth-fifth columns of the Table) or full-wave rectified and smoothed (the second-third columns of the Table) EMG plus the knee and ankle angle-time histories (EMG^+ Model). In each table the results for the full-wave rectified EMG, and the full-wave rectified and smoothed EMG are given.

Table 1.a: Inter-subject-A (EMG Model[1])

Training Sets[2] (speed)	Force Predictions			
	rectified & smoothed EMG		rectified EMG	
	corr.coeff	RMS error[3]	corr.coeff	RMS error[3]
0.4 m/s	0.95	2.10 (9%)	0.94	2.69 (11%)
0.8 m/s	0.96	2.74 (7%)	0.95	3.32 (9%)
1.2 m/s	0.92	4.63 (11%)	0.91	4.73 (11%)

1. The input to the network is the EMG signal.
2. Training data are from cat 1 and 2.
3. The unit of values is Newton, and the percentage of the corresponding maximum peak force also is shown in this column.

Table 1.b: Inter-subject-A (EMG^+ Model[1])

Training Sets[2] (speed)	Force Predictions			
	rectified & smoothed EMG		rectified EMG	
	corr.coeff	RMS error[3]	corr.coeff	RMS error[3]
0.8 m/s	0.96	2.84 (7%)	0.93	3.73 (10%)
1.2 m/s	0.91	4.73 (11%)	0.91	4.82 (11%)

1. The input to the network is the EMG signal and the knee and ankle angles.
2. Training data are from cat 1 and 2.
3. The unit of values is Newton, and the percentage of the corresponding maximum peak force also is shown in this column.

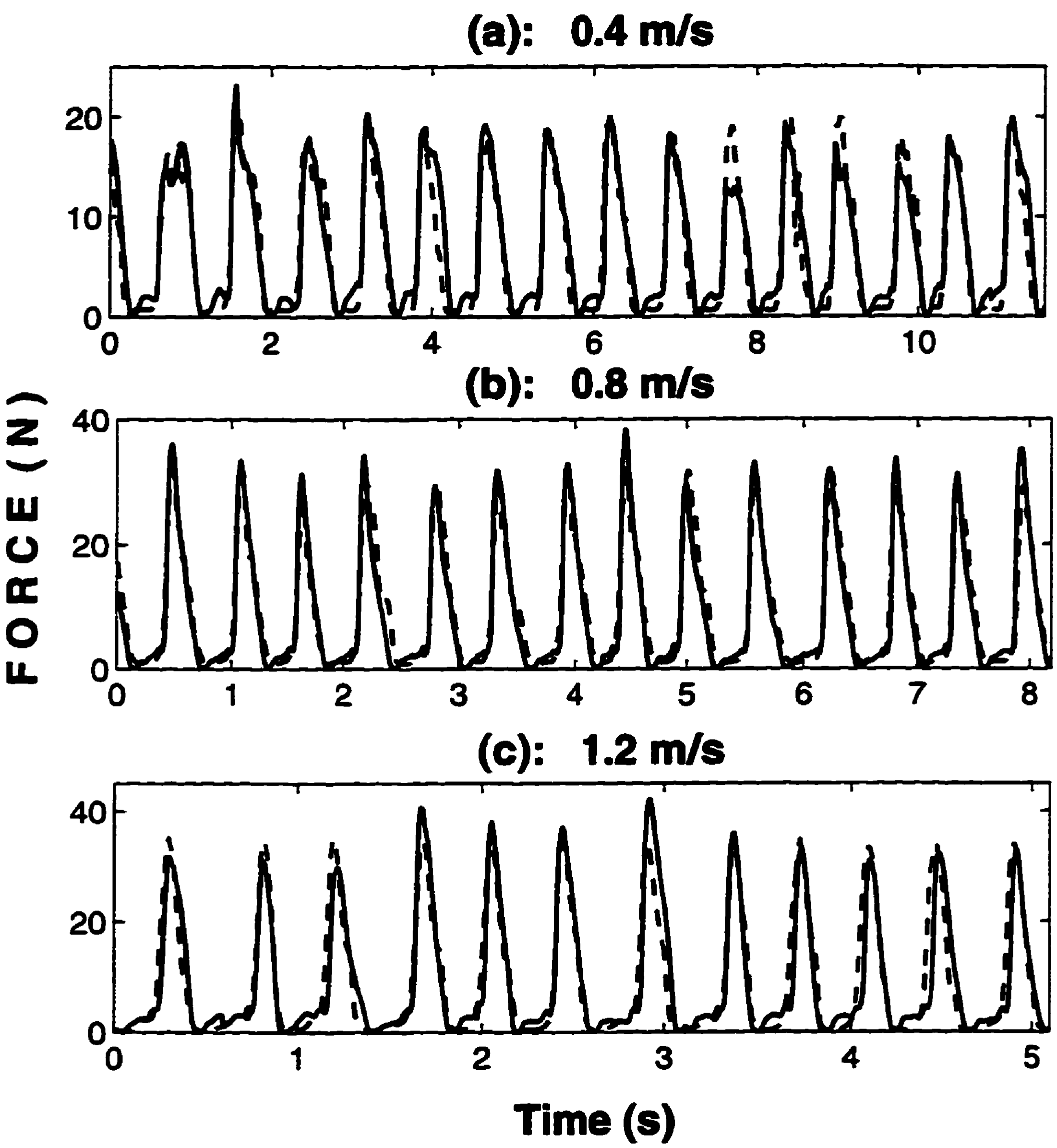

Figure 4.1.1 Inter-subject-A tests:Comparisons of the predicted forces (dashed-line) with the actual gastrocnemius forces (solid-line) for cat 3 walking at (a) 0.4 m/s, when the network was trained with the full-wave rectified and smoothed EMG and muscular force data from cat1 and 2 walking at 0.4 m/s; (b) 0.8 m/s, when the network was trained with the full-wave rectified and smoothed EMG and muscular force data from cat 1 and 2 walking at 0.8 m/s; (c) 1.2 m/s, when the network was trained with the full-wave rectified and smoothed EMG and muscular force data from cat1 and 2 walking at 1.2 m/s.

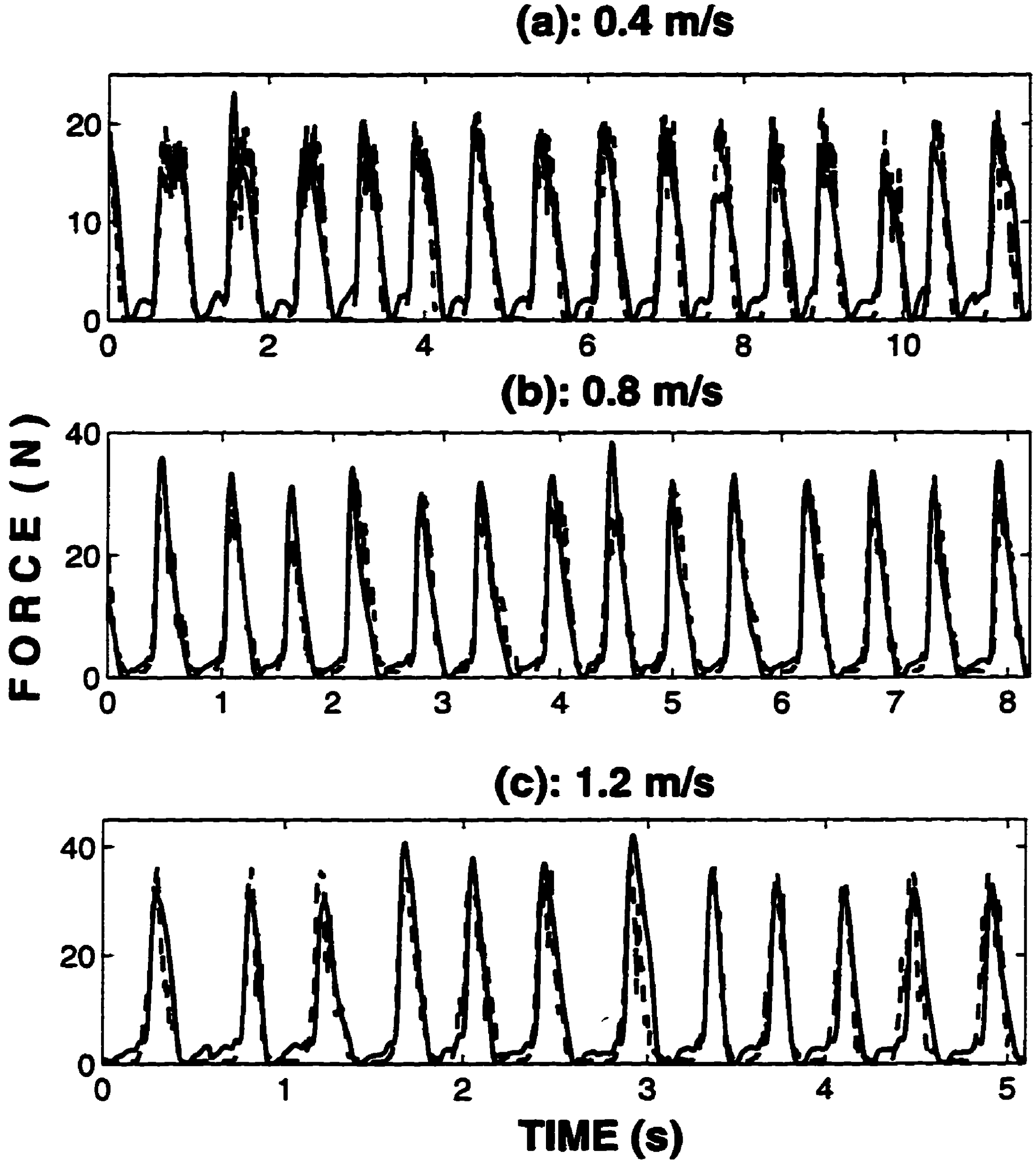

Figure 4.1.2 Inter-subject-A tests:Comparisons of the predicted forces (dashed-line) with the actual gastrocnemius forces (solid-line) for cat 3 walking at (a) 0.4 m/s, when the network was trained with the full-wave rectified EMG and muscular force data from cat1 and 2 walking at 0.4 m/s; (b) 0.8 m/s, when the network was trained with the full-wave rectified EMG and muscular force data from cat1 and 2 walking at 0.8 m/s; (c) 1.2 m/s, when the network was trained with the full-wave rectified EMG and muscular force data from cat1 and 2 walking at 1.2 m/s.

Figures 4.1.1 and 4.1.2 show comparisons of the predicted and the actual gastrocnemius forces for cat 3 walking at 0.4 m/s (Figure 4.1.1(a) and 4.1.2(a)), 0.8 m/s (Figure 4.1.1(b) and 4.1.2(b)),and 1.2 m/s (Figure 4.1.1(c) and 4.1.2(c)), respectively. The corresponding coefficients of cross-correlation are shown in the second and fourth column of Table 1.a. The corresponding RMS errors between the predicted and actual forces are shown in the third and fifth column of Table 1.a. For the test shown in Fig.4.1.1, the predicted and actual force curves were similar, and the root mean square (RMS) errors were 2.1 N (at 0.4 m/s) with the maximum peak force 23.2 N, 2.7 N (at 0.8 m/s) with the maximum peak force 38.4 N, and 4.6 N (at 1.2 m/s) with the maximum peak force 42.2 N, respectively. The correlation coefficients were generally better for walking at 0.4 and 0.8 m/s compared to walking at 1.2 m/s. After the force predictions for the first three steps, the differences in the peak magnitude between predicted and actual forces were generally large (>10%) when the peak of the current step was much lower (>10%) than the peak of the previous step at a speed of 0.4 m/s; and when the peak of the current step was much larger (>10%) than the peak of the previous step at speeds of 0.8, 1.2 m/s. There was a shift to the left of the predicted compared to the actual forces in several steps at a speed of 1.2 m/s. For the test shown in Fig. 4.1.2, the predicted force curves included more noise, especially for walking at 0.4 m/s, compared to the predicted forces in Fig. 4.1.1. This indicates that the high frequency content in the raw EMG signal is an unwanted component of the input to the network for the muscle force predictions.

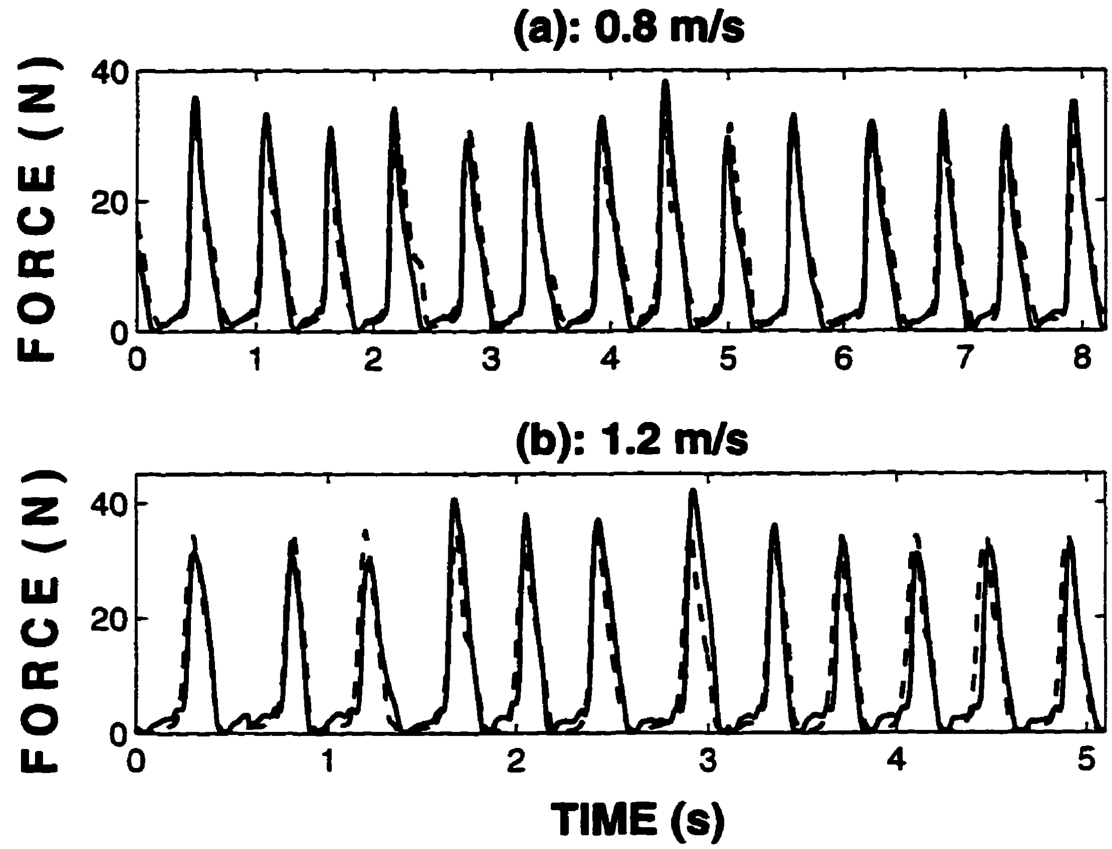

Figure 4.1.3 Inter-subject-A tests:Comparisons of the predicted forces (dashed-line) with the actual gastrocnemius forces (solid-line) for cat 3 walking at (a) 0.8 m/s, when the network was trained with the full-wave rectified and smoothed EMG plus the knee and ankle angle-time histories, and muscular force data from cat1 and 2 walking at 0.8 m/s; (b) 1.2 m/s, when the network was trained with the full-wave rectified and smoothed EMG plus the knee and ankle angle-time histories, and muscular force data from cat1 and 2 walking at 1.2 m/s.

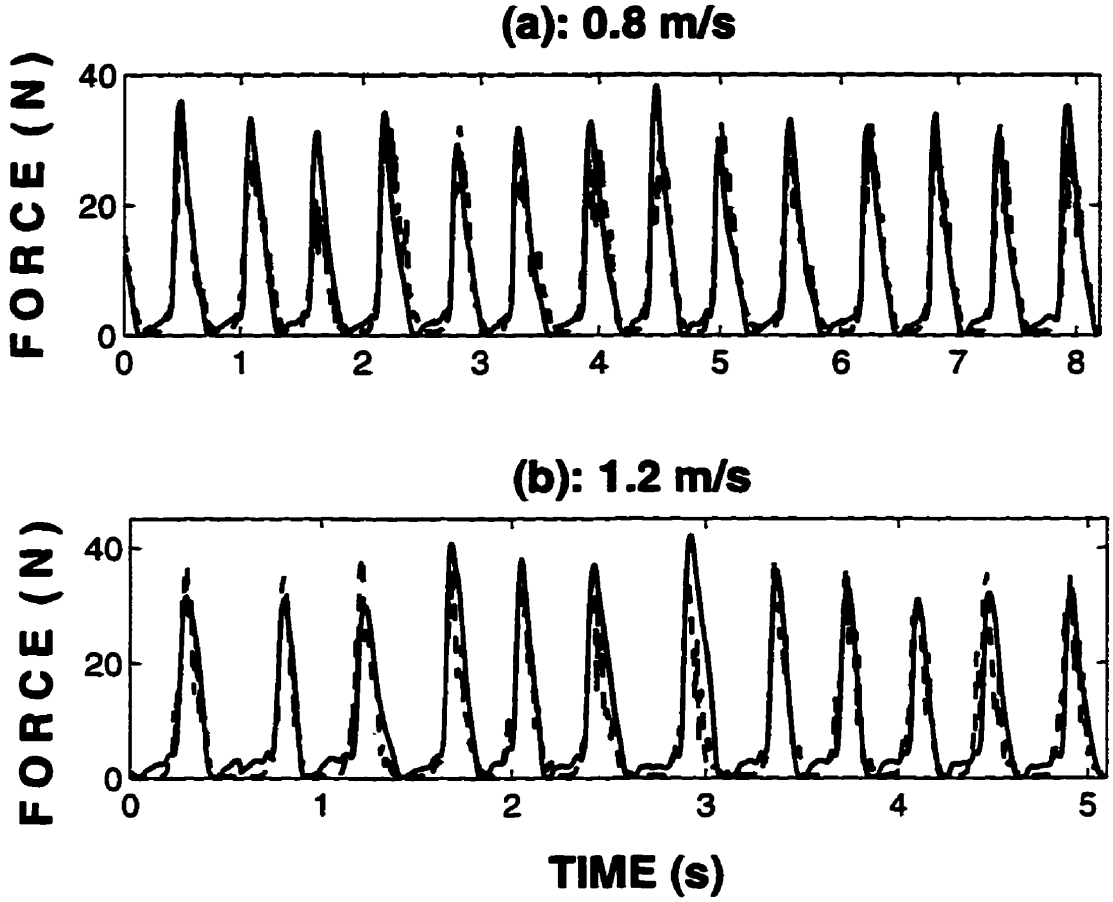

Figure 4.1.4 Inter-subject-A tests: Comparisons of the predicted forces (dashed-line) with the actual gastrocnemius forces (solid-line) for cat 3 walking at (a) 0.8 m/s, when the network was trained with the full-wave rectified EMG plus the knee and ankle angle-time histories, and muscular force data from cat1 and 2 walking at 0.8 m/s. (b) 1.2 m/s, when the network was trained with the full-wave rectified EMG plus the knee and ankle angle-time histories,and muscular force data from cat1 and 2 walking at 1.2 m/s.

Figures 4.1.3 and 4.1.4 show comparisons of the predicted and the actual gastrocnemius forces for cat 3 walking at 0.8 m/s (Figure 4.1.3(a) and 4.1.4(a)),and 1.2 m/s (Figure 4.1.3(b) and 4.1.4(b)), respectively for the tests in Table 1.b. The correlation coefficients shown in Fig 4.1.3 are similar to those shown in Fig. 4.1.1, and so are the prediction results shown in Fig. 4.1.2 and 4.1.4. The results indicate that adding the kinematics to the input for the ANN did not improve the force predictions in these tests.

4.2 Inter-subject-B tests

Force predictions for the inter-subject-B tests are shown in Tables 2.a, and 2.b. The coefficients of cross-correlation ranged from 0.73-0.95 (the third and fifth column of Tables 2.a and 2.b). The RMS errors are shown in the fourth and sixth column of Tables 2.a and 2.b, respectively. The training data were taken from cat 1 and 2 and the muscle predictions were made for cat 3 for walking at speeds of 0.4, 0.8, 1.2 m/s respectively. For the predictions shown in Table 2.a, only EMG signal was used as input (EMG Model); for the predictions shown in Table 2.b, EMG plus knee and ankle angles were used as input (EMG^+ Model). Results are shown for the full-wave rectified and the full-wave rectified and smoothed EMG. Adding the kinematics to the input improved the correlation coefficients and decreased the RMS errors in the tests using the rectified and smoothed EMG as input but not in the tests using only the rectified EMG as input (Table 2.a).

Table 2.a: Inter-subject-B tests (EMG Model[1])

Training Sets (speed)	speed (m/s)	rectified & smoothed EMG		rectified EMG	
		corr.coef.	RMS error[2]	corr.coef.	RMS error[2]
All available data from cat1 and 2	0.4	0.73	5.29 (23%)	0.87	3.67 (16%)
	0.8	0.88	5.29 (14%)	0.94	3.90 (10%)
	1.2	0.86	6.17 (15%)	0.93	4.42 (10%)

Force Predictions spans the speed and EMG columns.

1. The input to the network is the EMG signal.
2. The unit of values is Newton, and the percentage of the corresponding maximum peak force also is shown in this column.

Table 2.b: Inter-subject-B tests (EMG^+ Model[1])

Training Sets	speed (m/s)	rectified & smoothed EMG		rectified EMG	
		corr.coeff.	RMS error[2]	corr.coeff.	RMS error[2]
All available data from cat1 and 2	0.4	0.79	5.03 (22%)	0.83	4.51 (19%)
	0.8	0.95	3.92 (10%)	0.93	4.57 (12%)
	1.2	0.85	6.00 (14%)	0.91	5.09 (12%)

1. The input to the network is the EMG signal and the knee and ankle angles.
2. The unit of values is Newton, and the percentage of the corresponding maximum peak force also is shown in this column.

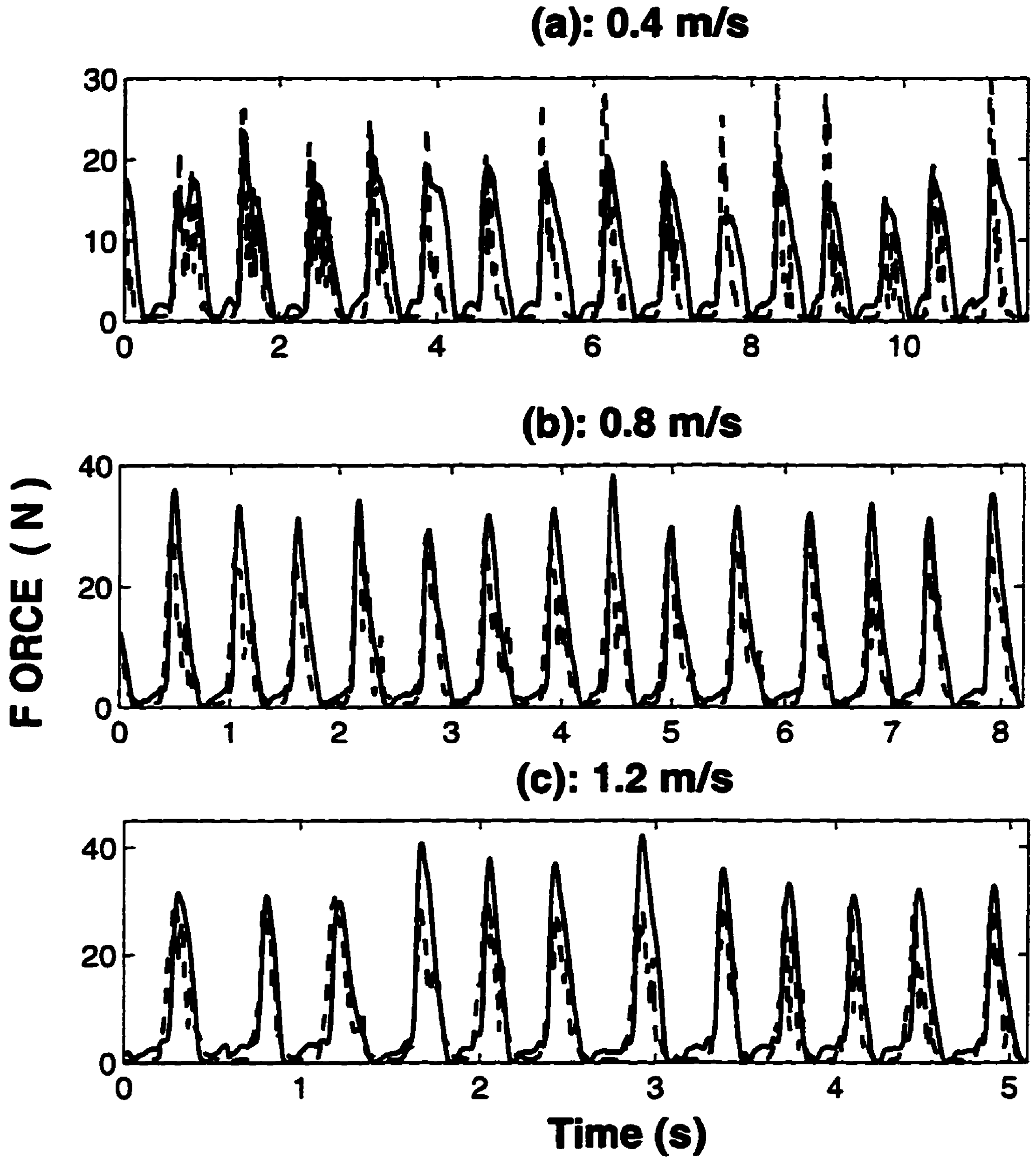

Figure 4.2.1 Inter-subject-B tests:Comparisons of the predicted forces (dashed-line) with the actual gastrocnemius forces (solid-line) for cat 3 walking at (a) 0.4 m/s; (b) 0.8 m/s; (c) 1.2 m/s, when the network was trained with all available full-wave rectified and smoothed EMG and muscular force from cat 1 and 2.

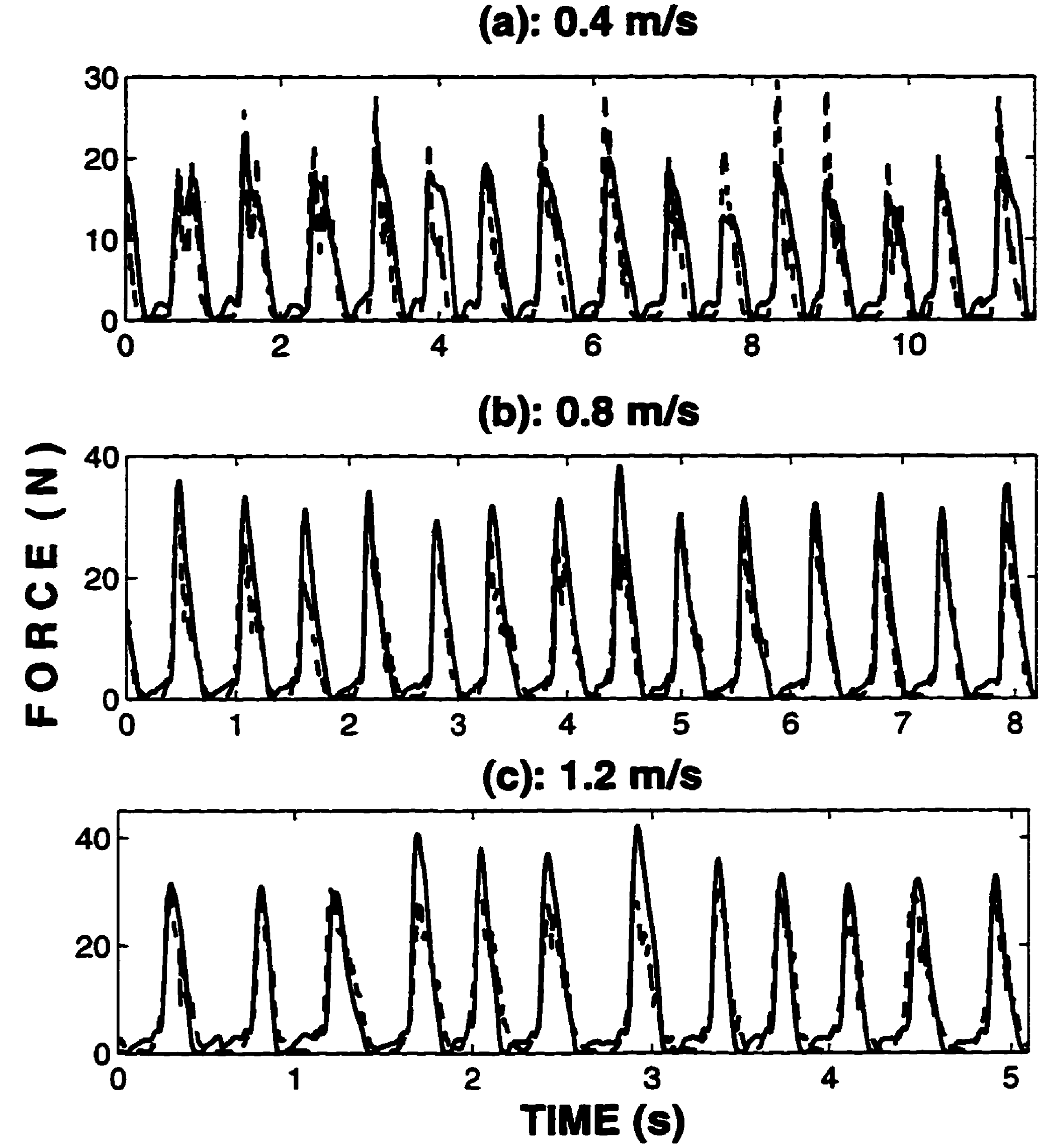

Figure 4.2.2 Inter-subject-B tests:Comparisons of the predicted forces (dashed-line) with the actual gastrocnemius forces (solid-line) for cat 3 walking at (a) 0.4 m/s; (b) 0.8 m/s; (c) 1.2 m/s, when the network was trained with all available full-wave rectified EMG and muscular force from cat 1 and 2.

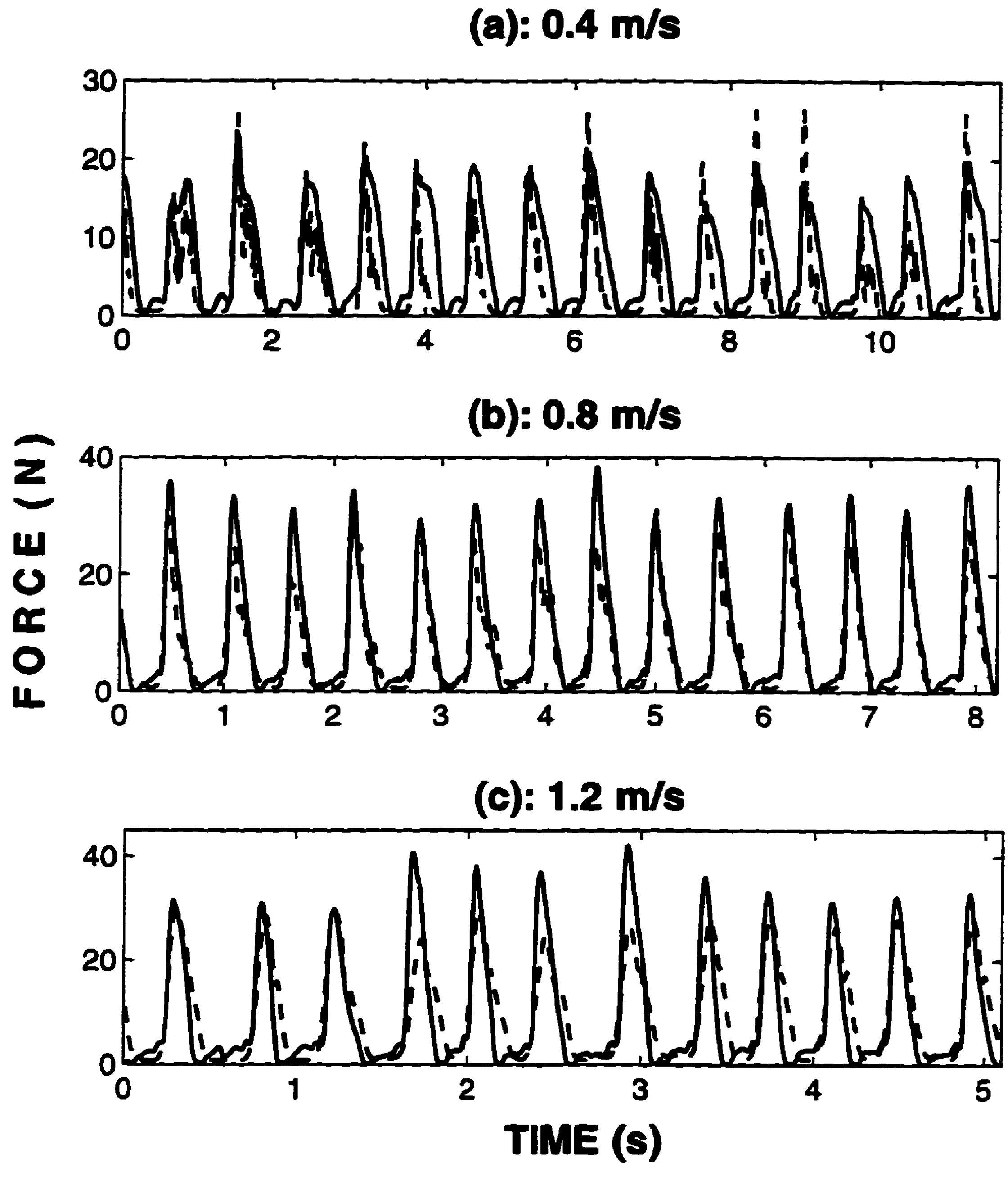

Figure 4.2.3 Inter-subject-B tests: Comparisons of the predicted forces (dashed-line) with the actual gastrocnemius forces (solid-line) for cat 3 walking at (a) 0.4 m/s; (b) 0.8 m/s; (c) 1.2 m/s, when the network was trained with all available full-wave rectified and smoothed EMG plus the knee and ankle angle-time histories, and muscular force data from cat1 and 2.

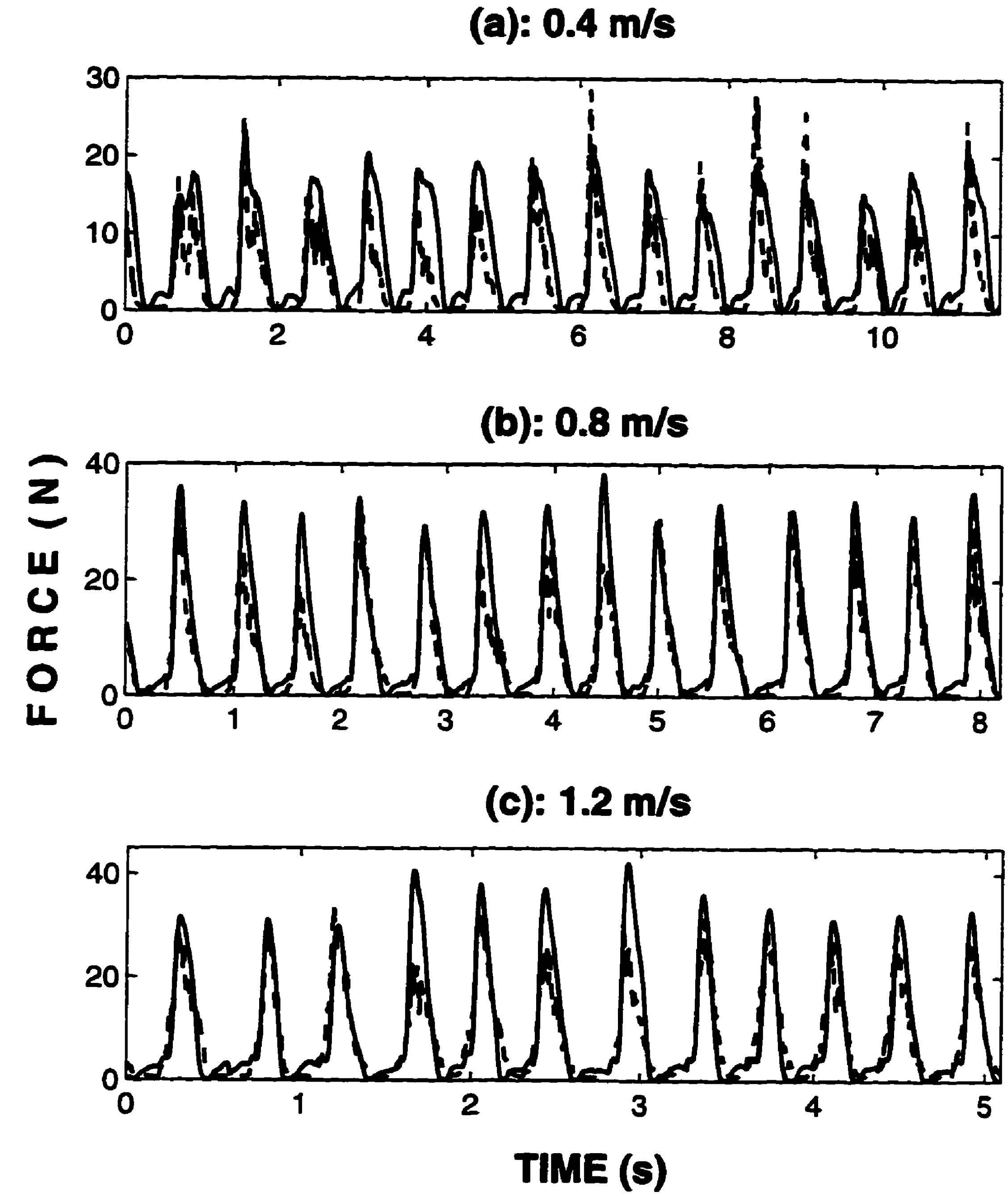

Figure 4.2.4 Inter-subject-B tests:Comparisons of the predicted forces (dashed-line) with the actual gastrocnemius forces (solid-line) for cat 3 walking at (a) 0.4 m/s; (b) 0.8 m/s; (c) 1.2 m/s, when the network was trained with all available full-wave rectified plus the knee and ankle angle-time histories, and muscular force data from cat 1 and 2.

Figures 4.2.1 and 4.2.2 show the comparison between the predicted and the actual forces for walking at 0.4 m/s, 0.8 m/s, and 1.2 m/s (Figure 4.2.1(a) and 4.2.2(a), 4.2.1(b) and 4.2.2(b), 4.2.1(c) and 4.2.2(c), respectively), when the network was trained with all available data from cat 1 and 2. Input for these tests was the full-wave rectified and smoothed EMG signal (Figure 4.2.1), or the full-wave rectified EMG signal (Fig. 4.2.2). The coefficients of cross-correlation and RMS errors of the results are listed in Table 2.a. While the coefficients of cross-correlation and RMS errors of the results shown in Figures 4.2.3 and 4.2.4 are listed in Table 2.b. The time histories of the predicted forces deviate systematically from those of the actual forces. The RMS prediction errors were generally high (>12% of the corresponding maximum peak force). Comparing the results in Figure 4.2 with the results in Figures 4.1, it is apparent that force predictions for the inter-subject-A tests were better than the corresponding predictions for the inter-subject-B tests. Therefore, increasing the number of training examples with non-specific walking trials decreased the predictive ability of the ANN in the gastrocnemius muscles.

4.3 Intra-subject tests

Force predictions for the intra-subject tests are shown in Table 3.a, and 3.b.

Table 3.a: Intra-subject tests (EMG Model[1])

Training Sets[2] (speed)	speed (m/s)	Force Predictions: rectified & smoothed EMG		rectified EMG	
		corr.coeff.	RMS error[3]	corr.coeff.	RMS error[3]
0.8, 1.2, 1.8 m/s	0.4	0.87	3.96 (17%)	0.85	4.07 (18%)
0.4, 1.2, 1.8 m/s	0.8	0.93	4.25 (11%)	0.93	4.11 (11%)
0.4, 0.8, 1.8 m/s	1.2	0.92	4.49 (11%)	0.92	4.55 (11%)
0.4, 0.8, 1.2 m/s	1.8	0.88	5.70 (14%)	0.90	5.20 (12%)

1. The input to the network is the EMG signal.
2. Training data are from cat 3.
3. The unit of values is Newton, and the percentage of the corresponding maximum peak force also is shown in this column.

Table 3.b: Intra-subject tests (EMG^+ Model[1])

Training Sets[2] (speed)	speed (m/s)	Force Predictions: rectified & smoothed EMG		rectified EMG	
		corr.coeff.	RMS error[3]	corr.coeff	RMS error[3]
0.8, 1.2, 1.8 m/s	0.4	0.83	4.61 (20%)	0.80	4.71 (20%)
0.4, 1.2, 1.8 m/s	0.8	0.93	4.39 (11%)	0.93	4.08 (11%)
0.4, 0.8, 1.8 m/s	1.2	0.90	4.92 (12%)	0.90	4.89 (12%)
0.4, 0.8, 1.2 m/s	1.8	0.88	5.74 (14%)	0.89	5.52 (13%)

1. The input to the network is the EMG signal and the knee and ankle angles
2. Training data are from cat 3.
3. The unit of values is Newton, and the percentage of the corresponding maximum peak force also is shown in this column.

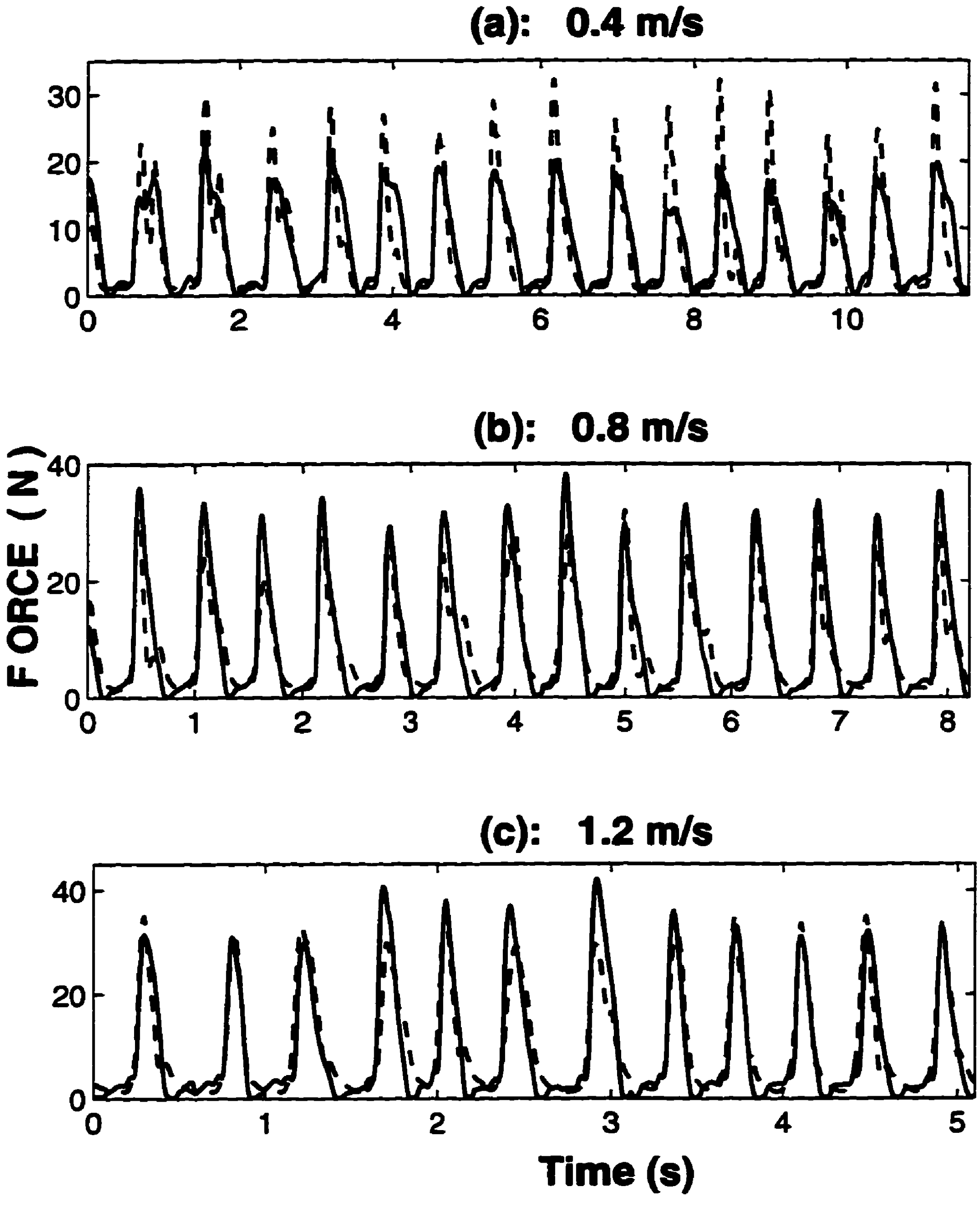
(a): 0.4 m/s
30
20
10
0
0
2
4
6
8
10
(b): 0.8 m/s
FORCE (N)
40
20
0
0
1
2
3
4
5
6
7
8
(c): 1.2 m/s
40
20
0
0
1
2
3
4
5
Time (s)

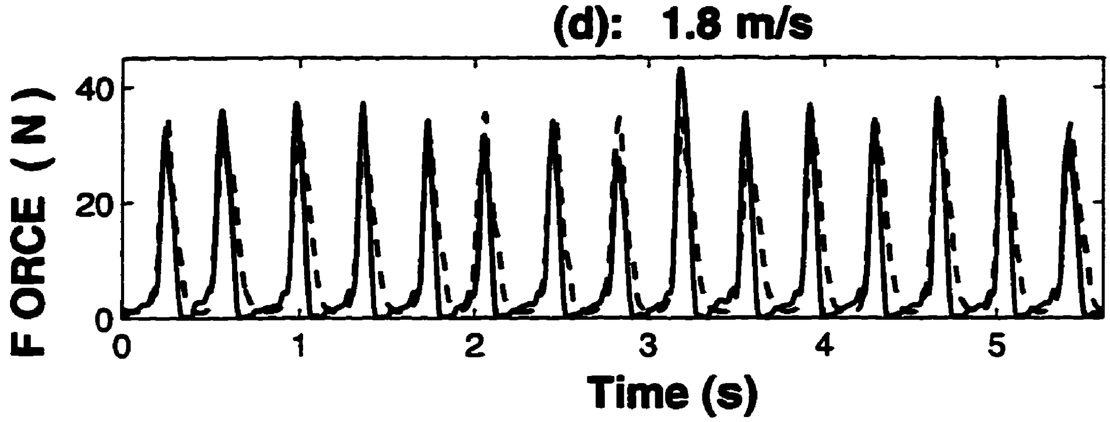

Figure 4.3.1 Intra-subject tests: Comparisons of the predicted forces (dashed-line) with the actual gastrocnemius forces (solid-line) for a representative cat walking at (a) 0.4 m/s, when the network was trained with the full-wave rectified and smoothed EMG and force data from the same cat while walking/trotting at speeds of 0.8, 1.2, 1.8 m/s; (b) 0.8 m/s, when the network was trained with the full-wave rectified and smoothed EMG and force data from the same cat while walking/trotting at speeds of 0.4, 1.2, 1.8 m/s; (c) 1.2 m/s, when the network was trained with the full -wave rectified and smoothed EMG and force data from the same cat while walking/trotting at speeds of 0.4, 0.8, 1.8 m/s; (d) 1.8 m/s, when the network was trained with the full-wave rectified and smoothed EMG and force data from the same cat while walking at speeds of 0.4,0.8,1.2, m/s.

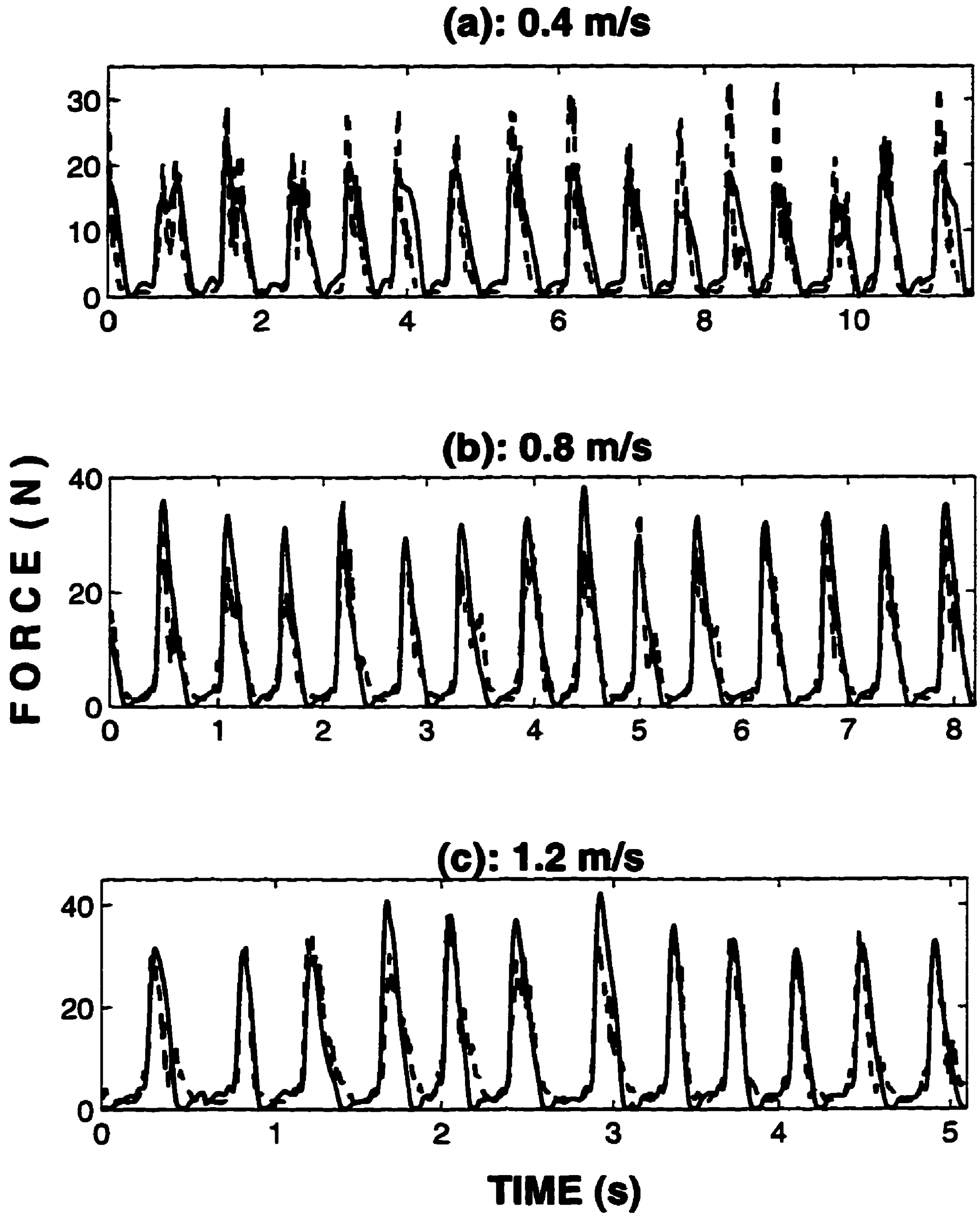
(a): 0.4 m/s
30
20
10
0
0
2
4
6
8
10
(b): 0.8 m/s
FORCE (N)
40
20
0
0
1
2
3
4
5
6
7
8
(c): 1.2 m/s
40
20
0
0
1
2
3
4
5
TIME (s)

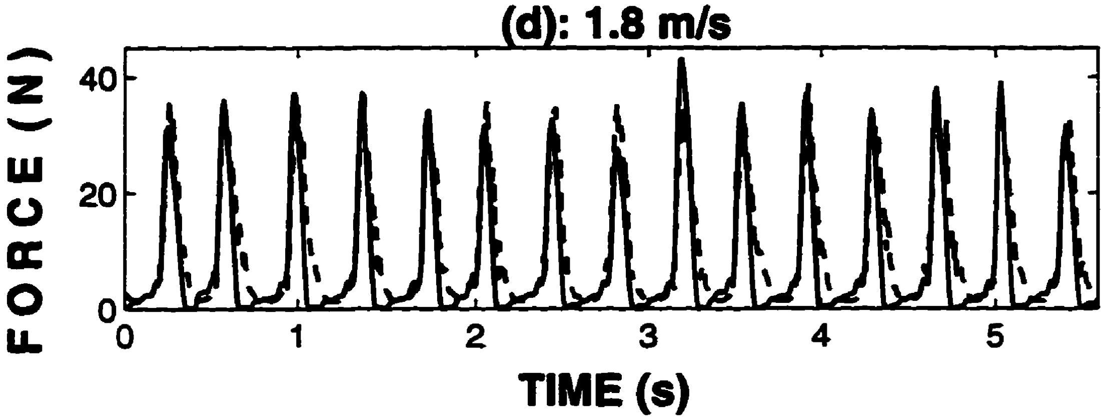

Figure 4.3.2 Intra-subject tests: Comparisons of the predicted forces (dashed-line) with the actual gastrocnemius forces (solid-line) for a representative cat walking at (a) 0.4 m/s, when the network was trained with the full-wave rectified EMG and force data from the same cat while walking/trotting at speeds of 0.8, 1.2, 1.8 m/s;(b) 0.8 m/s, when the network was trained with the full-wave rectified EMG and force data from the same cat while walking/trotting at speeds of 0.4, 1.2, 1.8 m/s; (c) 1.2 m/s, when the network was trained with the full-wave rectified EMG and force data from the same cat while walking/trotting at speeds of 0.4, 0.8, and 1.8 m/s; (d) 1.8 m/s, when the net work was trained with the full-wave rectified EMG and force data from the same cat while walking at speeds of 0.4, 0.8,1.2, m/s.

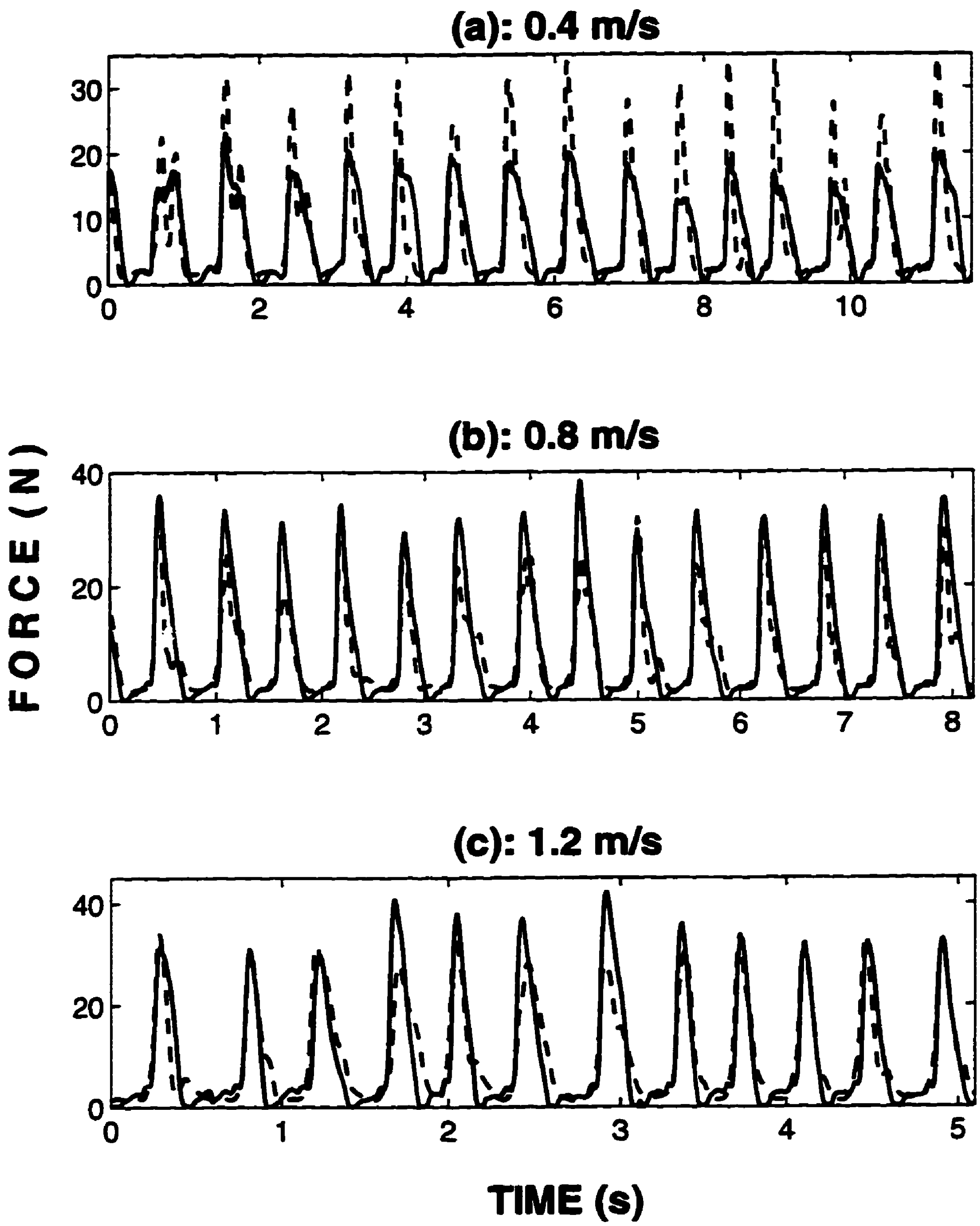
(a): 0.4 m/s
30
20
10
0
0
2
4
6
8
10
(b): 0.8 m/s
FORCE (N)
40
20
0
0
1
2
3
4
5
6
7
8
(c): 1.2 m/s
40
20
0
0
1
2
3
4
5
TIME (s)

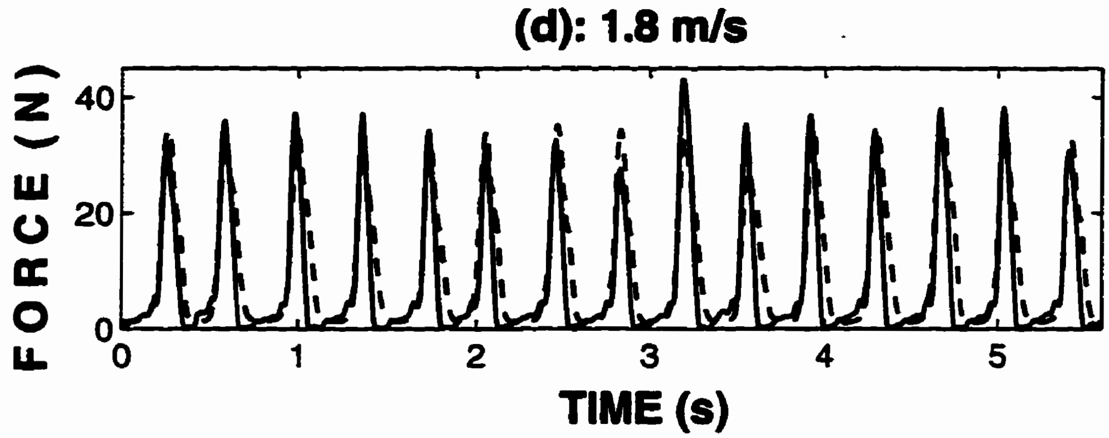

Figure 4.3.3 Intra-subject tests: Comparisons of the predicted forces (dashed-line) with the actual gastrocnemius forces (solid-line) for a representative cat walking at (a) 0.4 m/s,when the network was trained with the full-wave rectified and smoothed EMG plus the knee and ankle angle-time histories, and muscular force data from the same cat while walking/trotting at speeds of 0.8, 1.2, 1.8 m/s; (b) 0.8 m/s, when the network was trained with the full-wave rectified and smoothed EMG plus the knee and ankle angle-time histories, and muscular force data from the same cat while walking/trotting at speeds of 0.4, 1.2, 1.8 m/s; (c) 1.2 m/s, when the network was trained with the full -wave rectified and smoothed EMG plus the knee and ankle angle-time histories, and muscular force data from the same cat while walking/trotting at speeds of 0.4, 0.8, 1.8 m/s; (d) 1.8 m/s, when the network was trained with the full-wave rectified and smoothed EMG plus the knee and ankle angle-time histories, and muscular force data from the same cat while walking at speeds of 0.4,0.8,1.2, m/s.

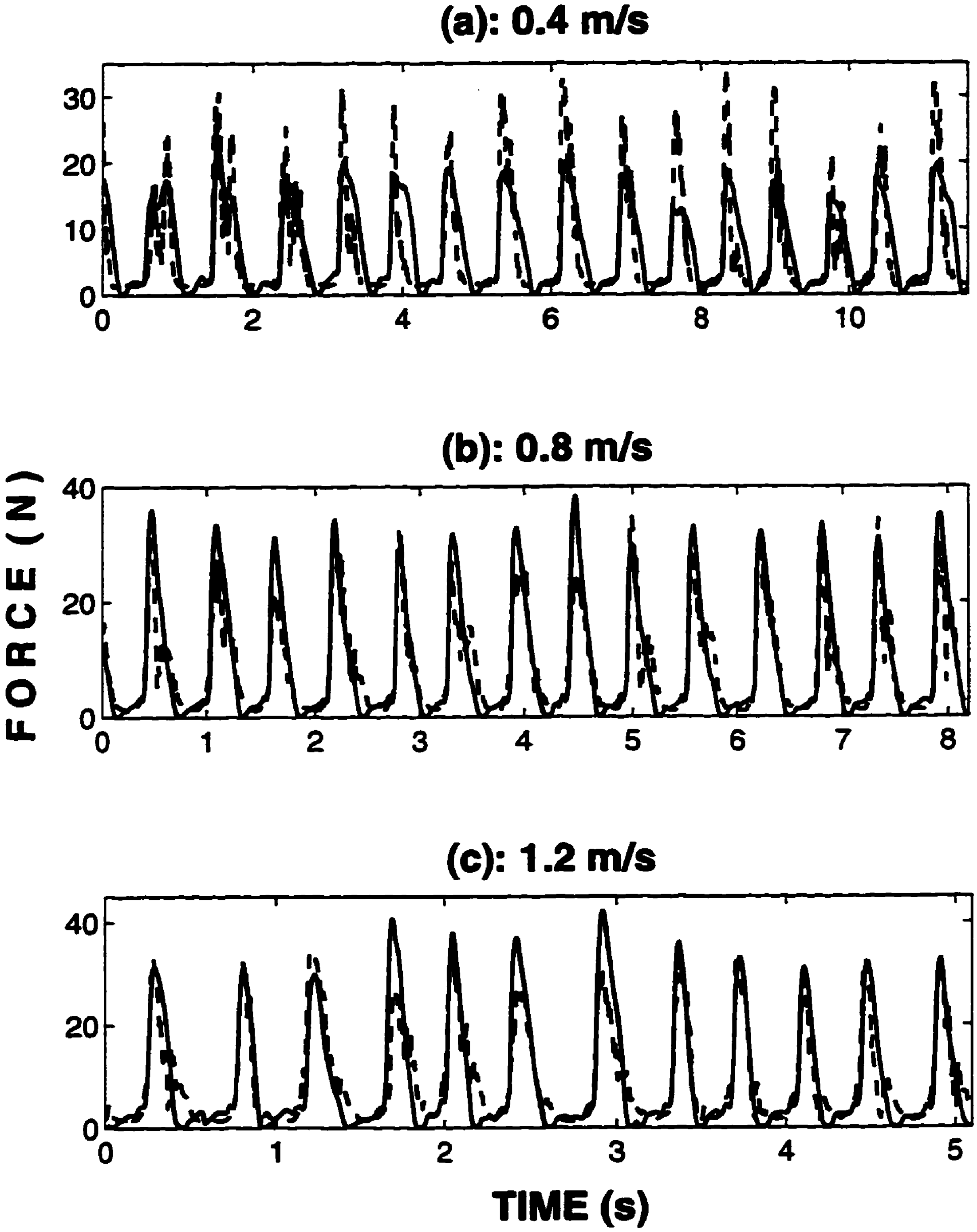
(a): 0.4 m/s
30
20
10
0
0
2
4
6
8
10
(b): 0.8 m/s
FORCE (N)
40
20
0
0
1
2
3
4
5
6
7
8
(c): 1.2 m/s
40
20
0
0
1
2
3
4
5
TIME (s)

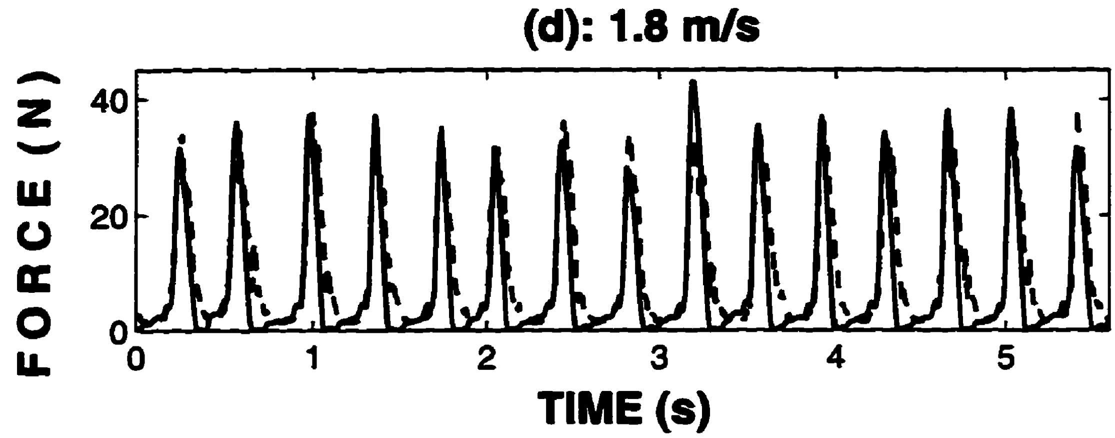

Figure 4.3.4 Intra-subject tests: Comparisons of the predicted forces (dashed-line) with the actual gastrocnemius forces (solid-line) for a representative cat walking at (a) 0.4 m/s, when the network was trained with the full-wave rectified EMG plus the knee and ankle angle-time histories, and muscular force data from the same cat while walking/trotting at speeds of 0.8, 1.2, 1.8 m/s; (b) 0.8 m/s,when the network was trained with the full-wave rectified EMG plus the knee and ankle angle-time histories, and muscular force data from the same cat while walking / trotting at speeds of 0.4, 1.2,1.8 m/s; (c) 1.2 m/s, when the network was trained with the full-wave rectified EMG plus the knee and ankle angle-time histories,and muscular force data from the same cat while walking /trotting at speeds of 0.4,0.8,1.8 m/s; (d) 1.8 m/s,when the network was trained with the full-wave rectified EMG plus the knee and ankle angle-time histories,and muscular force data from the same cat while walking at speeds of 0.4,0.8,1.2, m/s.

Figures 4.3.1 and 4.3.2, respectively show the predicted forces for one representative cat walking/trotting at one speed while the network was trained with the full-wave rectified and smoothed EMG (Figure 4.3.1) or the full-wave rectified EMG (Figure 4.3.2) and force data from the same cat walking/trotting at the three remaining speeds. The coefficients of cross-correlation for the experiments shown in Figures 4.3.1 and 4.3.2

are listed in the third and fifth column of Table 3.a, respectively. The cross-correlation coefficients for the experiments shown in Figures 4.3.3 and 4.3.4 are listed in the third and fifth column of Table 3.b. The corresponding RMS prediction errors shown in Figure 4.3 are listed in the fourth and last column of Tables 3.a and 3.b, respectively. The root mean square errors shown in Figure 4.3.1 are 4.0 N (at 0.4 m/s) with the maximum peak force of 23.2 N, 4.3 N (at 0.8 m/s) with the maximum peak force of 38.4 N, 4.5 N (at 1.2 m/s) with the maximum peak force of 42.2 N, and 5.7 N (at 1.8 m/s) with the maximum peak force of 43.0 N, respectively.

The coefficients of cross-correlation were higher (>0.9) when the speed for the force predictions was intermediate compared to the situation when the speed for the force predictions was higher or lower than the speeds used for training the network. Differences in the peak force were larger at 0.4 than at 0.8 or 1.2 m/s (compare Figure 4.3.1a (0.4 m/s) to Figure 4.3.1b,c (0.8 and 1.2 m/s), respectively). The RMS errors ranged from 11%-20% of the corresponding maximum peak forces. There is a systematic shift to the right of the time histories in the descending part of the predicted compared to the actual force time histories at 1.8 m/s (Figure 4.3.1(d), 4.3.2(d), 4.3.3(d), and 4.3.4(d)), and a systematic shift to the left for the corresponding comparison at 0.4 m/s (Figure 4.3.1(a), 4.3.2(a), 4.3.3(a), and 3.4(a)). The shifts resulted in low (<0.90) coefficients of cross-correlation and high RMS errors (12%-14% of the corresponding maximum peak forces) for walking at 1.8 m/s.

4.4 Intra-session tests

Force predictions for the intra-session tests are shown in Tables 4.a, and 4.b.

Table 4.a: Intra-session tests (EMG Model[1])

Training Sets[2] (steps)	Force predictions				
	steps	rectified & smoothed EMG		rectified EMG	
		corr.coeff.	RMS error[3]	corr.coeff.	RMS error[3]
0-1.5	10-14	0.97	2.82 (8%)	0.90	4.89 (14%)
0-2.5	10-14	0.95	3.31 (9%)	0.89	5.07 (14%)
0-3.5	10-14	0.95	3.41 (10%)	0.93	4.26 (12%)
0-4.5	10-14	0.97	2.34 (7%)	0.91	4.44 (12%)
0-5.5	10-14	0.98	2.36 (7%)	0.92	4.41 (12%)
0-6.5	10-14	0.98	2.21 (6%)	0.93	3.96 (11%)
0-7.5	10-14	0.97	2.44 (7%)	0.92	4.36 (12%)
0-8.5	10-14	0.97	2.55 (7%)	0.91	4.42 (12%)
0-9.5	10-14	0.97	2.53 (7%)	0.94	3.57 (10%)

1. The input to the network is the EMG signal.
2. Training data are from an increasing number of step cycles of a representative cat walking at 0.8 m/s.
3. The unit of values is Newton, and the percentage of the corresponding maximum peak force also is shown in this column

Table 4.b: Intra-session tests (EMG$^+$ Model[1])

Training Sets[2] (steps)	Force Predictions				
	steps	rectified & smoothed EMG		rectified EMG	
		corr.coeff.	RMS error[3]	corr.coeff.	RMS error[3]
0-1.5	10-14	0.97	3.06 (9%)	0.92	4.33 (12%)
0-2.5	10-14	0.97	2.60 (7%)	0.93	3.98 (11%)
0-3.5	10-14	0.96	3.11 (9%)	0.94	3.74 (10%)
0-4.5	10-14	0.97	2.37 (7%)	0.96	3.09 (9%)
0-5.5	10-14	0.98	2.34 (7%)	0.96	3.09 (9%)
0-6.5	10-14	0.98	2.15 (6%)	0.95	3.39 (10%)
0-7.5	10-14	0.97	2.49 (7%)	0.94	3.52 (10%)
0-8.5	10-14	0.97	2.45 (7%)	0.96	2.99 (9%)
0-9.5	10-14	0.98	2.34 (7%)	0.96	2.90 (8%)

1. The input to the network is the EMG signal and the knee and ankle angles.
2. Training data are from an increasing number of step cycles of a representative cat walking at 0.8 m/s.
3. The unit of values is Newton, and the percentage of the corresponding maximum peak force also is shown in this column.

Force predictions for the intra-session tests were good when the EMG signal was full-wave rectified and smoothed (the third and fourth columns of Table 4.a and 4.b). The coefficients of cross-correlation for the tests ranged from 0.95-0.98 (the third column of Table 4.a and 4.b) and the RMS prediction errors ranged from 6%- 9% of the maximum peak force of 35.2 N (the fourth column of Table 4.a and 4.b), when the network was trained with information of 1.5 steps or more.

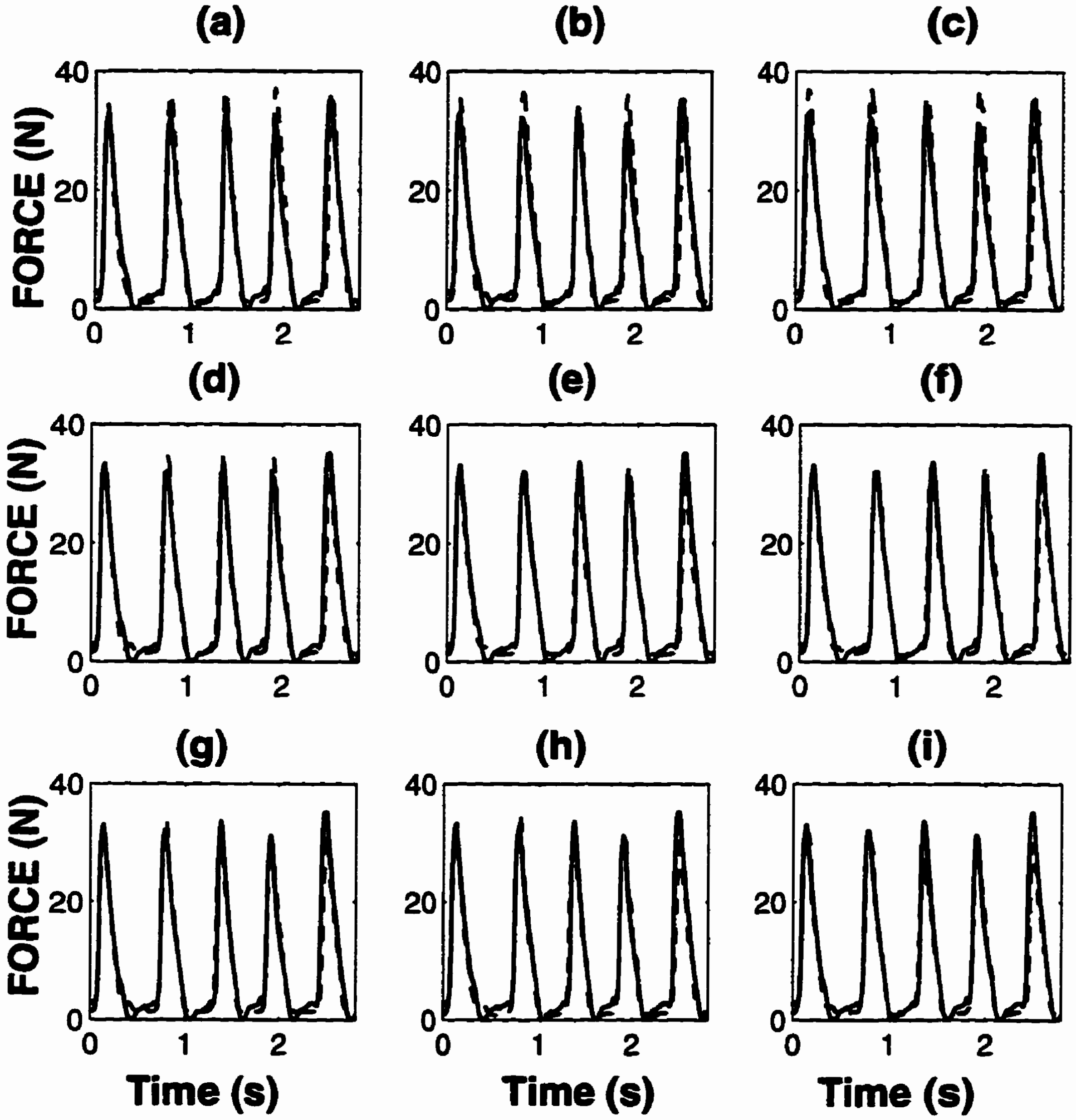

Figure 4.4.1 Intra-session tests: Comparisons of the predicted forces (dashed-line) with the actual gastrocnemius forces (solid-line) for the last five steps of a representative cat at 0.8 m/s, when the network was trained using the full-wave rectified and smoothed EMG and force data from the first 1.5 (a), 2.5 (b), 3.5 (c), 4.5 (d), 5.5 (e), 6.5 (f), 7.5 (g), 8.5 (h), and 9.5 (i) steps of that session.

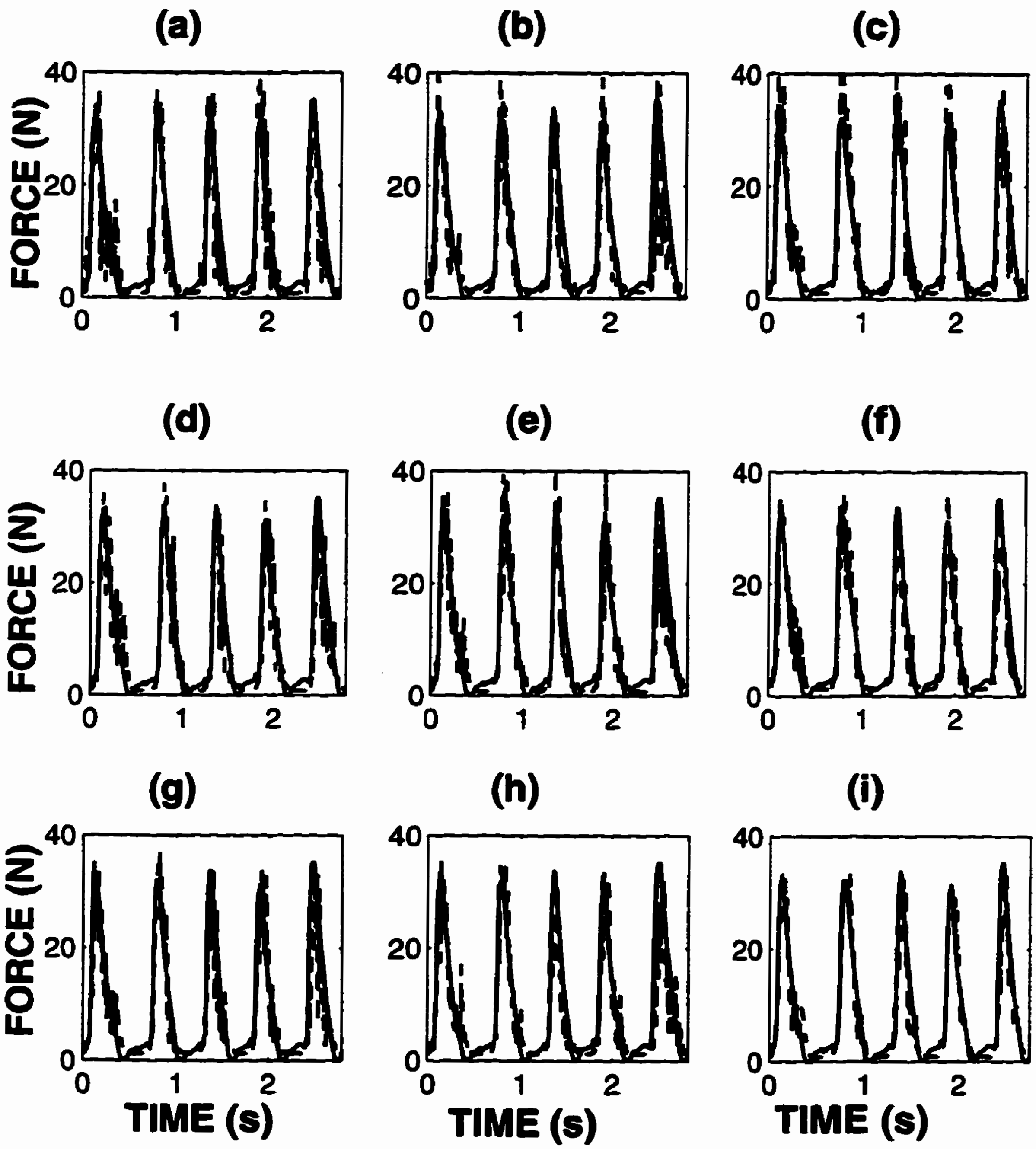

Figure 4.4.2 Intra-session tests: Comparisons of the predicted forces (dashed-line) with the actual gastrocnemius forces (solid-line) for the last five steps of a representative cat at 0.8 m/s, when the network was trained using the full-wave rectified EMG and force data from the first 1.5 (a), 2.5 (b), 3.5 (c), 4.5 (d), 5.5 (e), 6.5 (f), 7.5 (g), 8.5 (h), and 9.5 (i) steps of that session.

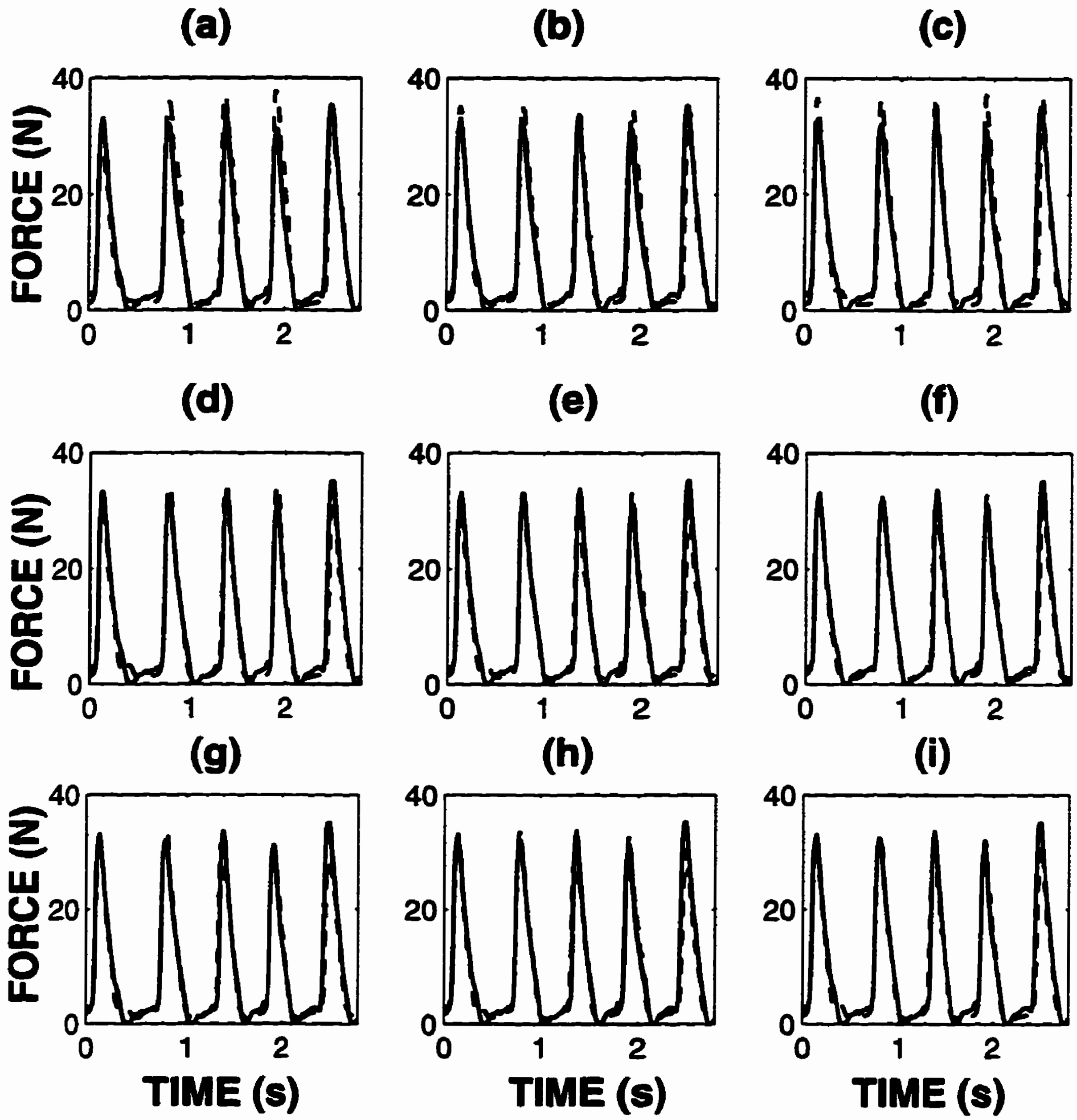

Figure 4.4.3 Intra-session tests: Comparisons of the predicted forces (dashed-line) with the actual gastrocnemius forces (solid-line) for the last five steps of a representative cat at 0.8 m/s, when the network was trained using the full-wave rectified and smoothed EMG plus the knee and ankle angle-time histories, and force data rom the first 1.5 (a), 2.5 (b), 3.5 (c),4.5 (d), 5.5 (e), 6.5 (f),7.5 (g),8.5 (h),and 9.5 (i) steps of that session.

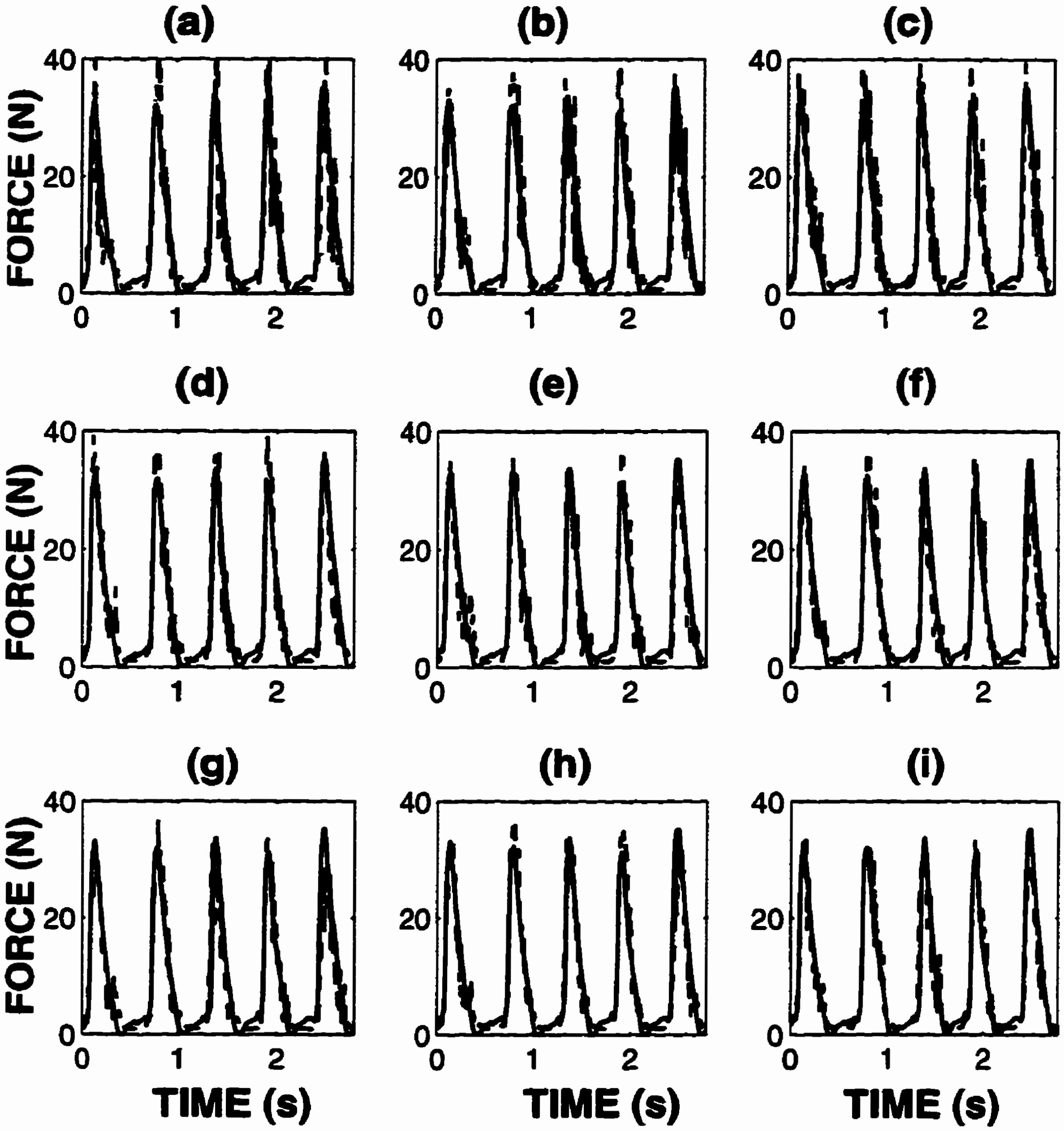

Figure 4.4.4 Intra-session tests: Comparisons of the predicted forces (dashed-line) with the actual gastrocnemius forces (solid-line) for the last five steps of a representative cat at 0.8 m/swhen the network was trained using the full-wave rectified EMG plus the knee and ankle angle-time histories, and force data from the first 1.5 (a), 2.5 (b), 3.5 (c),4.5 (d), 5.5 (e), 6.5 (f), 7.5 (g), 8.5 (h), and 9.5 (i) steps of that session

Figures 4.4.1(a)-(i) and 4.4.2(a)-(i) show the comparisons of the predicted and the actual forces for the last five steps of a representative cat in one session when the network was trained using the full-wave rectified and smoothed EMG or the full-wave rectified EMG, and force data from an increasing number of steps (1.5, 2.5, 3.5, 4.5, 5.5, 6.5, 7.5, 8.5, and 9.5 steps) of that session, respectively. The corresponding coefficients of cross-correlation for the tests are shown in the third and fifth columns of Table 4.a. The corresponding RMS errors are shown in the fourth and sixth columns of Table 4.a.

Figures 4.4.3(a)-(i) and 4.4.4(a)-(i) show the prediction results listed in Table 4.b. The coefficients of cross-correlation were higher (>0.95) when the network was trained using the full-wave rectified and smoothed EMG (the third column of Table 4.a and 4.b) compared to using the full-wave rectified and unsmoothed EMG (the fifth column of Table 4.a and 4.b). Also, the RMS errors were lower (<9% of the maximum peak force) when the network was trained using the smoothed (the fourth column of Table 4.a and 4.b) compared to using the unsmoothed EMG (the last column of Tables 4.a and 4.b). For the tests shown in Figures 4.4.2 and 4.4.4, the predicted force curves included more noise compared to the predicted forces in Figures 4.4.1 and 4.4.3.

For the results shown in Figures 4.4.1 and 4.4.3, the coefficient of cross-correlation ranged from 0.97-0.98, the RMS errors ranged from 2.2-2.5 N with the maximum peak force of 35.2 N, and the time histories of the predicted and actual forces matched almost perfectly when the number of steps used for the training session was 4.5 or more (Figure 4.4.1 and 4.4.3).

Chapter five: Force Predictions for the Cat Soleus

5.1 Inter-subject-A tests

Soleus force predictions for the inter-subject-A tests are shown in Tables 5.a. and 5.b. All training examples were from cat 1 and 2 and the force predictions were made for cat 3. The coefficients of cross-correlation for the tests ranged between 0.93-0.96 (the second and fourth columns of Table 5.a and 5.b). The corresponding RMS errors between the predicted and actual force were 11% of the corresponding maximum peak force of 14.8 N at 0.4 m/s, 12% of the corresponding maximum peak force of 16.7 N at 0.8 m/s, and 10% of the corresponding maximum peak force of 17.3 N at 1.2 m/s (the third and fifth columns of Tables 5.a and 5.b). In each table, the results for the full-wave rectified EMG (the fourth-fifth columns of the Table), and the full-wave rectified and smoothed EMG (the second-third columns of the Table) are given.

Figures 5.1.1 and 5.1.2 show comparisons of the predicted and the actual soleus forces for cat 3 walking at 0.4 m/s (Figures 5.1.1(a) and 5.1.2(a)), 0.8 m/s (Figures 5.1.1(b) and 5.1.2(b)),and 1.2 m/s (Figures 5.1.1(c) and 5.1.2(c)), respectively. The corresponding coefficients of cross-correlation are shown in the second and fourth columns of Table 5.a. The corresponding RMS errors between the predicted and actual forces are shown in the third and fifth column of Table 5.a. Figures 5.1.3 and 5.1.4 show the results listed in Table 5.b. The figures and statistical

Table 5.a: Inter-subject-A (EMG Model[1])

Training Sets[2] (speed)	Force prediction			
	rectified & smoothed EMG		rectified EMG	
	corr.coeff.	RMS error[3]	corr.coeff.	RMS error[3]
0.4 m/s	0.96	1.61 (11%)	0.95	1.79 (12%)
0.8 m/s	0.94	2.21 (13%)	095	2.01 (12%)
1.2 m/s	0.93	1.83 (10%)	0.93	1.81 (10%)

1. The input to the network is the EMG signal.
2. Training data are from cat 1 and 2.
3. The unit of values is Newton, and the percentage of the corresponding maximum peak force alsc is shown in this column.

Table 5.b: Inter-subject-A (EMG^+ Model[1])

Training Sets[2] (speed)	Force prediction			
	rectified & smoothed EMG		rectified EMG	
	corr.coeff.	RMS error[3]	corr.coeff.	RMS error[3]
0.4 m/s	0.95	1.69 (11%)	0.95	1.82 (12%)
0.8 m/s	0.94	2.32 (14%)	0.93	2.25 (13%)
1.2 m/s	0.94	1.75 (10%)	0.93	1.84 (11%)

1. The input to the network are the EMG signal and the knee and ankle angles.
2. Training data are from cat 1 and 2.
3. The unit of values is Newton, and the percentage of the corresponding maximum peak force also is shown in this column.

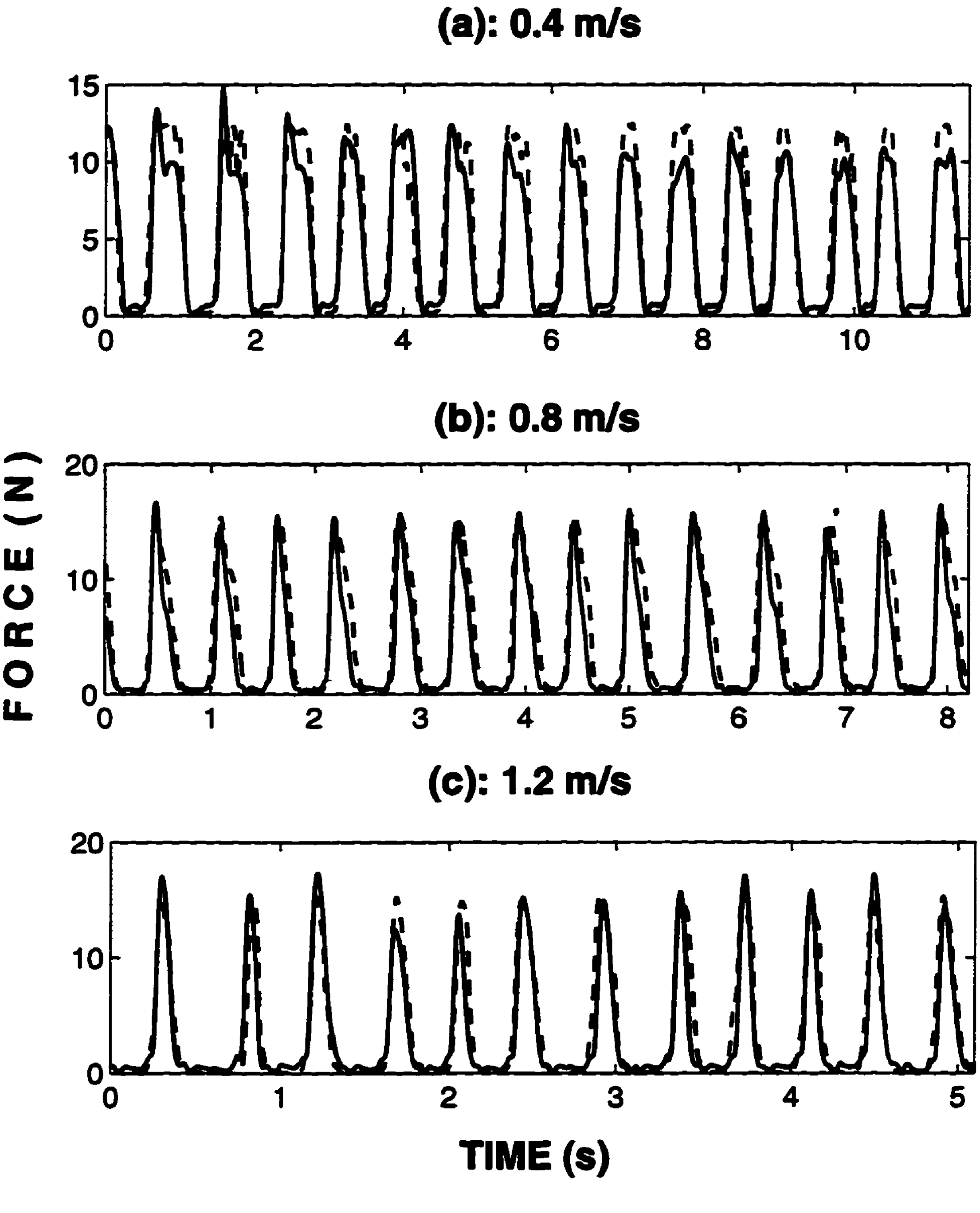

Figure 5.1.1 Inter-subject-A tests: Comparisons of the predicted forces (dashed-lines) with the actual soleus forces (solid-lines) for one cat walking at (a) 0.4 m/s, when the network was trained with the full-wave rectified and smoothed EMG and muscular force data from the remaining two cats walking at 0.4 m/s; (b) the corresponding results for walking at 0.8 m/s; (c) the corresponding results for walking at 1.2 m/s.

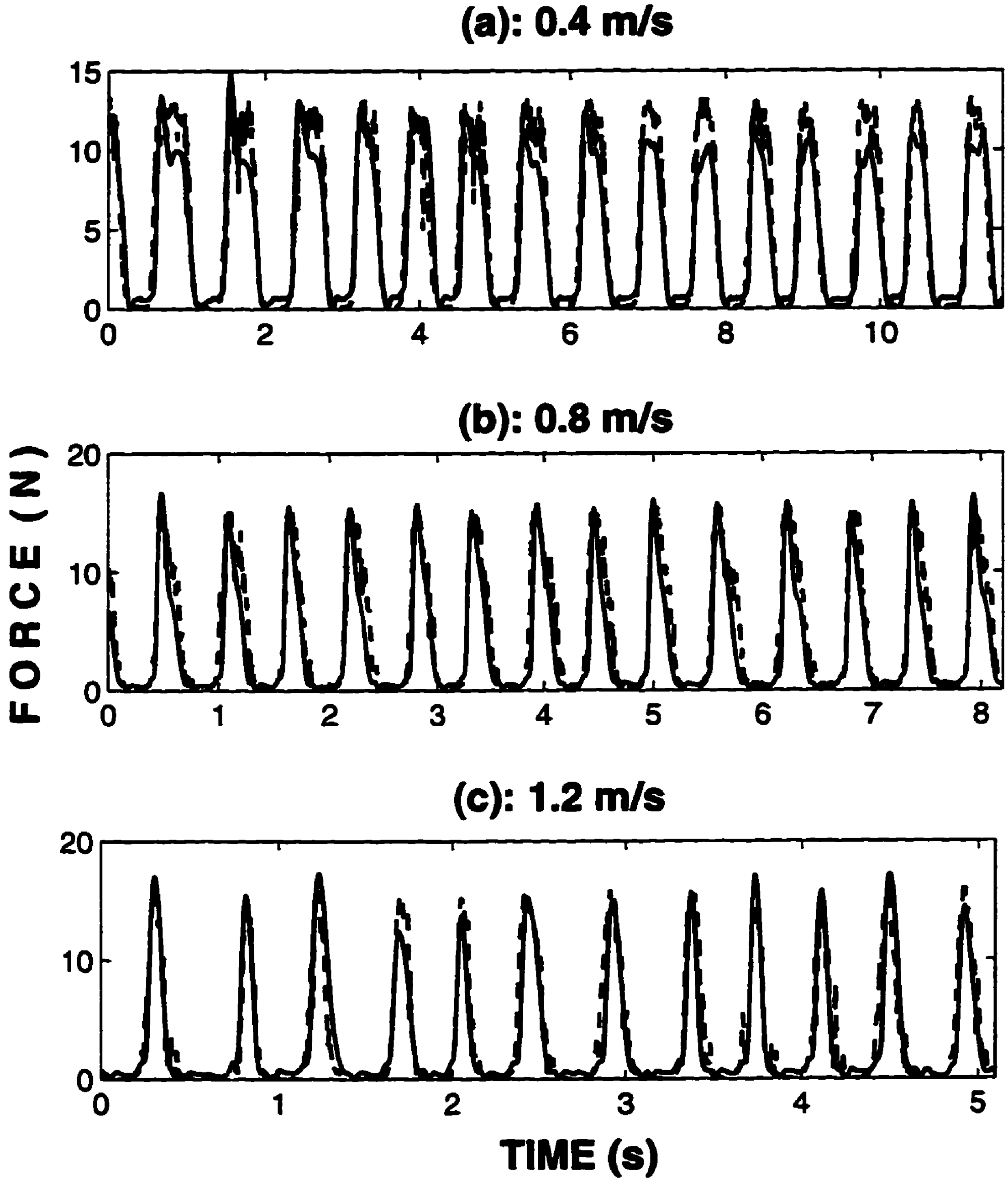

Figure 5.1.2 Inter-subject-A tests: Comparisons of the predicted forces (dashed-lines) with the actual soleus forces (solid-lines) for one cat walking at (a) 0.4 m/s, when the network was trained with the full-wave rectified EMG and muscular force data from the remaining two cats walking at 0.4 m/s; (b) the corresponding results for walking at 0.8 m/s; (c) the corresponding results for walking at 1.2 m/s.

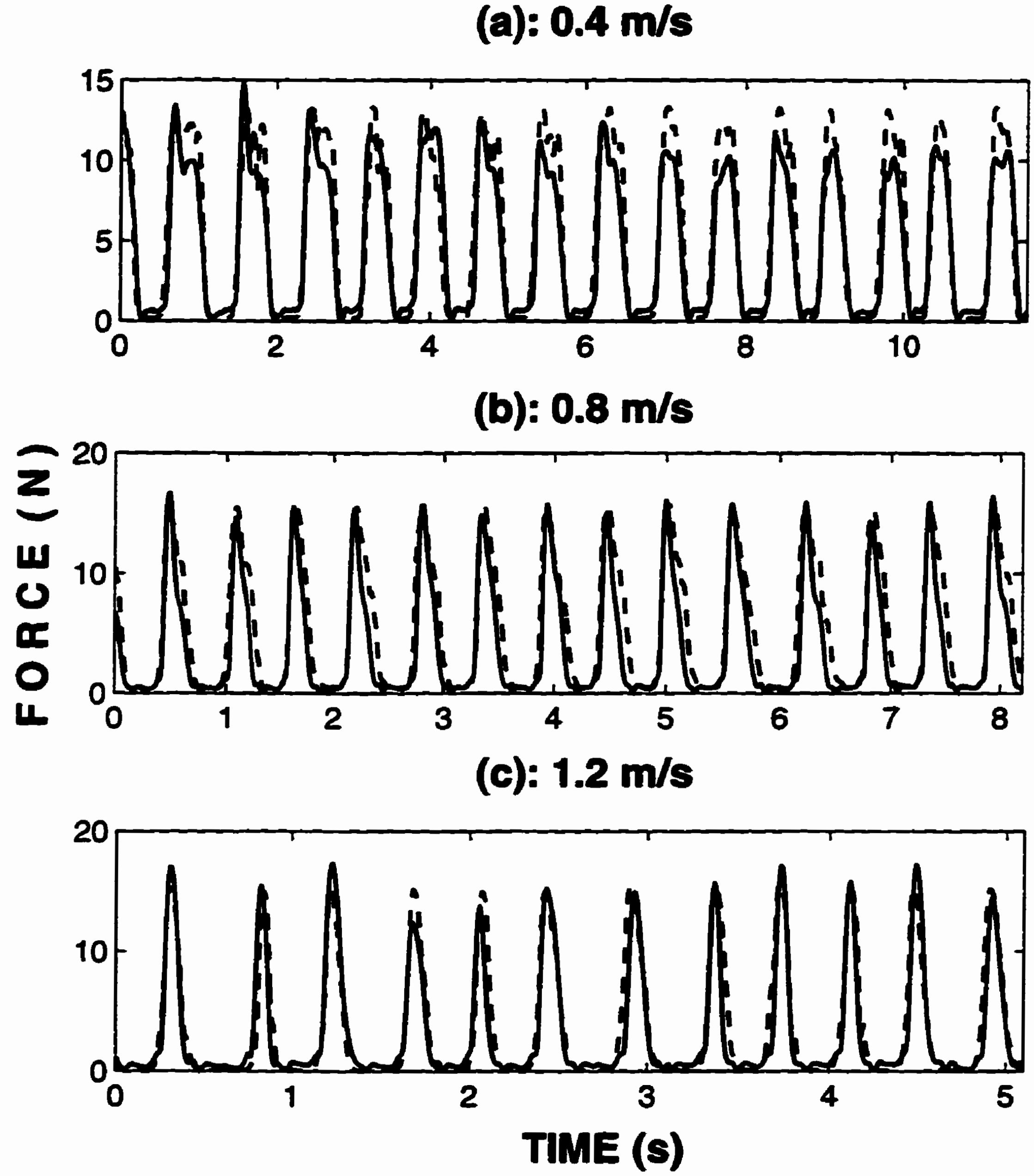

Figure 5.1.3 Inter-subject-A tests: Comparisons of the predicted forces (dashed-lines) with the actual soleus forces (solid-lines) for one cat walking at (a) 0.4 m/s, when the network was trained with the full-wave rectified and smoothed EMG plus the knee and ankle angle-time histories and force data from the remaining two cats walking at 0.4 m/s; (b) the corresponding results for walking at 0.8 m/s; (c) the corresponding results for walking at 1.2 m/s.

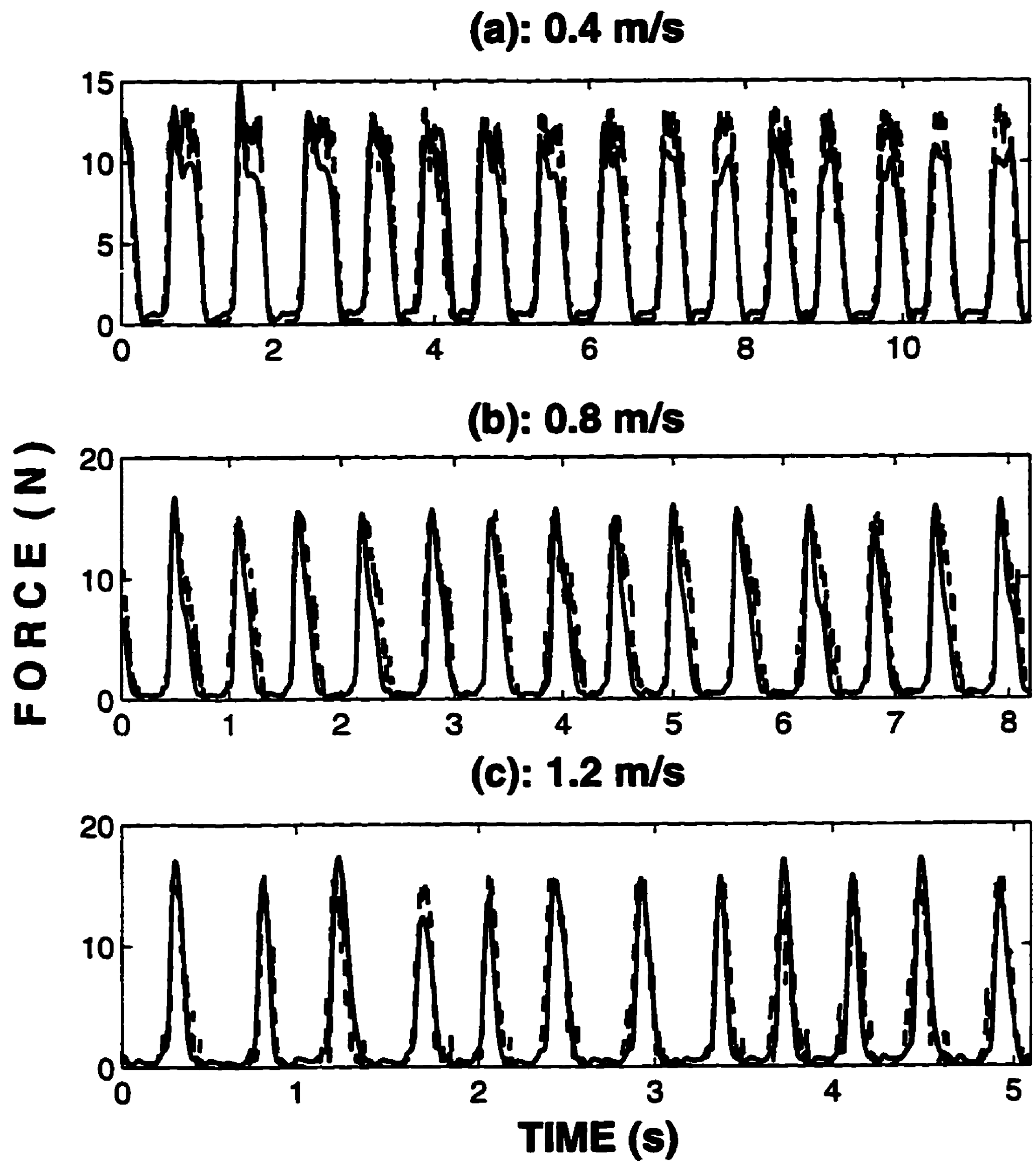

Figure 5.1.4 Inter-subject-A tests: Comparisons of the predicted forces (dashed-lines) with the actual soleus forces (solid-lines) for one cat walking at (a) 0.4 m/s, when the network was trained with the full-wave rectified EMG plus the knee and ankle angle-time histories, and force data from the remaining two cats walking at 0.4 m/s; (b)the corresponding results for walking at 0.8 m/s; (c) the corresponding results for walking at 1.2 m/s.

results showed that the predicted and actual force curves were similar for walking at speeds of 0.8, 1.2 m/s. The peak force amplitudes matched better for walking at 0.8 and 1.2 m/s compared to walking at 0.4 m/s. The differences in the peak magnitude between predicted and actual forces were generally large (>10%) when the peak of the current step was much lower (>10%) than the peak of the previous step or the following step at a speed of 0.4 m/s; and when the peak of the current step was much larger (>10%) than the peak of the previous step at speeds of 0.8, 1.2 m/s. There was a systematic shift to the right of the descending part of the predicted compared to the actual force at a speed of 0.8 m/s (Figures 5.1.1b, 5.1.2b, 5.1.3b, and 5.1.4b). The shifts resulted in increasing RMS errors (12%-14% of the corresponding maximum peak forces) for walking at 0.8 m/s. The predicted force curves shown in Fig. 5.1.2 and 5.1.4 included more noise, especially for walking at 0.4 m/s, compared to the predicted forces in Fig. 5.1.1 and 5.1.3. The results indicated that adding the knee and ankle angle time histories to the input of the ANN did not improve the force predictions in these tests.

5.2 Inter-subject-B tests

Soleus force predictions for the inter-subject-B tests are shown in Tables 6.a, and 6.b. The coefficients of cross-correlation ranged between 0.91-0.94 (the second and fourth columns of Table 6.a and 6.b). The corresponding RMS errors between the predicted and actual forces ranged from 1.65 N to 2.17N (the third and fifth columns of the Table 6.a and 6.b). The training data were taken from cat 1 and 2 and the muscle predictions were made for cat 3 for walking at speeds of 0.4, 0.8, 1.2 m/s respectively. For the predictions shown in Table 6.a, only EMG signal was used as input (EMG Model); for the predictions shown in Table 6.b, EMG plus knee and ankle angle time histories were used as input (EMG^+ Model). Results are shown for the full-wave rectified and the full-wave rectified and smoothed EMG. Adding the kinematics to the input of the ANN (Table 6.b) did not improve the correlation coefficients and RMS errors between the predicted and actual forces in these tests (Table 6.a).

Figures 5.2.1 and 5.2.2 show the comparison between the predicted (dashed lines) and the actual (solid lines) forces for walking at 0.4 m/s (Fig. 5.2.1(a) and 5.2.2(a)), 0.8 m/s (Fig. 5.2.1(b) and 5.2.2(b)), and 1.2 m/s (Figure 5.2.1(c) and 5.2.2(c)), respectively, when the network was trained with all available data from cats 1 and 2. Input for these tests was the full-wave rectified and smoothed EMG signal (Figure 5.2.1), or the full-wave rectified, unsmoothed EMG signal (Fig. 5.2.2). The coefficients of cross-correlation and RMS errors are listed in Table 6.a. Figures 5.2.3 and 5.2.4 show the results listed in Table 2.b. The predictions of the peak magnitudes were generally better for walking at 0.8 m/s and 1.2 m/s than for walking at 0.4 m/s. Typically, the peak magnitudes were overestimated at speeds of walking of 0.4 m/s, and underestimated at 0.8 m/s. Comparing the results shown in Figure 5.2 with those shown in

Figure 5.1, soleus force predictions for the inter-subject-A tests were slightly better than the corresponding predictions for the inter-subject-B tests. Therefore, increasing the number of training examples with non-specific walking trials decreased the predictive ability of the ANN.

Table 6.a: Inter-subject-B (EMG Model[1])

Training Sets (speed)	speed (m/s)	Force Prediction			
		rectified & smoothed EMG		rectified EMG	
		corr.coeff	RMS error[2]	corr.coeff	RMS error[2]
All available data from cat1 and 2	0.4	0.92	1.91 (13%)	0.91	2.17 (15%)
	0.8	0.94	1.82 (11%)	0.93	2.01 (12%)
	1.2	0.92	2.08 (12%)	0.93	1.73 (10%)

1. The input to the network is the EMG signal.
2. The unit of values is Newton, and the percentage of the corresponding maximum peak force also is shown in this column.

Table 6.b: Inter-subject-B (EMG^+ Model[1])

Training Sets	speed (m/s)	Force Prediction			
		rectified & smoothed EMG		rectified EMG.	
		corr.coeff	RMS error[2]	corr.coeff	RMS error[2]
All available data from cat 1, cat 2	0.4	0.91	2.04 (14%)	0.91	2.14 (14%)
	0.8	0.94	1.67 (10%)	0.93	2.01 (12%)
	1.2	0.92	1.94 (11%)	0.94	1.65 (10%)

1. The input to the network are the EMG signal and the knee and ankle angles.
2. The unit of values is Newton, and the percentage of the corresponding maximum peak force also is shown in this column.

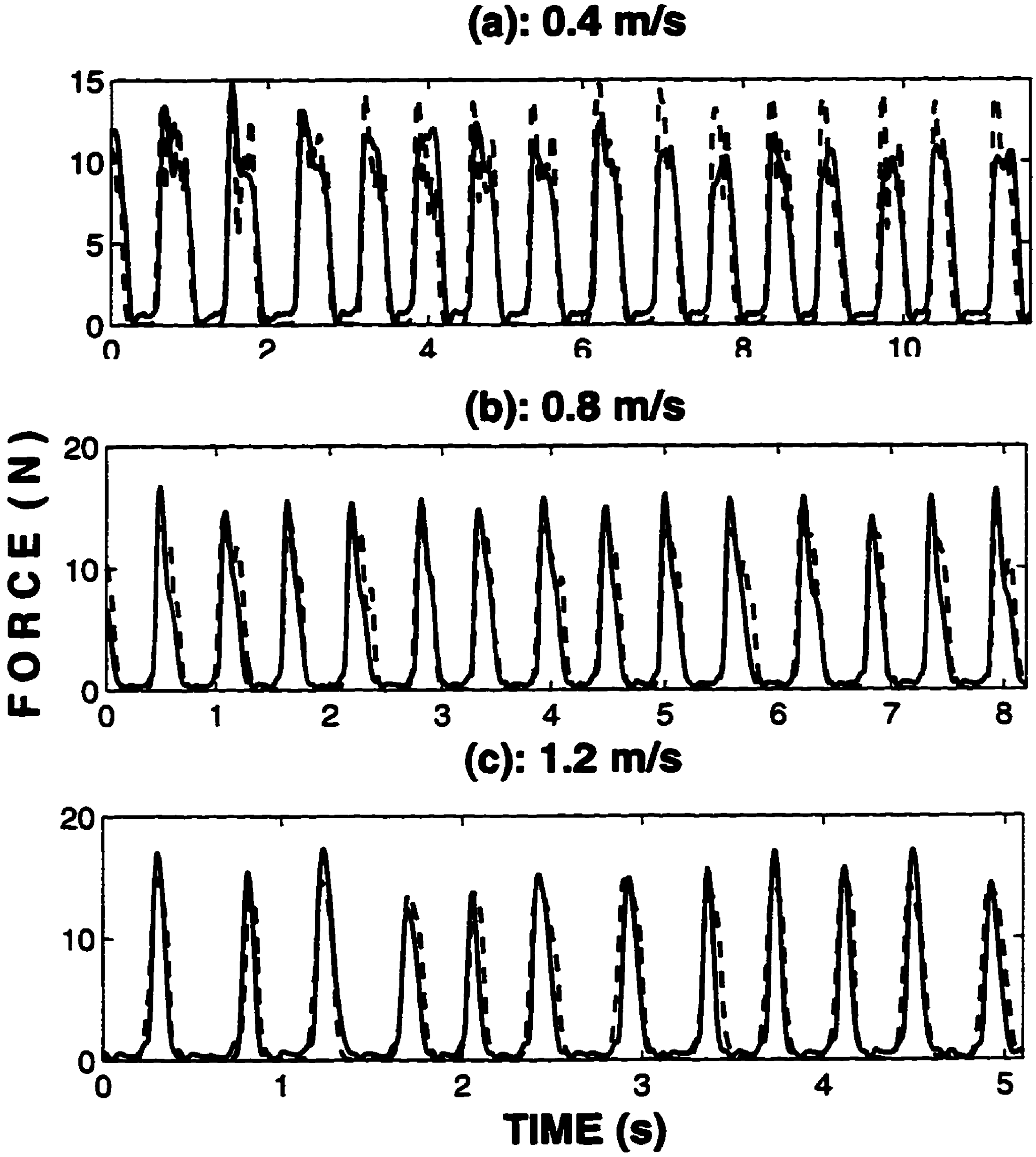

Figure 5.2.1 Inter-subject-B tests: Comparisons of the predicted forces (dashed-lines) with the actual soleus forces (solid-lines) for one cat walking at (a) 0.4 m/s; (b) 0.8 m/s;(c)1.2 m/s, when the network was trained with all available full-wave rectified and smoothed EMG and muscular force data from cat 1 and 2.

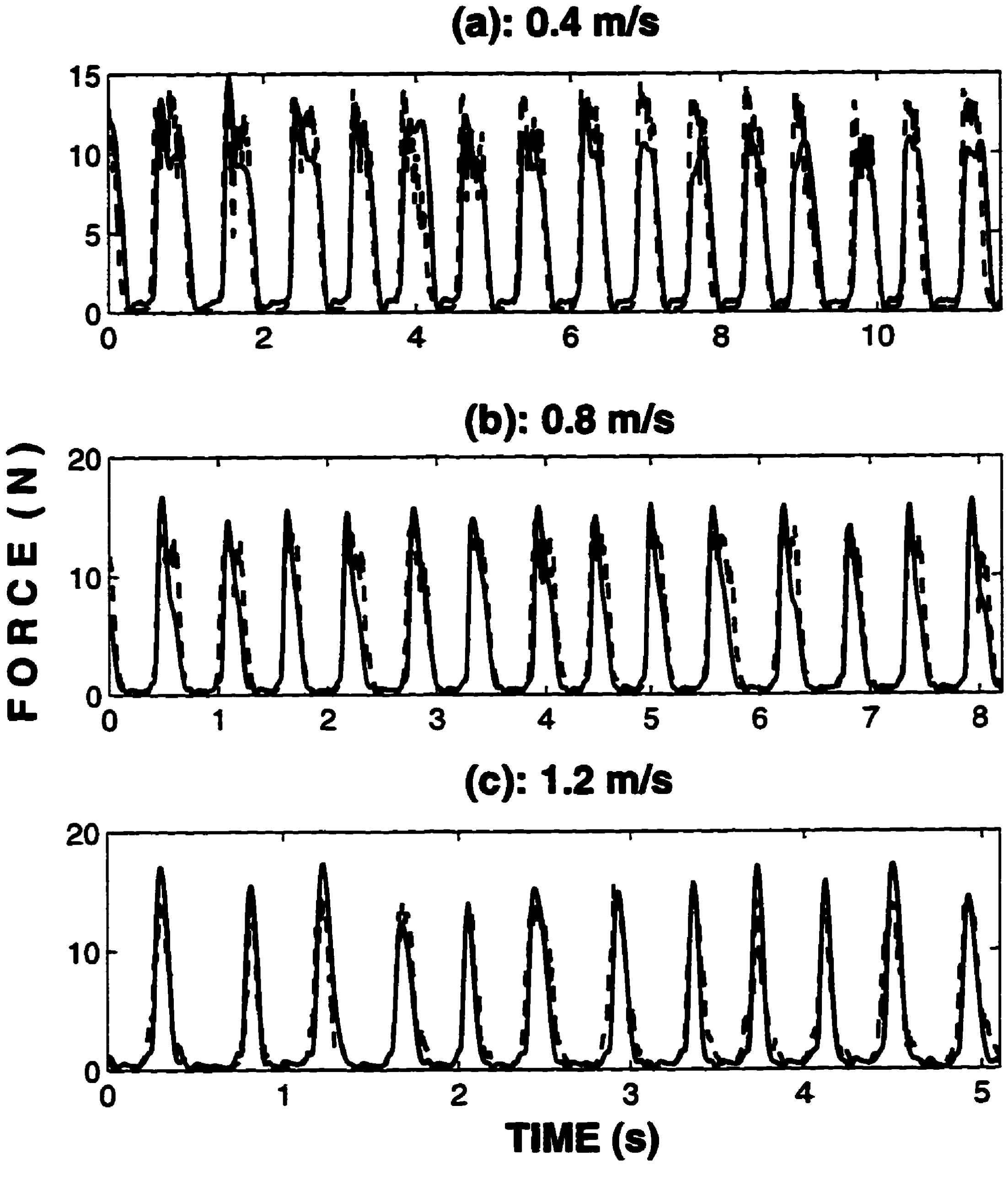

Figure 5.2.2 Inter-subject-B tests: Comparisons of the predicted forces (dashed-lines) with the actual soleus forces (solid-lines) for one cat walking at (a) 0.4 m/s; (b) 0.8 m/s;(c)1.2 m/s, when the network was trained with all available full-wave rectified EMG and muscular force data from cat 1 and 2.

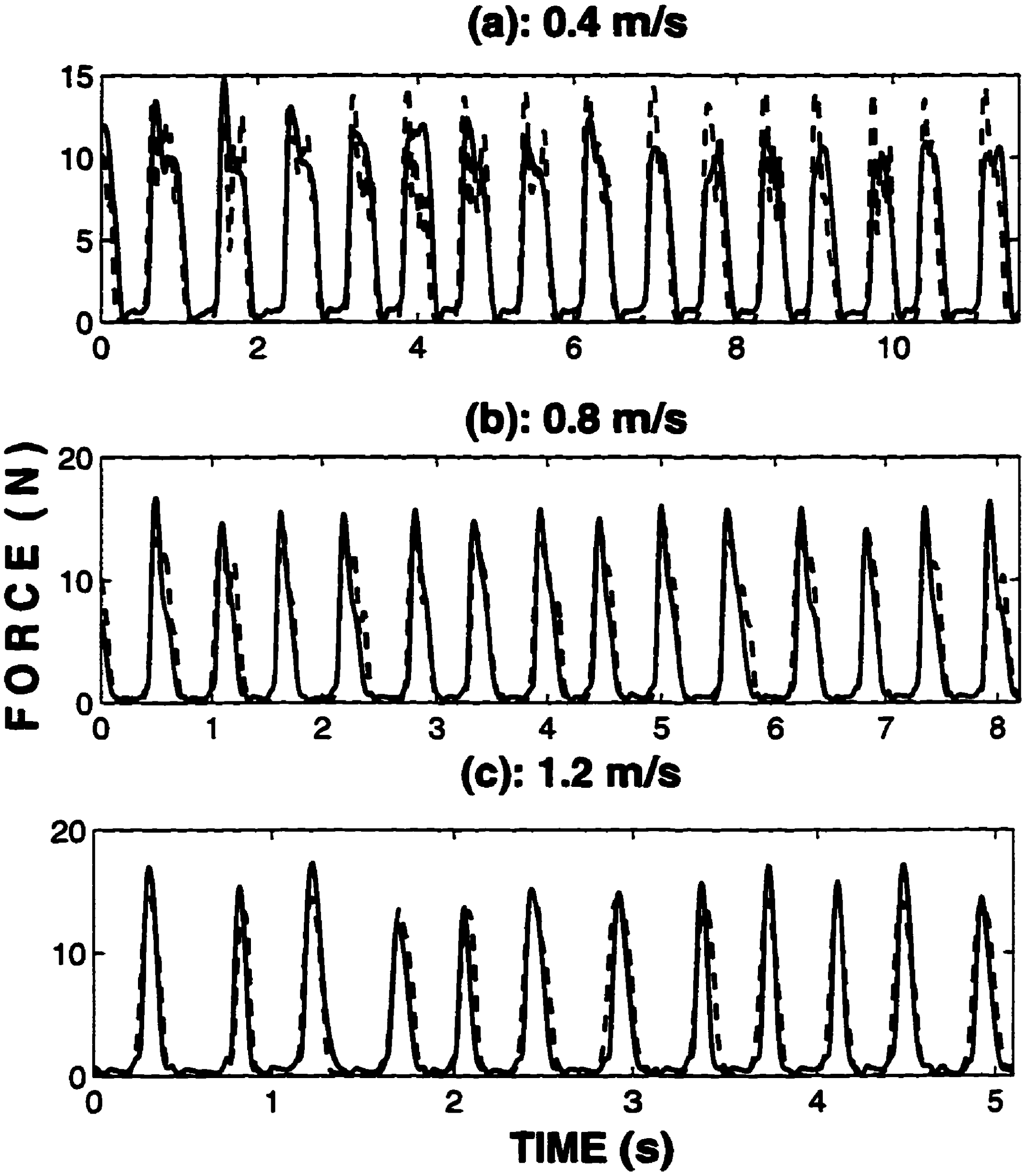

Figure 5.2.3 Inter-subject-B tests: Comparisons of the predicted forces (dashed-lines) with the actual soleus forces (solid-lines) for one cat walking at (a) 0.4 m/s; (b) 0.8 m/s;(c)1.2 m/s, when the network was trained with all available full-wave rectified and smoothed EMG plus the knee and ankle angle-time histories, and force data from cat 1 and 2.

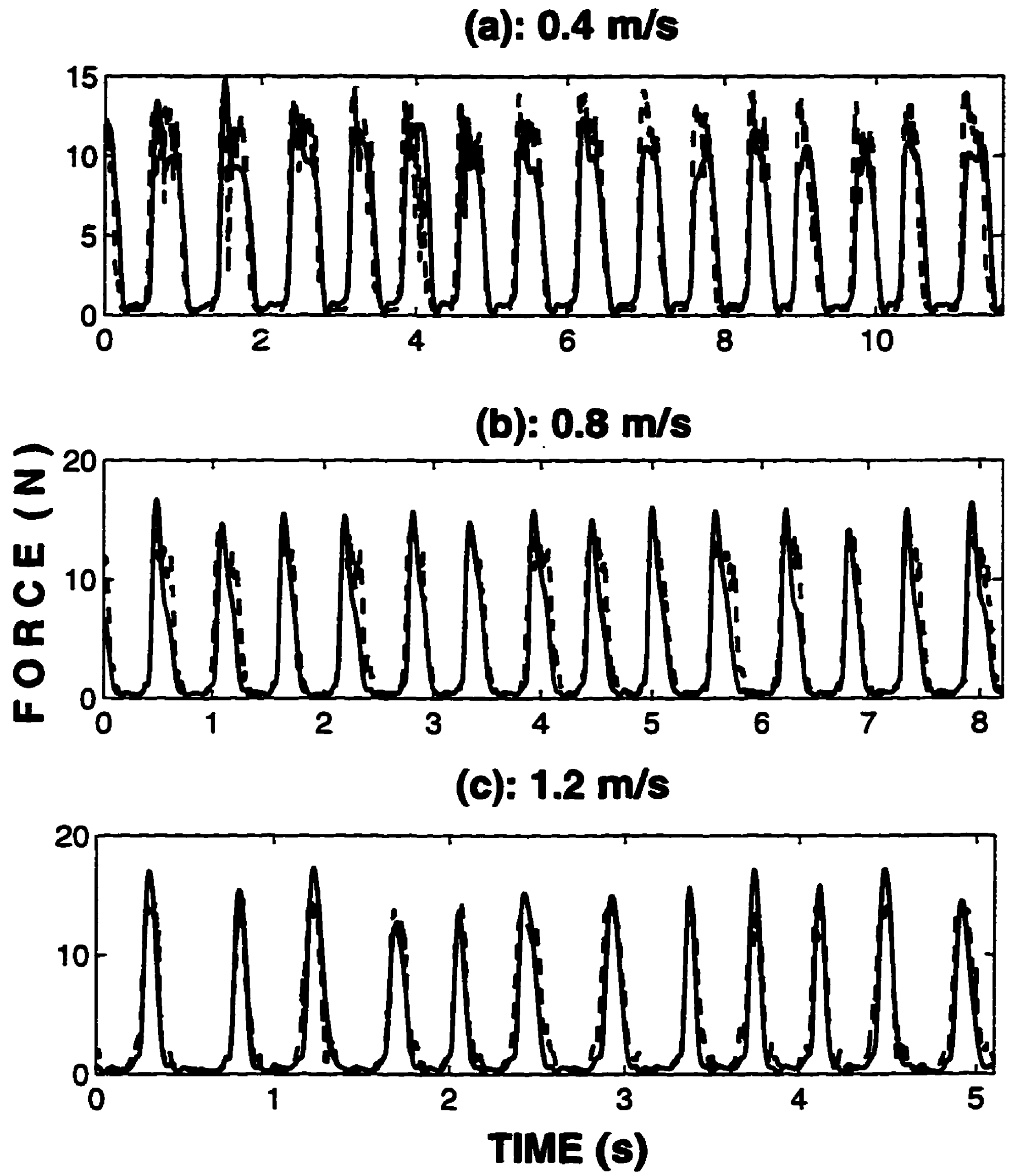

Figure 5.2.4 Inter-subject-B tests: Comparisons of the predicted forces (dashed-lines) with the actual soleus forces (solid-lines) for one cat walking at (a) 0.4 m/s; (b) 0.8 m/s;(c)1.2 m/s, when the network was trained with all available full-wave rectified EMG plus the knee and ankle angle time histories, and force data from cat 1 and 2.

5.3 Intra-subject tests

Table 7.a: Intra-subject (EMG Model[1])

Training Sets[2] (speed)	speed (m/s)	rectified & smoothed EMG		rectified EMG	
		corr.coeff.	RMS error[3]	corr.coeff.	RMS error[3]
0.8, 1.2, 1.8 m/s	0.4	0.75	3.52 (24%)	0.79	3.12 (21%)
0.4, 1.2, 1.8 m/s	0.8	0.87	2.53 (15%)	0.89	2.21 (13%)
0.4, 0.8, 1.8 m/s	1.2	0.91	1.98 (11%)	0.92	2.05 (12%)
0.4, 0.8, 1.2 m/s	1.8	0.84	2.63 (15%)	0.87	2.24 (13%)

(Force prediction spans the speed and EMG columns.)

1. The input to the network is the EMG signal.
2. Training data are from cat 3.
3. The unit of values is Newton, and the percentage of the corresponding maximum peak force also is shown in this column.

Table 7.b: Intra-subject (EMG$^+$ Model[1])

Training Sets[2] (speed)	speed (m/s)	rectified & smoothed EMG		rectified EMG	
		corr.coeff.	RMS error[3]	corr.coeff.	RMS error[3]
0.8, 1.2, 1.8 m/s	0.4	0.66	4.08 (27%)	0.75	3.41 (23%)
0.4, 1.2, 1.8 m/s	0.8	0.94	1.68 (10%)	0.93	1.88 (11%)
0.4, 0.8, 1.8 m/s	1.2	0.93	1.94 (11%)	0.93	1.70 (10%)
0.4, 0.8, 1.2 m/s	1.8	0.85	2.57 (15%)	0.88	2.26 (13%)

1. The inputs to the network are the EMG signal and the knee and ankle angles
2. Training data are from cat 3.
3. The unit of values is Newton, and the percentage of the corresponding maximum peak force also is shown in this column.

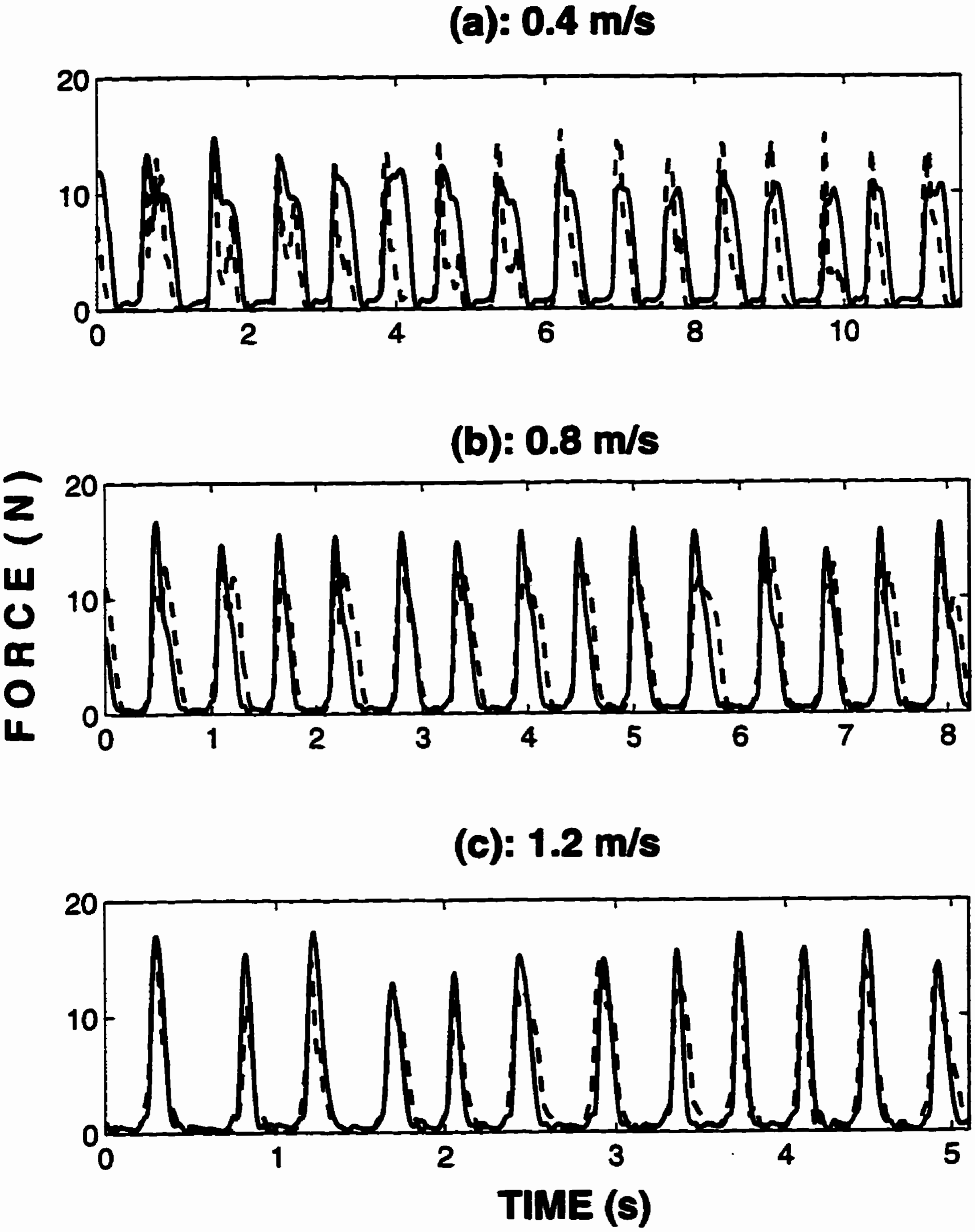
(a): 0.4 m/s
20
10
0
0
2
4
6
8
10
(b): 0.8 m/s
FORCE (N)
20
10
0
0
1
2
3
4
5
6
7
8
(c): 1.2 m/s
20
10
0
0
1
2
3
4
5
TIME (s)

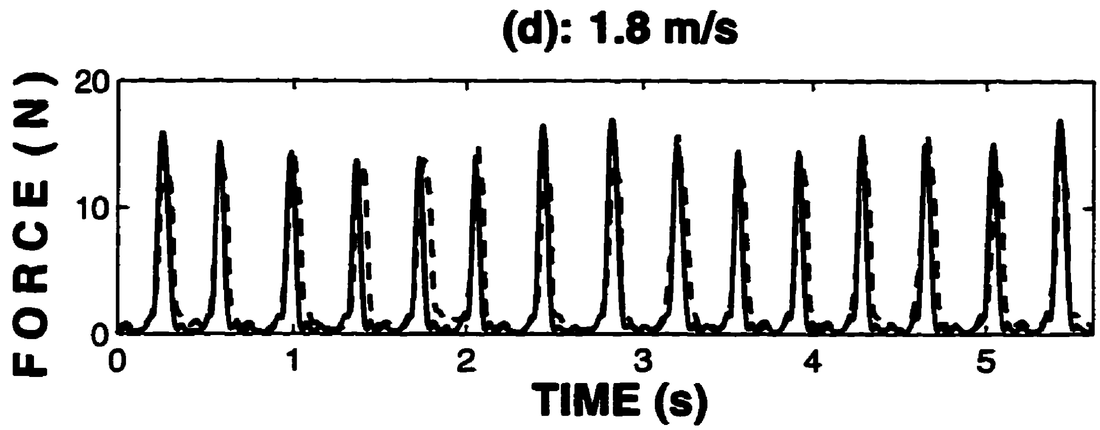

Figure 5.3.1 Intra-subject tests: Comparisons of the predicted forces (dashed-lines) with the actual soleus forces (solid-lines) for a representative cat walking at (a) 0.4 m/s,when the network was trained with the full-wave rectified and smoothed EMG and force data from the same cat while walking/trotting at speeds of 0.8, 1.2, 1.8 m/s; (b) 0.8 m/s, when the network was trained with the full-wave rectified and smoothed EMG and force data from the same cat while walking/trotting at speeds of 0.4, 1.2, 1.8 m/s; (c) 1.2 m/s, when the network was trained with the full-wave rectified and smoothed EMG and force data from the same cat while walking/trotting at speeds of 0.4, 0.8, 1.8 m/s; (d) 1.8 m/s, when the network was trained with the full-wave rectified and smoothed EMG and force data from the same cat while walking at speeds of 0.4, 0.8, 1.2 m/s.

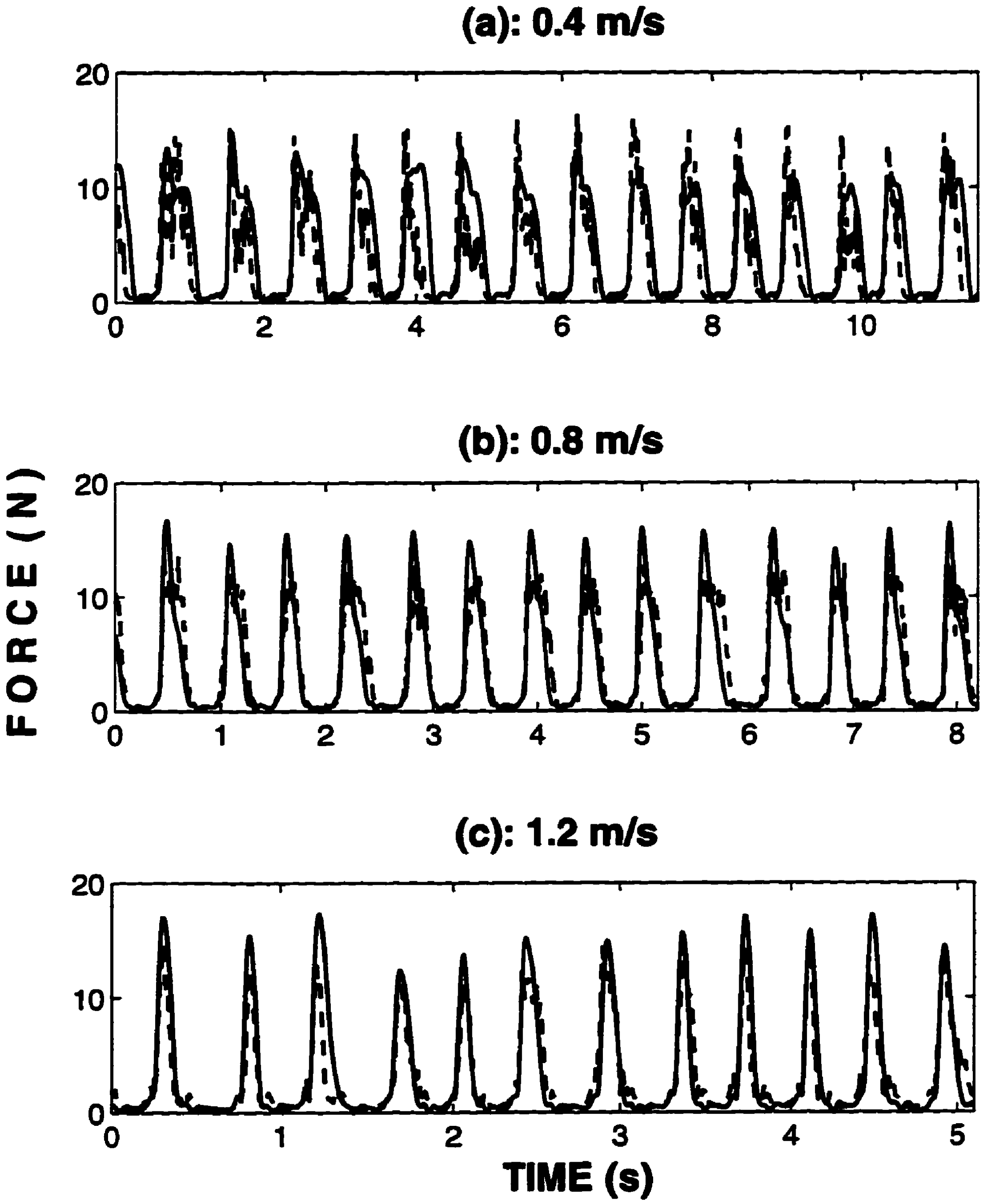
(a): 0.4 m/s
(b): 0.8 m/s
(c): 1.2 m/s
FORCE (N)
TIME (s)
0
10
20
0
2
4
6
8
10
0
1
2
3
4
5
6
7
8
0
1
2
3
4
5

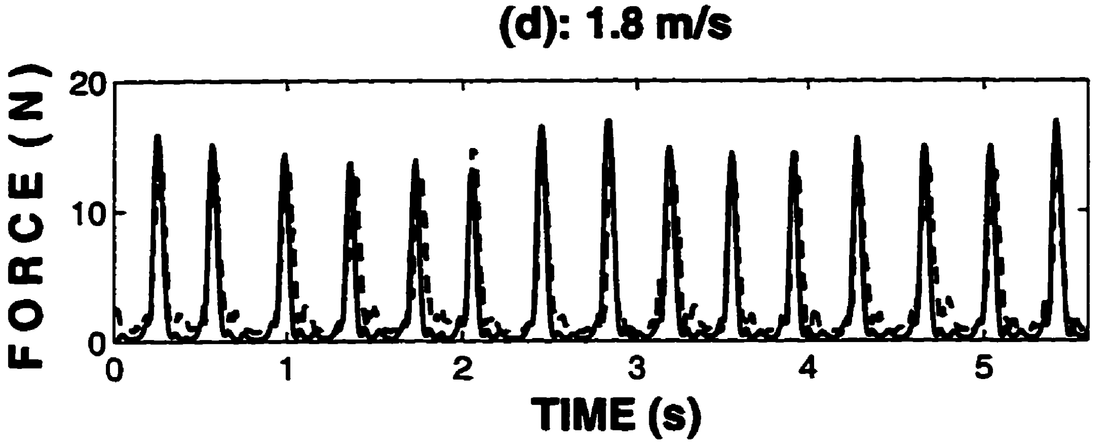

Figure 5.3.2 Intra-subject tests: Comparisons of the predicted forces (dashed-lines) with the actual soleus forces (solid-lines) for a representative cat walking at (a) 0.4 m/s,when the network was trained with the full-wave rectified EMG and force data from the same cat while walking /trotting at speeds of 0.8, 1.2, 1.8 m/s; (b) 0.8 m/s, when the network was trained with the full-wave rectified EMG and force data from the same cat while walking/trotting at speeds of 0.4,1.2,1.8 m/s;(c) 1.2 m/s, when the network was trained with the full-wave rectified EMG and force data from the same cat while walking/trotting at speeds of 0.4,0.8, 1.8 m/s; (d) 1.8 m/s, when the network was trained with the full-wave rectified EMG and force data from the same cat while walking/trotting at speeds of 0.4,0.8,1.2 m/s.

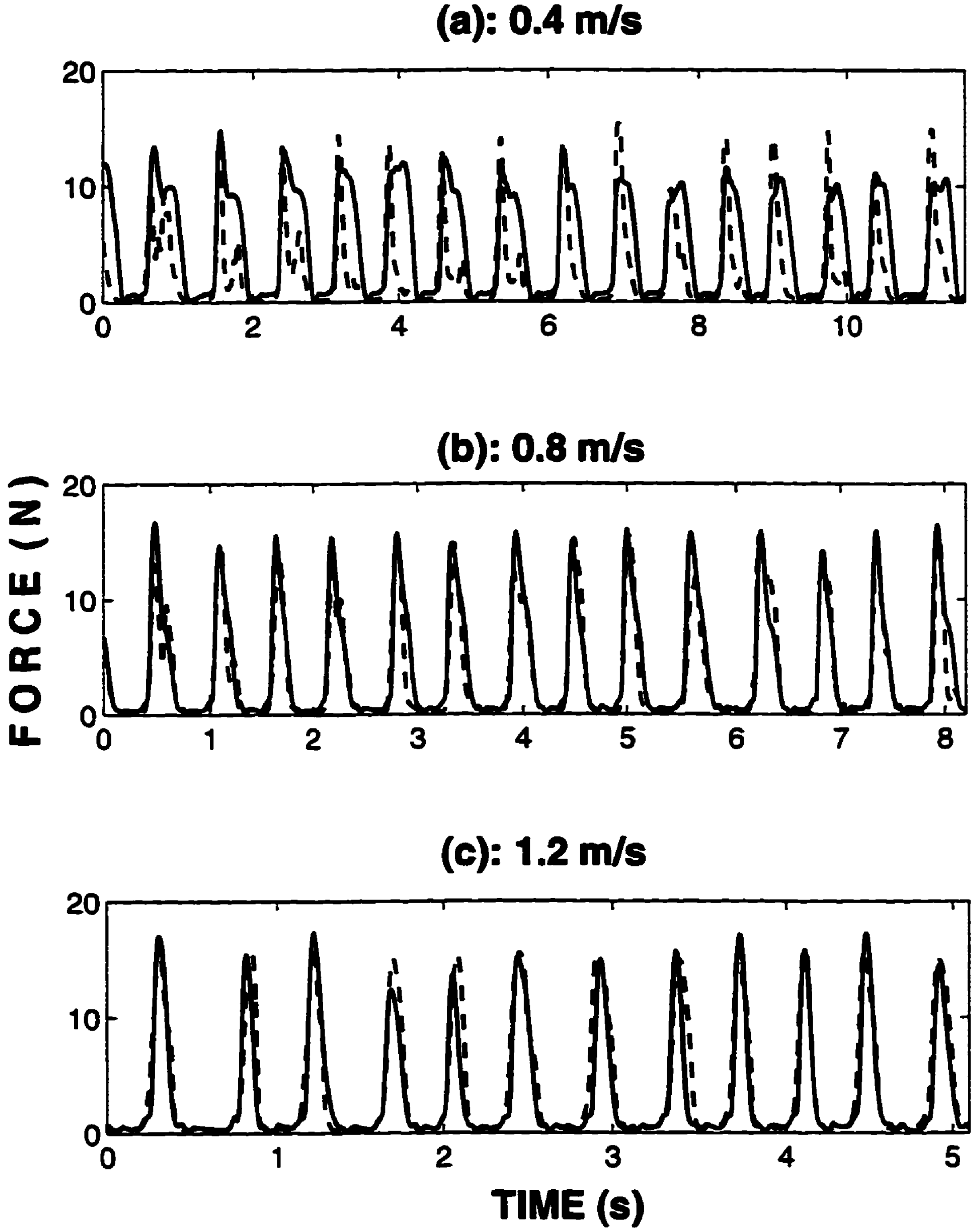
(a): 0.4 m/s
20
10
0
0
2
4
6
8
10
(b): 0.8 m/s
FORCE (N)
20
10
0
0
1
2
3
4
5
6
7
8
(c): 1.2 m/s
20
10
0
0
1
2
3
4
5
TIME (s)

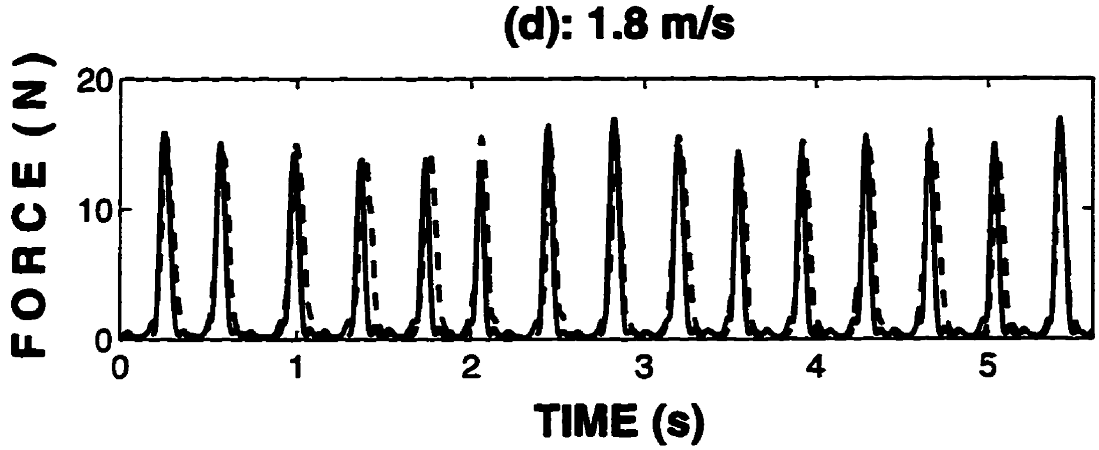

Figure 5.3.3 Intra-subject tests: Comparisons of the predicted forces (dashed-lines) with the actual soleus forces (solid-lines) for a representative cat walking at (a) 0.4 m/s, when the network was trained with the full-wave rectified and smoothed EMG plus the knee and ankle angle-time histories,and force data from the same cat while walking /trotting at speeds of 0.8,1.2,1.8 m/s; (b) 0.8 m/s, when the network was trained with the full-wave rectified and smoothed EMG plus the knee and ankle angle-time histories, and force data from the same cat while walking/trotting at speeds of 0.4, 1.2,1.8 m/s; (c) 1.2 m/s, when the network was trained with the full-wave rectified and smoothed EMG plus the knee and ankle angle-time histories, and force data from the same cat while walking /trotting at speeds of 0.4, 0.8, 1.8 m/s; (d) 1.8 m/s,when the network was trained with the full-wave rectified and smoothed EMG plus the knee and ankle angle-time histories, and force data from the same cat while walking/trotting at speeds of 0.4,0.8,1.2 m/s.

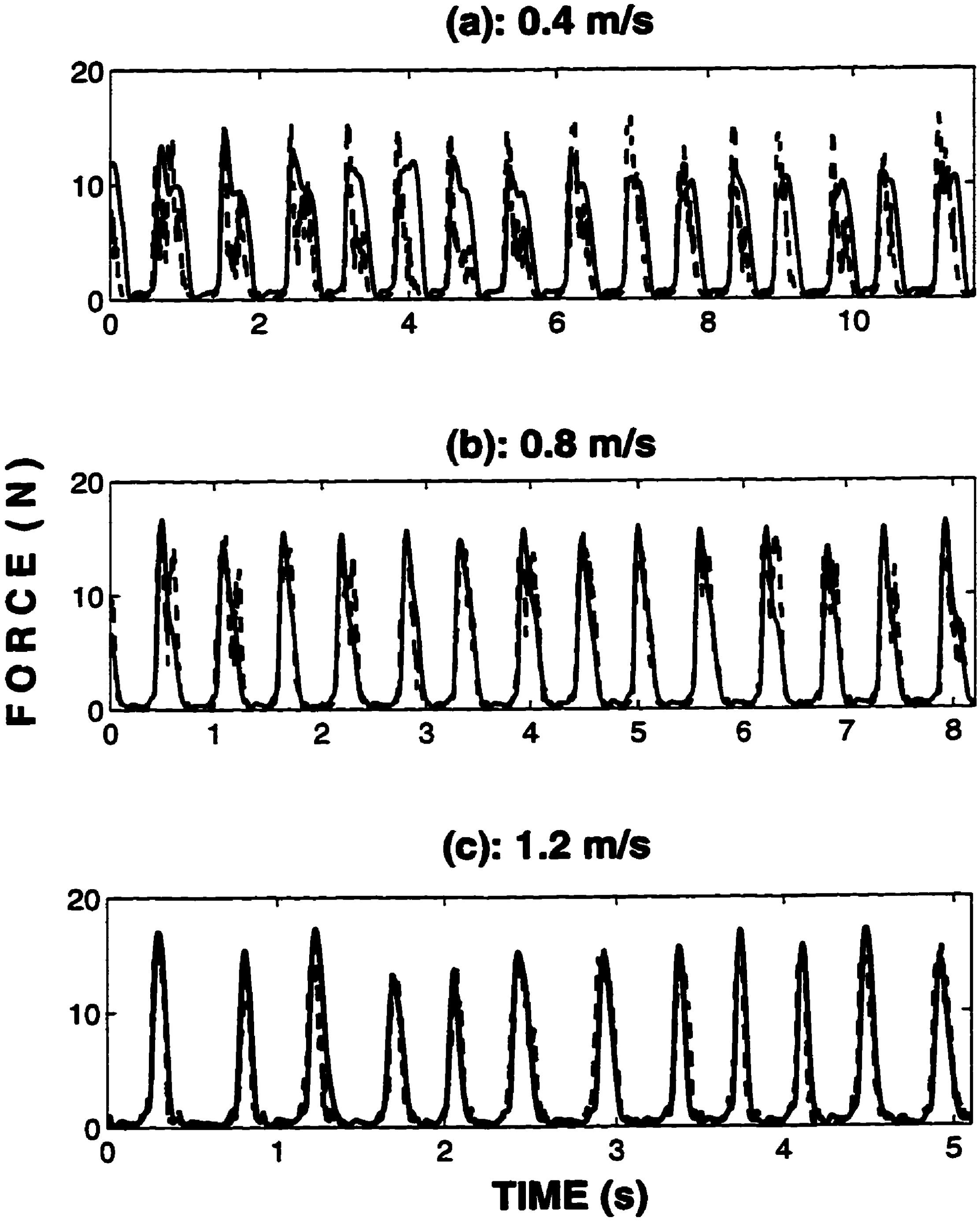
(a): 0.4 m/s
(b): 0.8 m/s
(c): 1.2 m/s
FORCE (N)
TIME (s)
0
10
20
0
2
4
6
8
10
0
1
2
3
4
5
6
7
8
0
1
2
3
4
5

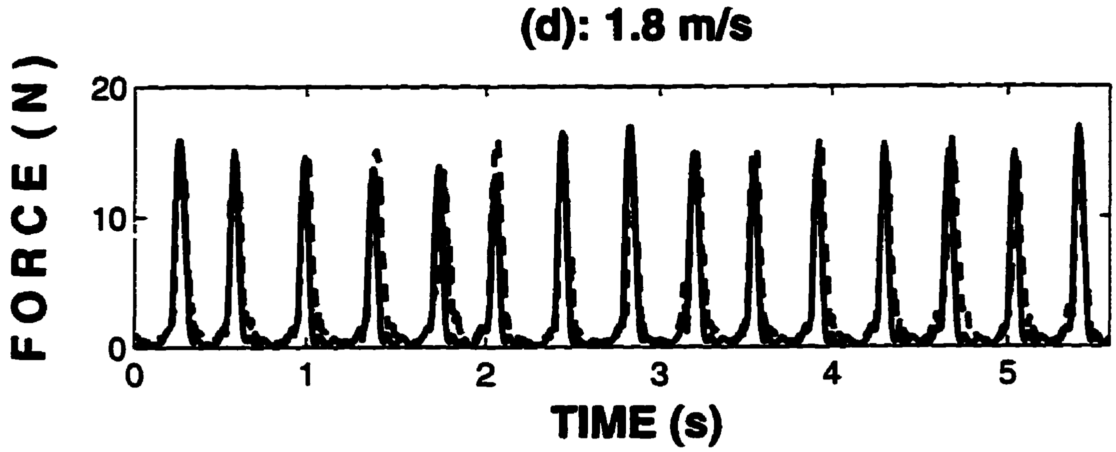

Figure 5.3.4 Intra-subject tests: Comparisons of the predicted forces (dashed-lines) with the actual soleus forces (solid-lines) for a representative cat walking at (a) 0.4 m/s, when the network was trained with the full-wave rectified EMG plus the knee and ankl e angle-time histories, and force data from the same cat while walking /trotting at speeds of 0.8,1.2, 1.8 m/s; (b) 0.8 m/s, when the network was trained with the full-wave rectified EMG plus the knee and ankle angle-time histories, and force data from the same cat while walking /trotting at speeds of 0.4, 1.2, 1.8 m/s; (c) 1.2 m/s, when the network was trained with the full-wave rectified EMG plus the knee and ankle angle-time histories, and force data from the same cat while walking /trotting at speeds of 0.4, 0.8, 1.8 m/s; (d) 1.8 m/s,when the network was trained with the full-wave rectified EMG plus the knee and ankle angle-time histories, and force data from the same cat while walking /trotting at speeds of 0.4, 0.8, 1.2 m/s.

Soleus force predictions for the intra-subject tests are shown in Tables 7.a, and 7.b.

Figures 5.3.1 and 5.3.2 show the predicted soleus forces for one representative cat walking/trotting at a given speed while the network was trained with the full-wave rectified and smoothed EMG or the full-wave rectified and unsmoothed EMG and force data from the same cat walking/trotting at the three other speeds. The coefficients of cross-correlation for the experiments shown in Figures 5.3.1 and 5.3.2 are listed in the third and fifth columns of Table 7.a, respectively; the corresponding RMS errors are listed in the fourth and sixth columns of Table 7.a. The cross-correlation coefficients and RMS errors for the experiments shown in Figures 5.3.3 and 5.3.4 are listed in Table 7.b. The time histories of the predicted forces deviated systematically from those of the actual forces at a speed of 0.4 m/s in all intra-subject prediction tests. At speeds of 0.8 and 1.2 m/s, the predicted forces underestimated the actual forces when the input for the ANN was the EMG signal only (Figure 5.3.1 and 5.3.2). Adding the kinematics to the input for the ANN improved significantly the cross-correlation coefficients and produced an improved match of the peak amplitudes between predicted and actual forces at speeds of 0.8 and 1.2 m/s. The corresponding prediction results (Figures 5.3.3 and 5.3.4) at 0.8 and 1.2 m/s were almost as good as those in the inter-subject-A prediction tests. For example, when adding the kinematic information to the training input of the ANN, the coefficients of cross-correlation were improved (from 0.87 (Figure 5.1.1b) to 0.94 (Figure 5.1.3b) at 0.8 m/s; from 0.91 (Figure 5.1.1c) to 0.93 (Figure 5.1.3c) at 1.2 m/s) (the third column of Table 3b) and the RMS errors decreased (from 2.5 N to 1.7 N at 0.8 m/s, and from 2.0 N to 1.9 N at 1.2 m/s) (the fourth column of Table 3b). Differences between the predicted and actual peak forces were larger at a walking speed of 0.4 than at 0.8 or 1.2 m/s. Also, there was a systematic shift of the time histories to the right on the descending part of the predicted compared to the actual force time histories at 1.8 m/s (Figure 5.3.3(d),and 5.3.4(d)), and a systematic shift to the left for the corresponding comparison at 0.4 m/s (Figure 5.3.3(a),and 5.3.4(a)). This shift resulted in low (<=0.88) coefficients of cross-correlation and slightly large RMS errors (>= 13% of the corresponding maximum peak forces) for walking at 1.8 m/s (Figure 5.3.1(d), 5.3.2(d), 5.3.3(d),and 5.3.4(d)).

5.4 Intra-session tests

Force predictions for the intra-session tests are shown in Table 8.a, and 8.b.

Soleus force predictions for the intra-session tests were excellent (Table 8.a, and 8.b) when the EMG signal was full-wave rectified and smoothed. The coefficients of cross-correlation for the tests ranged from 0.96-0.98 (the third column of Table 8.a and 8.b), and the corresponding RMS errors were small (<= 8% of the corresponding maximum peak forces), when trained with information from 1.5 steps or more. Figures 5.4.1(a)-(i) and 5.4.2(a)-(i) show the comparisons of the predicted and the actual forces for the last five steps of a representative cat in one session when the network was trained using the full-wave rectified and smoothed EMG, or the full-wave rectified EMG alone, and force data from an increasing number of steps (1.5, 2.5, 3.5, 4.5, 5.5, 6.5, 7.5, 8.5, and 9.5 steps) of that session, respectively. The corresponding coefficients of cross-correlation for the tests are shown in the third and fifth columns of Table 8.a.

Table 8.a: Intra-session (EMG Model[1])

Training Sets[2] (steps)	Force prediction				
	steps	rectified & smoothed EMG		rectified EMG	
		corr.coeff.	RMS error[3]	corr.coeff.	RMS error[3]
0-1.5	10-14	0.97	1.32 (8%)	0.92	1.98 (12%)
0-2.5	10-14	0.97	1.29 (8%)	0.92	1.99 (12%)
0-3.5	10-14	0.97	1.15 (7%)	0.93	1.78 (11%)
0-4.5	10-14	0.97	1.14 (7%)	0.94	1.67 (10%)
0-5.5	10-14	0.97	1.08 (6%)	0.95	1.52 (9%)
0-6.5	10-14	0.98	1.02 (6%)	0.96	1.37 (8%)
0-7.5	10-14	0.98	1.03 (6%)	0.95	1.51 (9%)
0-8.5	10-14	0.98	1.04 (6%)	0.96	1.37 (8%)
0-9.5	10-14	0.98	1.00 (6%)	0.96	1.37 (8%)

1. The input to the network is the EMG signal.
2. Training data are from an increasing number of step cycles of a representative cat walking at 0.8 m/s.
3. The unit of values is Newton, and the percentage of the corresponding maximum peak force also is shown in this column.

Table 8.b: Intra-session (EMG$^+$ Model[1])

Training Sets[2] (steps)	Force prediction				
	steps	rectified & smoothed EMG		rectified EMG	
		corr.coeff.	RMS error[3]	corr.coeff.	RMS error[3]
0-1.5	10-14	0.96	1.57 (9%)	0.91	2.42 (15%)
0-2.5	10-14	0.96	1.55 (9%)	0.92	2.05 (12%)
0-3.5	10-14	0.97	1.32 (8%)	0.93	1.81 (11%)
0-4.5	10-14	0.97	1.15 (7%)	0.94	1.74 (11%)
0-5.5	10-14	0.97	1.28 (8%)	0.94	1.74 (11%)
0-6.5	10-14	0.97	1.20 (8%)	0.94	1.69 (10%)
0-7.5	10-14	0.97	1.16 (7%)	0.94	1.82 (11%)
0-8.5	10-14	0.97	1.08 (6%)	0.95	1.59 (9%)
0-9.5	10-14	0.97	1.08 (6%)	0.95	1.54 (9%)

1. The inputs to the network are the EMG signal and the knee and ankle angles.
2. Training data are from an increasing number of step cycles of a representative cat walking at 0.8 m/s.
3. The unit of values is Newton, and the percentage of the corresponding maximum peak force also is shown in this column.

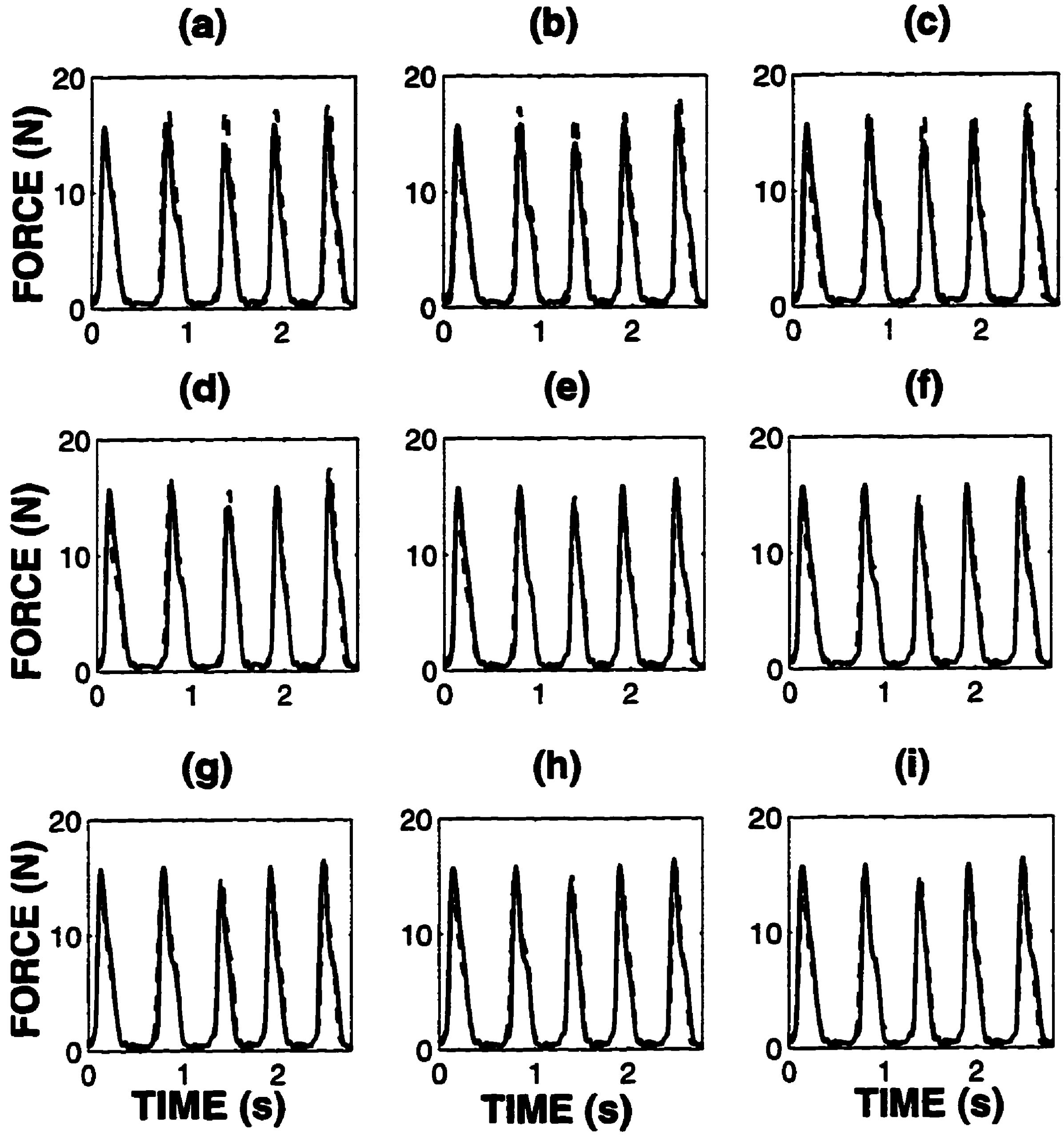

Figure 5.4.1 Intra-session tests: Comparisons of the predicted forces (dashed-lines) with the actual soleus forces (solid-lines) for the last five steps of a representative cat at 0.8 m/s, when the network was trained using the full-wave rectified and smoothed EMG and force data from the first 1.5 (a),2.5 (b), 3.5 (c), 4.5 (d),5.5 (e),6.5 (f), 7.5 (g),8.5 (h),and 9.5 (i) steps of that session.

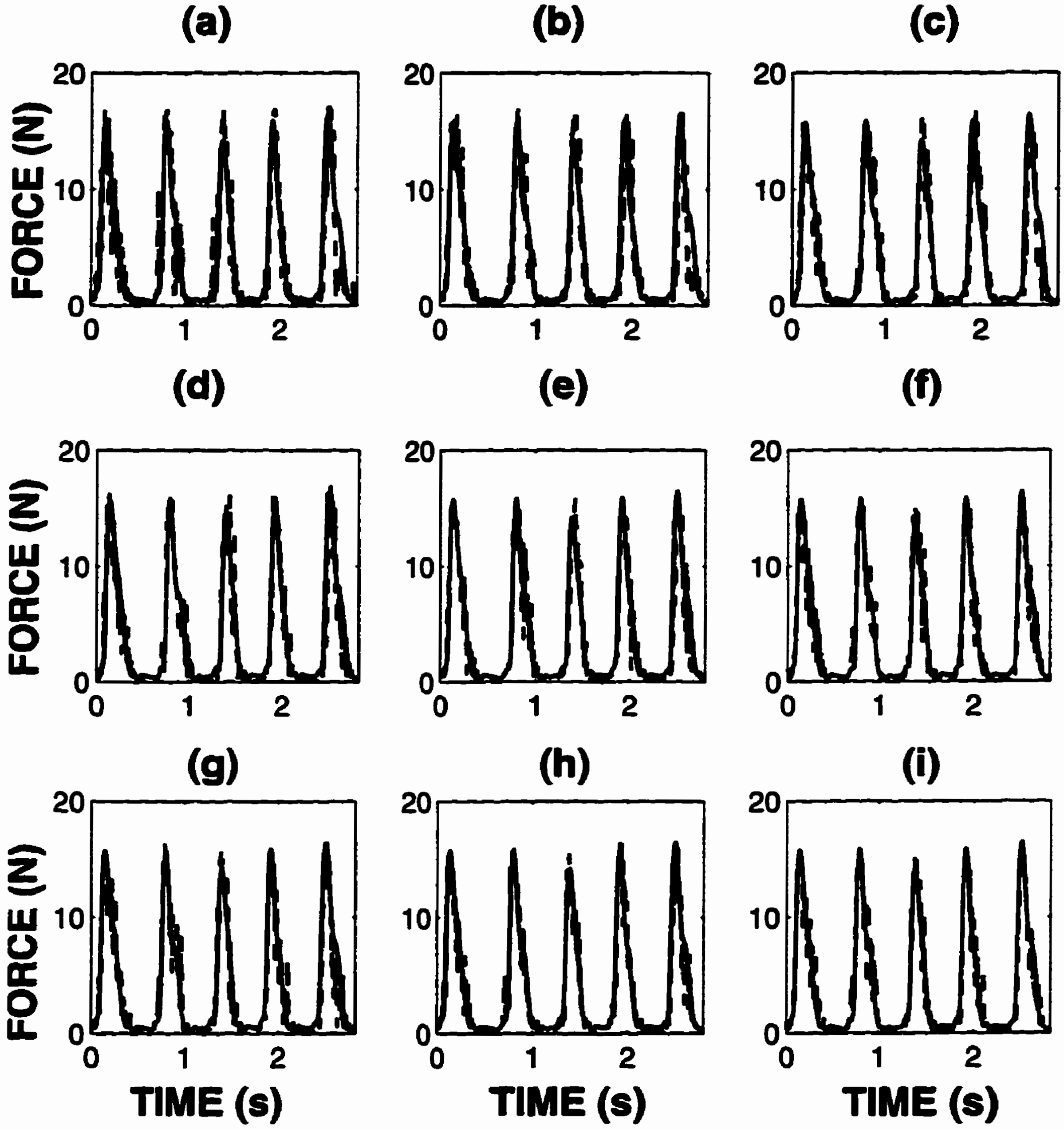

Figure 5.4.2 Intra-session tests: Comparisons of the predicted forces (dashed-lines) with the actual soleus forces (solid-lines) for the last five steps of a representative cat at 0.8 m/s, when the network was trained using the full-wave rectified EMG and force data from the first 1.5 (a), 2.5 (b), 3.5 (c), 4.5 (d), 5.5 (e), 6.5 (f), 7.5 (g), 8.5 (h), and 9.5 (i) steps of that session.

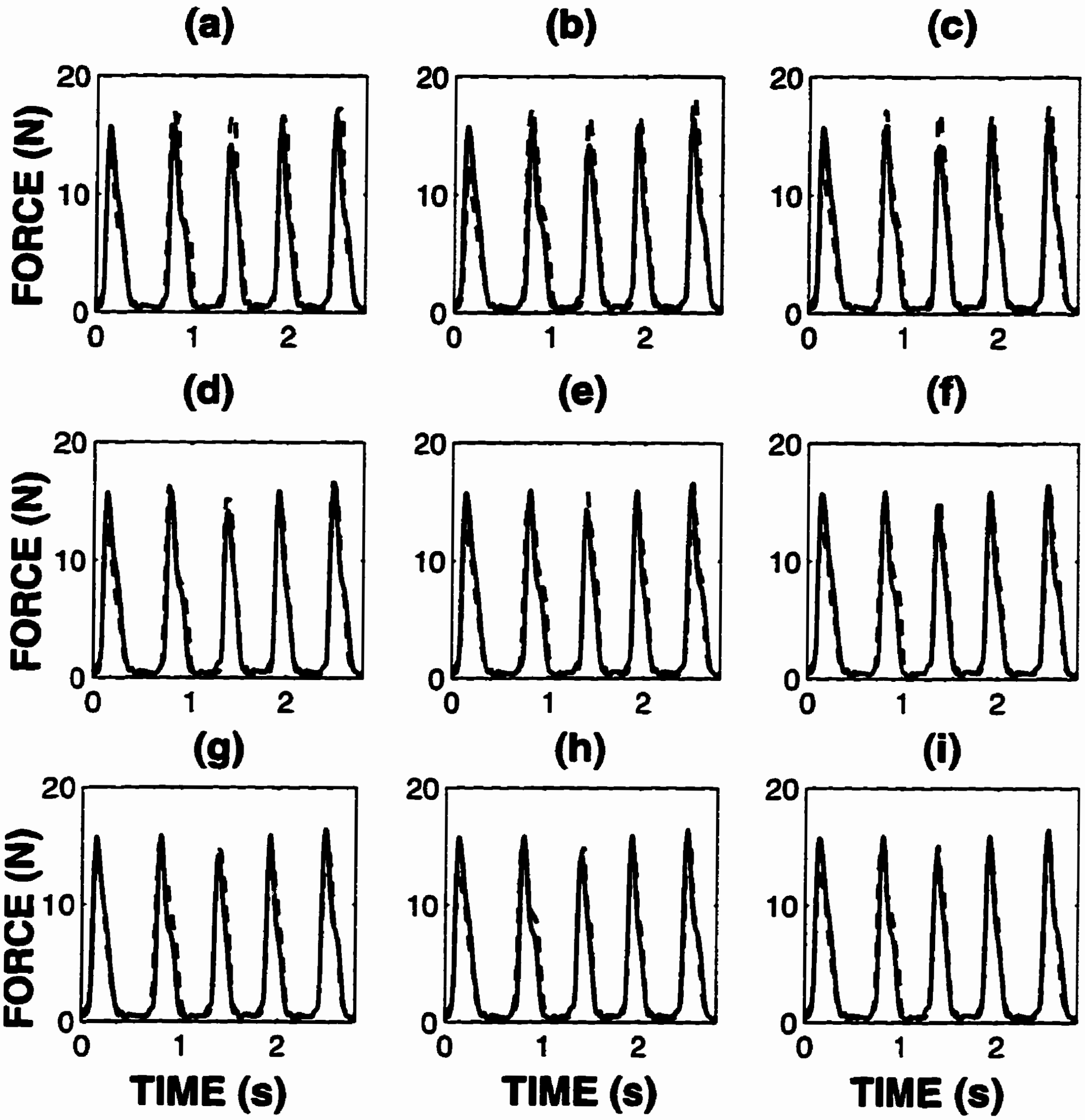

Figure 5.4.3 Intra-session tests:Comparisons of the predicted forces (dashed-lines) with the actual soleus forces (solid-lines) for the last five steps of a representative cat at 0.8 m/s, when the network was trained using the full-wave rectified and smoothed EMG plus the knee and ankle angle-time histories, and force data from the first 1.5 (a), 2.5 (b), 3.5 (c), 4.5 (d), 5.5 (e), 6.5 (f), 7.5 (g), 8.5 (h), and 9.5 (i) steps of that session.

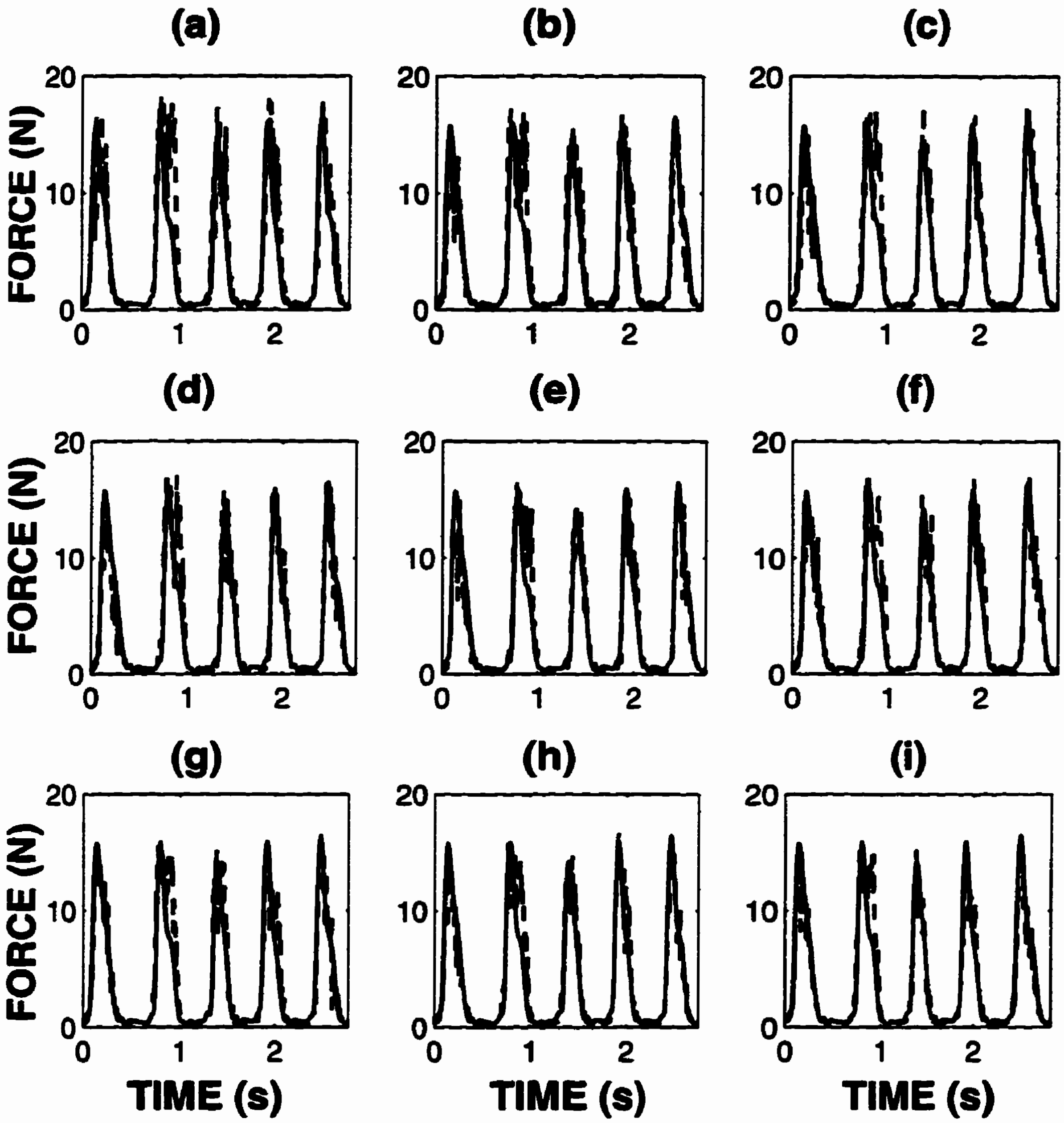

Figure 5.4.4 Intra-session tests: Comparisons of the predicted forces (dashed-lines) with the actual soleus forces (solid-lines) for the last five steps of a representative cat at 0.8 m/s, when the network was trained using the full-wave rectified EMG plus the knee and ankle angle-time histories, and force data from the first 1.5 (a), 2.5 (b), 3.5 (c), 4.5 (d), 5.5 (e), 6.5 (f), 7.5 (g), 8.5 (h), and 9.5 (i) steps of that session.

Figures 5.4.3(a)-(i) and 5.4.4(a)-(i) show the force-time predictions for the results listed in the third and fifth columns of Table 8.b. The soleus force predictions were virtually perfect, when the network was trained using the full-wave rectified and smoothed EMG and when the number of steps used for training exceeded 4.5 (the third and fourth columns of Tables 8.a and 8.b). For the tests shown in Figures 5.4.2 and 5.4.4, the predicted force curves contained more noise compared to the predicted forces in Figures 5.4.1 and 5.4.3.

Chapter six: Discussions

The cat gastrocnemius and soleus have different architecture and mechanical, morphological, and biochemical properties which affect the force output of these muscles during locomotion. Peak forces and EMGs of the gastrocnemius increase in parallel with increasing speeds of locomotion, whereas peak soleus forces remain about constant and EMGs increase with increasing speeds of locomotion (Herzog et al., 1993). In this study, we made force predictions for the cat gastrocnemius and soleus using an ANN approach. The results found here demonstrated that adequate force predictions could be made for two very different muscles with different properties functional abilities, and control function.

6.1 Dynamic force predictions for the cat gastrocnemius

The dynamic force predictions made using the ANN were excellent for the inter-subject-A and the intra-session prediction schemes for the gastrocnemius. The coefficients of cross-correlation in these tests exceeded 0.91 and RMS errors were equal to or less than 11% of the corresponding maximum peak forces in all cases. The time histories of the predicted forces agreed well with those of the actual forces. These results suggest that the dynamic EMG-force relationships and the mechanical properties of gastrocnemius muscles are similar across cats walking/trotting at a given speed of locomotion. One limitation of the inter-subject-A predictions was that the predicted peak forces were over- or underestimated when the peak force of the target step was much lower or higher than the peak force of the previous step. This limitation could probably be eliminated if data from more cats had been available for the training of the ANN.

For the intra-session predictions of gastrocnemius forces, the force predictions were bad if the number of steps used for training the ANN was less than one (i.e. 0.5 steps, Figure 6.1.1). An example where 0.5 steps were used for training is shown in Figure 6.1.1. The RMS error was 5.1 N with the maximum peak force of 35.2 N, (14%). However, the force predictions were excellent and the coefficients of cross-correlation remained virtually constant (Figure 6.1.2, Tables 4.a, 4.b) once the number of steps used for training the ANN exceeded five. This result indicates that the essential features of the EMG-force relationship for a cat walking at a given speed are captured by the ANN within about five to six full step cycles.

The inter-subject-B predictions were not as good as the inter-subject-A predictions for the cat gastrocnemius. The root mean square (RMS) errors were large (e.g. Figure 4.2.1), about 23% (0.4 m/s), 14% (0.8 m/s), and 15% (1.2 m/s) of the corresponding maximum peak forces. The primary difference between the inter-subject-B and the inter-subject-A schemes was that in the former all speeds of locomotion were used in the training set, whereas in the latter, only the speed of locomotion for which the predictions were made was used in the training set. Therefore, it appears that the ANN can generalize better when little but specific training input is provided compared to when a great deal of non-specific input is added.

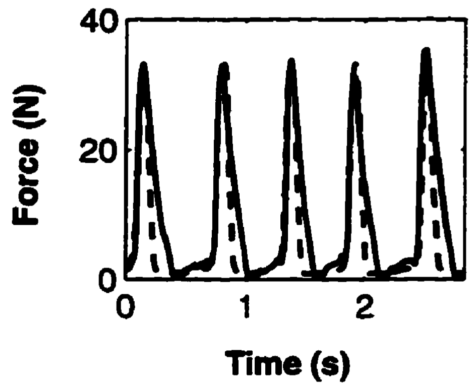

Figure 6.1.1 Intra-session test:
Comparisons of the predicted forces (dashed-line) with the actual gastrocnemius forces (solid-line) for the last five steps of the same representative cat as used in Figure4.41(0.8 m/s),when the network was trained using the full-wave rectified and smoothed EMG and force data from the first 0.5 steps of that session, corr.coef.=0.90, RMS error=5.1 N.

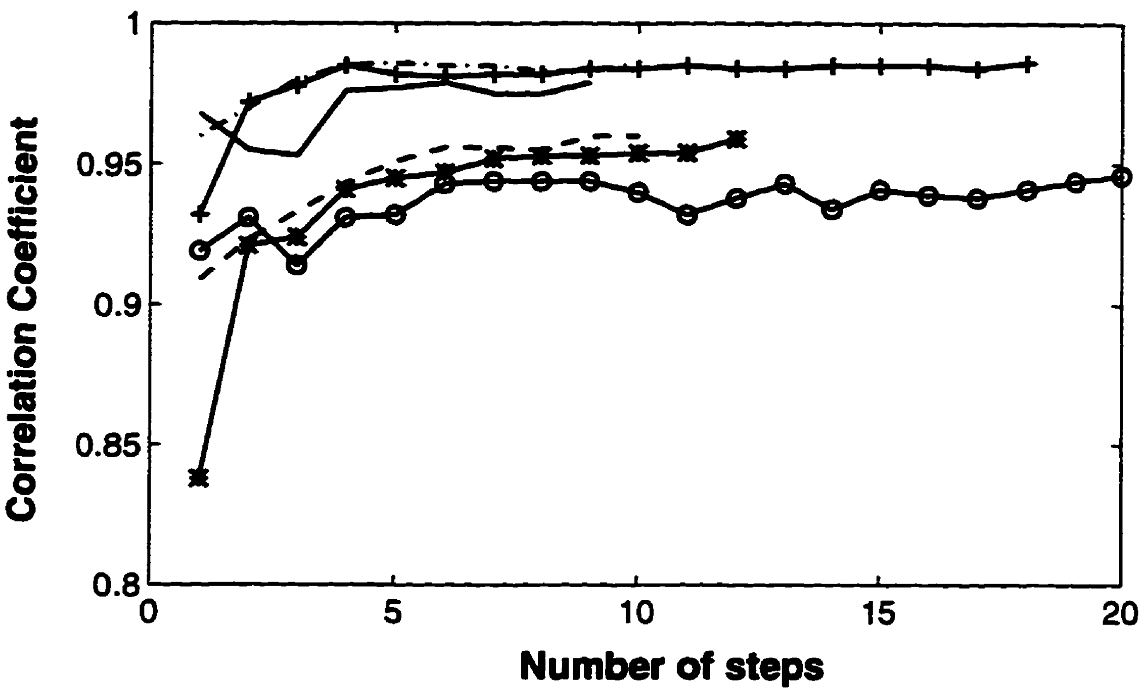

Figure 6.1.2 The dependency of the cross-correlation coefficient on the number of steps used to train the ANN in the Intra-session prediction tests for the last five steps of cat 1 walking at 0.8 (solid-line with '*'), 1.2 m/s (solid line with '+'),and cat 2 walking at 0.8 m/s (solid-line with 'o'), and cat 3 walking at 0.4 (dashed-line), 0.8 (solid-line), 1.8 m/s (dashed-dot-line).

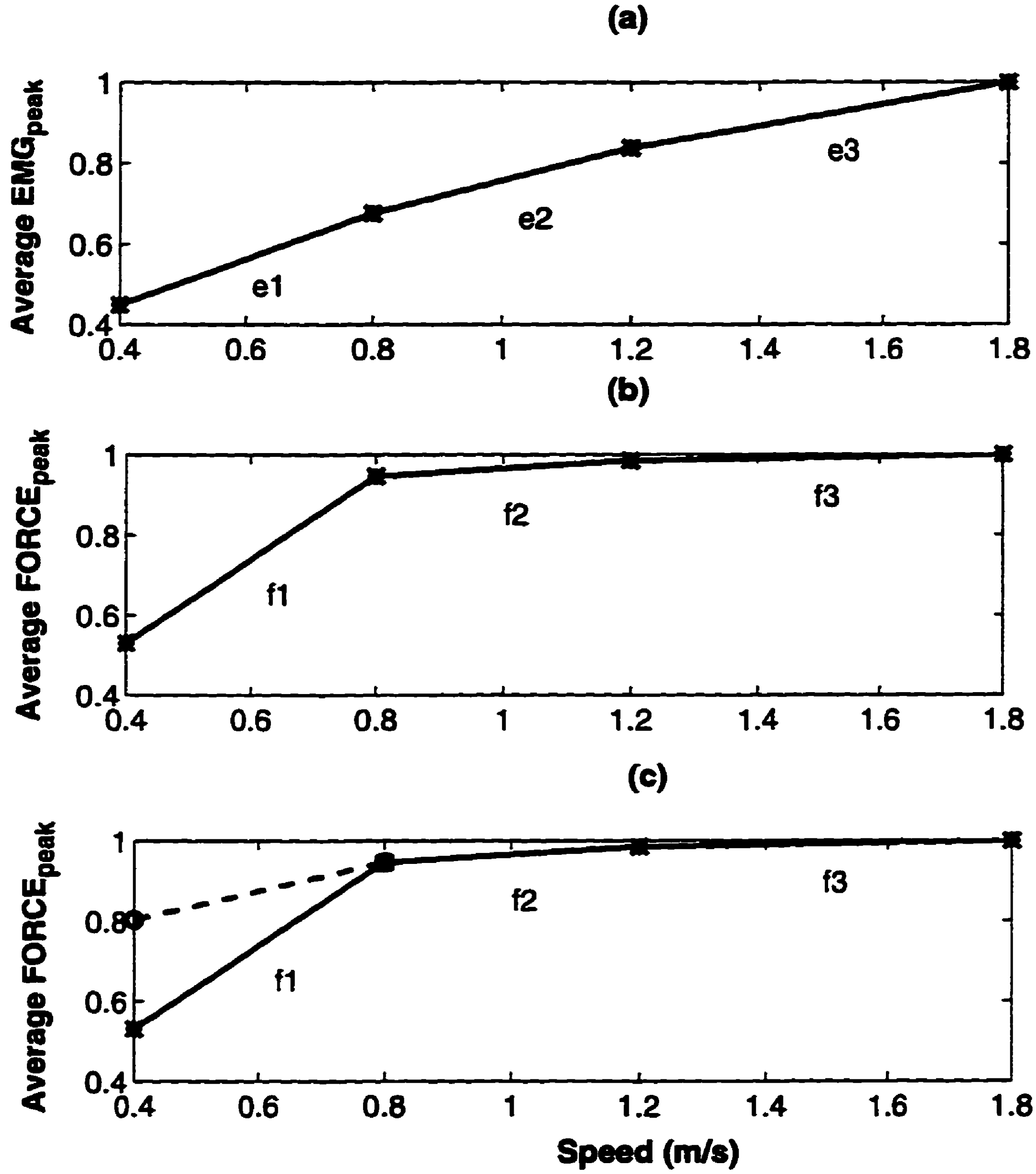

Figure 6.1.3 (a) The average peak values (marked by '*') of the processed EMG signals measured from a representative cat at speeds of locomotion of 0.4, 0.8, 1.2, and 1.8 m/s. (b) The average peak force values (marked by '*') measured from a representative cat at speeds of locomotion of 0.4, 0.8, 1.2, and 1.8 m/s. (c) Comparison of the average predicted peak force (marked by 'o') with the average actual peak force (marked by '*') for a representative cat walking at 0.4 m/s when the network was trained with the full-wave rectified and smoothed EMG and force data from the same cat while walking /trotting at speeds of 0.8, 1.2, 1.8 m/s.

The neural network could not predict well the force in the intra-subject prediction schemes for the gastrocnemius for walking at 0.4 m/s (e.g. Figure 4.3.1(a)). The RMS errors (Figure 4.3.1) were 17% (0.4 m/s), 11% (0.8 m/s), 11% (1.2 m/s), and 13% (1.8 m/s) of the corresponding maximum peak forces. The predictions were worse for the lowest and highest speeds of locomotion. This result is probably caused by an insufficient amount of information (EMG-force pattern) in the training phase.

Figure 6.1.3(a) shows the average peak values of the processed EMGs from the gastrocnemius of one cat at speeds of walking/trotting of 0.4, 0.8, 1.2, and 1.8 m/s. e1, e2, and e3 represent the slopes of the lines connecting the average peak EMG values at speeds of 0.4 m/s to 0.8 m/s, 0.8 m/s to 1.2 m/s, and 1.2 m/s to 1.8 m/s, respectively. Figure 6.1.3(b) shows the corresponding average peak force values. f1, f2, and f3, represent the slopes of the lines connecting the average peak force values at speeds of 0.4 to 0.8 m/s, 0.8 to 1.2 m/s, and 1.2 to 1.8 m/s. The value for e1, e2, and e3 are similar (Figure 6.1.3(a)), whereas the value for f1 is much larger than that for f2 and f3. This result may explain why the peak forces for walking at 0.4 m/s were consistently predicted to be higher than the corresponding actual peak forces. Obviously, the EMG-force relationship had a different character for walking at 0.4 m/s than for any of the other speeds of locomotion. This fact may also influence the gastrocnemius force predictions at speeds of 0.8 and 1.2 m/s.

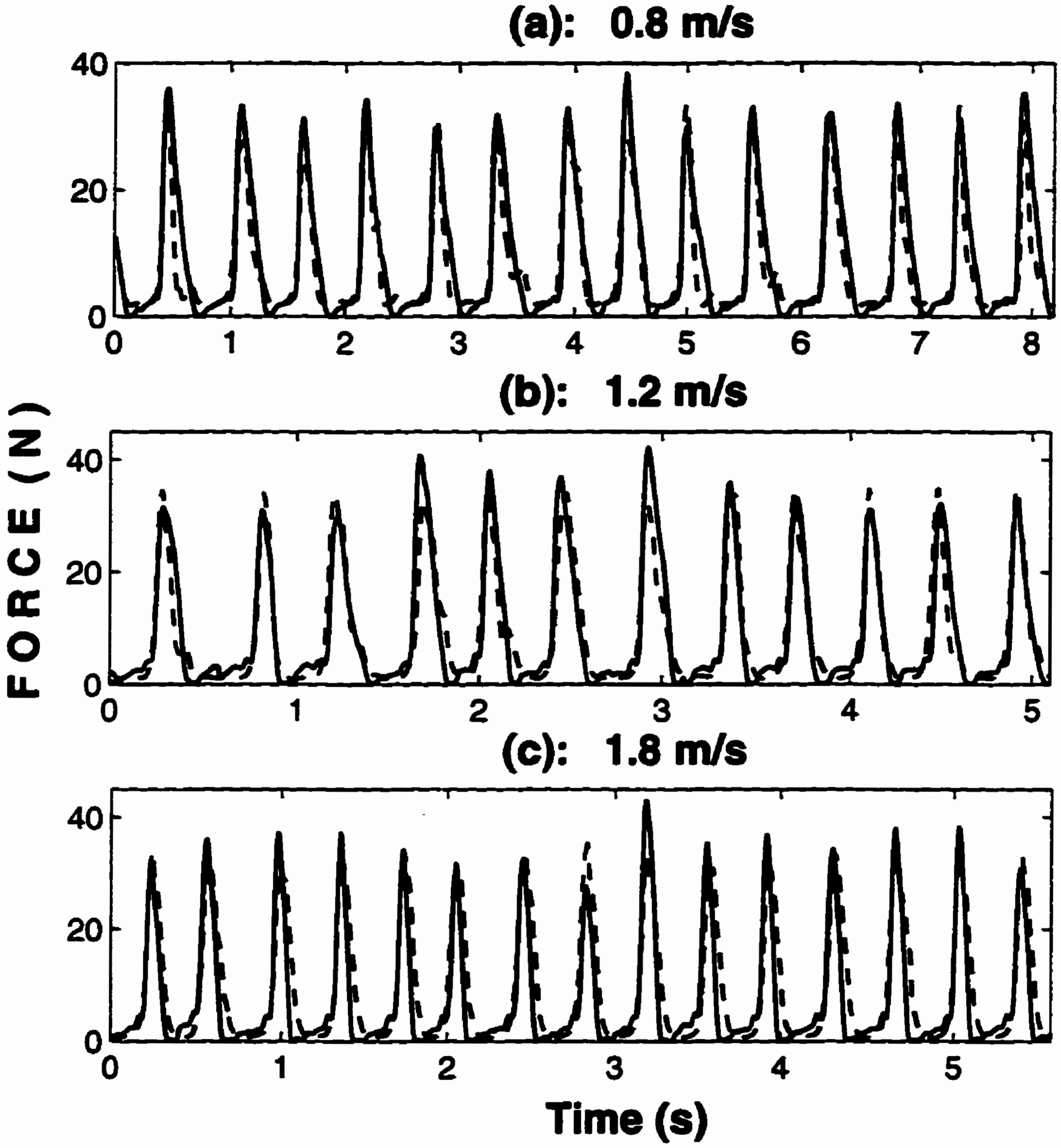

Figure 6.1.4 Intra-subject tests: Comparisons of the predicted forces (dashed-line) with the actual gastrocnemius forces (solid-line) for a representative cat walking (a) at 0.8 m/s, when the network was trained with the full-wave rectified and smoothed EMG and force data from the same cat while walking/trotting at speeds of 1.2, 1.8 m/s, RMS error = 3.8N; (b) at 1.2 m/s, when the network was trained with the full-wave rectified and smoothed EMG and force data from the same cat while walking/trotting at speeds of 0.8, 1.8 m/s, RMS error = 4.1N; and (c) at 1.8 m/s, when the network was trained with the full-wave rectified and smoothed EMG and force data from the same cat while walking/trotting at speeds of 0.8, 1.2 m/s, RMS error = 5.4N.

Based on our previous experience (inter-subject-B tests) in which it was found that non-specific training information could jeopardize the accuracy of the force predictions for the gastrocnemius, we repeated the intra-subject force predictions at 0.8, 1.2, and 1.8 m/s without using the information at 0.4 m/s as input into the ANN (Figure 6.1.4). When omitting the 0.4 m/s information for training the ANN, the coefficients of cross correlation for the remaining experiments improved (from 0.93 to 0.94 at 0.8 m/s; from 0.92 to 0.93 at 1.2 m/s; and from 0.88 to 0.89 at 1.8 m/s) and the RMS errors decreased (from 4.3 N to 3.8 N at 0.8 m/s; from 4.5 N to 4.1 N at 1.2 m/s; and from 5.7 N to 5.4 N at 1.8 m/s) compared to the intra- subject predictions including the 0.4 m/s values in the training input. Again, additional but non-specific input into the ANN appeared to be detrimental to the predictive ability of the ANN.

6.2 Dynamic force predictions for the cat soleus

The dynamic force predictions for the cat soleus were excellent for the inter-subject-A and the intra-session prediction schemes. The coefficients of cross-correlation in these tests exceeded 0.92 in all cases, and the time histories of the predicted forces generally agreed well with those of the actual forces. The RMS errors between the predicted and actual forces were equal to and less than 14% of the corresponding maximum peak forces in all inter-subject-A and the intra-session prediction tests. These results suggest that the dynamic EMG-force relationship and the mechanical properties of soleus muscles are similar across cats walking/trotting at a given speed of locomotion. One limitation of the inter-subject-A predictions for the soleus was that the predicted peak forces were over- or underestimated when the peak force of the target step was much lower or higher, respectively than the peak force of the previous step. Another limitation of the inter-subject-A predictions was that the predicted peak forces were generally overestimated for walking at 0.4 m/s.

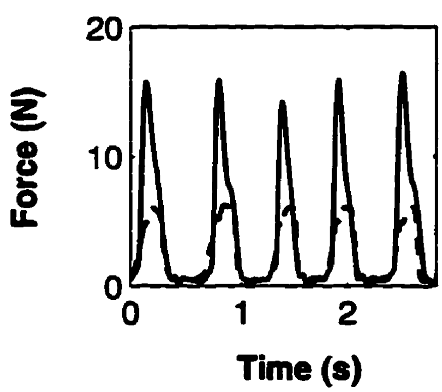

Figure 6.2.1 Intra-session test:
Comparisons of the predicted forces (dashed-line) with the actual soleus forces (solid-lines) for the last five steps of the same cat as used in Figure5.4.1(0.8 m/s),when the network was trained using the full-wave rectified and smoothed EMG and force data from the first 0.5 step of that session, corr.coef.=0.86, RMS error= 3.6 N.

In the intra-session prediction scheme for the soleus, the force predictions were bad if the number of steps used for training the ANN was less than one (i.e. 0.5 step, Figure 6.2.1). An example of predictions using just 0.5 steps for training is shown in Figure 6.2.1. The coefficient of cross-correlation was 0.86, the RMS error was 3.6 N with the maximum peak force of 16.4 N, (22%). However, the force predictions were excellent and the coefficients of cross-correlation remained virtually constant (0.98, third column of Table 8a) and the RMS errors were about 6% of the corresponding maximum peak forces, once the number of steps used for training the ANN exceeded five (Tables 8a and 8b). Therefore, the essential features of the EMG-force relationship for walking at a given speed are fully captured by the ANN within about five full step cycles.

The inter-subject-B predictions for the soleus were not as good as the inter-subject-A predictions despite the fact that the ANN was trained with the same plus additional information in the inter-subject-B compared to the inter-subject-A tests. Comparing this result with that of the inter-subject-B predictions in the gastrocnemius, one might conclude that the ANN can make better predictions (in both muscle) when little but specific training input is provided compared to when a great deal of non-specific input is added to the specific input.

The neural network did not perform well in the intra-subject prediction schemes for cat soleus when predicting the forces for walking at 0.4 m/s (Figures 5.3.1(a) and 5.3.2(a), 5.3.3(a), and 5.3.4(a)), and when only the EMG signal was used as input into the ANN (Figure 5.3.1). In Figure 5.1, the RMS errors were 24% (0.4 m/s), 15% (0.8 m/s), 11% (1.2 m/s), and 15% (1.8 m/s) of the corresponding maximum peak forces. Adding the kinematics to the input for the ANN improved the prediction results for the two intermediate speeds but not for the lowest and highest speeds of locomotion (Figure 5.3.2(a)-(d)). This result is probably caused because there is a limited amount of information provided to the training sets. It appears that the EMG-force relationship in the soleus had a different character for walking at 0.4 m/s than for any of the other speeds of locomotion. As the ANN is abstracting patterns from a data set that is averaged across subjects, it may be expected that more information, such as force and EMG data at speeds between 0.4 m/s and 0.8m/s, or at speeds below 0.4 m/s might have helped the force predictions for walking at 0.4 m/s. The results shown in Figure 5.3.1 and 5.3.3 also indicate that the kinematics play an important role in the intra-subject force predictions for the soleus muscle.

6.3 A brief comparison of dynamic force predictions between the cat gastrocnemius and soleus

In our study, we were able to predict and validate dynamic muscle forces for cat soleus and gastrocnemius across subjects based on measured EMG signals.

The force predictions across cats gave excellent results for the inter-subject-A but not the inter-subject-B tests. One limitation of the inter-subject-A predictions for both muscle was that the predicted peak forces were over- or underestimated when the peak force of the target step was much lower or higher, respectively than the peak force of the previous step. The pattern recognition scheme of the ANNs may partly explain this result. In our study, the training set only contained input-output patterns from two cats and eight to sixteen step cycles per speed of locomotion. This limited input may partly explain some of the inaccuracies in the force predictions.

Comparing the inter-subject-B prediction results of the gastrocnemius (Figures 4.2.1-4.2.4) with those of the soleus (Figures 5.2.1-5.2.4), it becomes apparent that the peak forces generally matched better for the soleus than the gastrocnemius. The inter-subject-B training sets contained all data which were used in the inter-subject-A training sets plus the data of all speeds of locomotion which were different from the speed for which the force predictions were made. This result suggests that the dynamic EMG-force relationship across cats is more similar than the relationship between speeds of locomotion in a given cat. For the gastrocnemius, the muscle force predictions were more variable across speeds than for the soleus.

For the force predictions across speeds in a given cat, the intra-subject prediction schemes, the neural network did not predict well the forces in the gastrocnemius and soleus for walking at 0.4 m/s. Obviously, the EMG-force relationship for both muscles had a different character for walking at 0.4 m/s than for any of the other speeds of locomotion. Adding the kinematics to the input for the ANN improved the prediction results for the soleus but not for the gastrocnemius. So, it seems that the soleus forces do not depend on the EMG primarily, but other factors, such as the length or rate of change in length, influence the muscle force substantially. The peak forces of soleus remained nearly constant for speeds of locomotion from 0.4 to 1.8 m/s as had been shown previously (e.g. Walmsley *et al.*, 1978), but the magnitudes of the corresponding EMG signals increased with increasing speeds of locomotion. Giving only EMG signals as input to the ANN could not successfully predict the dynamic soleus forces in the intra-subject prediction scheme. This result showed that the kinematics (or better, the contractile conditions of the muscle) appear to play an important role in soleus force prediction, wherease the contractile conditions might not be as important for the gastrocnemius, at least not at the relatively slow speeds of locomotion tested here. Prilutsky et al. (1994) reported that the relative shortening velocities of the soleus fibres were high compared to those of the gastrocnemius at all walking and slow trotting speeds. Therefore, these authors argued that the soleus could not produce an increased force at increasing speeds of locomotion, despite increased activation, because the contractile conditions imposed severe limitations on the force producing ability of the soleus.

The correlation coefficients were similar for all force predictions independent of whether the EMG signal input was smoothed or not. This result illustrates that the ANN could relate EMG and force signals quite successfully in most cases, independent of whether the frequency content of the EMG was completely different from that of the force (unsmoothed

EMG) or not.

6.4 Dynamic force predictions across muscles

Can the neural network generalize dynamic force predictions across muscles? The answer is no. The coefficient of cross-correlation of soleus force predictions using an ANN trained with gastrocnemius EMGs and forces was 0.5495, and the RMS error was 4.35 N with the maximum peak force of 16.7 N. Based on this result, it was concluded that the EMG-force relationship of different muscles in the same cat is inherently different.

6.5 Comparing current force predictions with previously published results

Previous research on the dynamic relationship between EMG and force suggested that the muscle contractile conditions must be known for adequate modelling of this relation (Hof and van den Berg, 1981a; Sherif et al., 1983; Olney and Winter, 1985; van den Bogert et al., 1988; Norman et al., 1988; van Ruijven and Weijs, 1990). The calibration procedures or estimation techniques used to determine parameters of the muscle model are lengthy and require extensive pretrials. However, the validity of estimating the variable contractile conditions of the muscle fibres during locomotion must still be established thoroughly in future experiments

(Herzog et al., 1994). Most of the studies mentioned above gave acceptable intra-subject force predictions from EMG over a limited range of conditions. However in none of these studies were inter-subject predictions made or were intra-subject predictions attempted across a variety of movements. Also, in none of the above studies were force predictions made and validated for more than one muscle.

The approach presented here does not consider the force-length-velocity properties of the target muscle. Nevertheless, the dynamic force predictions made here were comparable or better than those presented previously in similar studies [van den Bogert et al., 1988; Norman et al., 1988]. In the study of van den Bogert et al. (1988), the force predictions were made for the deep digital flexor muscle in the hindlimb of the horse. The muscle force predictions corresponded to what we termed the intra-subject prediction scheme. The parameters used in the muscle model were derived from "irregular" walking trials and the force predictions were made for "normal" walking of that same horse. Force predictions were made for one horse at one speed of locomotion only. The RMS prediction error for seven consecutive step cycles was 143 N (12% of the maximum peak force 1200 N). No cross-correlation coefficients were given. The RMS error was comparable to those obtained in our intra-subject tests for different speeds of locomotion in the same animal which covered walking and trotting gaits. The predicted forces in the study of van den Bogert et al. (1988) became negative when the actual forces were close to zero. No attempts were made to predict forces in the same horse for different speeds of locomotion, or to attempt force predictions across horses.

Norman et al. (1988) attempted to predict dynamic soleus forces from EMG in a walking cat. For their prediction model, the full wave rectified and smoothed (double-pass Butterworth filter, 5 Hz cut-off frequency) EMG signal and the soleus force during standing were required as input. The coefficients of cross-correlation and the RMS error between the predicted and measured soleus force while walking at 1.6 m/s were 0.91 and 23%, respectively. At first glance it appears that the result obtained by Norman et al. (1988) were close to those found in our studies, however their results were only obtained for four steps of a single walking condition after the model parameters had been adjusted to give the best least square fit between the actual and the "predicted" (i.e. fitted) forces. No attempts were made to perform predictions for other walking speeds of the same animal or across animals.

Chapter seven: Conclusions

The objective of this thesis was to revisit dynamic force predictions from EMG signals using an artificial neural network (ANN) approach. The basic concepts of predicting dynamic muscle forces from EMG were introduced and reviewed in Chapters 2 and 3. In Chapters 4, and 5, the results of our studies were described. In Chapter 6, the results were discussed.

The dynamic force predictions made using the ANN approach were good for the inter-subject-A and the intra-session prediction schemes. The inter-subject-B predictions were not as good as the inter-subject-A predictions. It appears, therefore that the ANN can generalize better when little but specific training input is provided compared to when a great deal of non-specific input is added to the specific input. This result may suggest that the dynamic EMG-force relationship across cats is more similar than the relationship between speeds of locomotion in a given cat.

From the results of the intra-session prediction tests, it becomes apparent that the correlation coefficients were similar whether the EMG signal input was smoothed or not.

The neural network could not perform well in the intra-subject prediction schemes, when predicting the force for walking at 0.4 m/s. It appears that the EMG-force relationship in the gastrocnemius and soleus had a different character for walking at 0.4 m/s than for any of the other speeds of locomotion. It may be expected that more information, such as force and EMG data at speeds between 0.4 m/s and 0.8m/s, or at speeds below 0.4 m/s, might have helped the force predictions for walking at 0.4 m/s. Adding the kinematics to the input for the ANN improved the prediction results for the soleus but not for the gastrocnemius. So, it seems that the soleus forces cannot be easily explained just by the EMG signals. The kinematics (or better, the contractile conditions of the muscle) appear to play an important role in soleus force production. The predictions were also not good for the highest speeds (1.8 m/s) of locomotion. This result is probably associated with the limited amount of information in the training sets. Probably, force and EMG data at speeds above 1.8 m/s might have helped the force predictions for trotting at 1.8 m/s.

One of the advantages of the ANN for predicting dynamic muscular forces from EMG is that it is simple to implement. Contractile conditions (i.e., the length and rate of change in length of the contractile element of the muscle), as well as the force-length and force-velocity relationships of the muscle do not need to be measured, which is particularly useful since it is nearly impossible to determine lengths and velocities of contractile elements of muscles accurately in-vivo. Therefore, another advantage of the ANN for predicting dynamic muscular forces from EMG is that complex muscle models are not required.

One of the limitations of the ANN approach is that the network must be trained at one stage; thus requiring force and EMG as input to train the network before meaningful predictions are possible. Another limitation of this approach is that the ANN method does not provide insight into the physiological and biological relationship of the EMG and muscle force because the method is purely numerical. However, these limitations should not detract from the excellent predictive ability of ANNs across movement patterns (walking and trotting) and across animals, once an appropriate data set of subjects and a minimal number of step cycles are available for training.

The results of this study indicate that ANNs are able to identify the highly non-linear relation between EMG and muscular force, and that ANNs are able to generalize, to a certain degree, this relationship. Although, the ANN approach can not give additional insight into the physiological relation between EMG and force, it is able to provide force predictions from the EMG signals which are accurate, and so, may prove to be useful in practical applications in which the result is important rather than the underlying mechanism, for example, in functional electrical stimulation or the control of prosthetic devices.

Bibliography

Andrews, J. G. (1974) Biomechanical analysis of human motion. *Kinesiology* **4**, pp. 32-42.

Basmajian, J.V. and De Luca, C.J. (1985), *Muscles Alive. Their Functions Revealed by Electromyography* (5th Ed.). Williams and Wilkins, Baltimore.

Bouisset, S. and Maton, M.S. (1972) Quantitative relationship between surface EMG and intramuscular electromyographic activity in voluntary movement. *Am. J. Phys. Med.* **51**, pp. 285-295.

Chen, J., Vandwalle, J., Sansen, W., Vantrappen, G. and Janssens, J. (1990) Multichannel adaptive enhancement of the electrogastrogram. *IEEE Trans. Biomech. Engn.* **37**, pp. 285-294.

Ericson, B.E. and Hagberg, M. (1978) EMG signal level versus external force: a methodological study on computer aided analysis. *Biomechanics VI-A* (Edited by Asmussen, E. and Jorgensen, K.). pp. 251-255. University Park Press, Baltimore.

Ferrara, E. R. and Widrow, B. (1982) Fetal electrocardiogram enhancement by time-sequenced adaptive filtering. *IEEE Trans. Biomed. Engn.* **29**, pp. 458-460.

Grossberg, S. (1988) *Neural Networks and Natural Intelligence.* Cambridge, MA: MIT Press.

Hassoun, M. H., Wang, C. and Spitzer, A.R. (1994) NNERVE: Neural Network Extraction of Repetitive Vectors for Electromyography-Part I: Algorithm *Transactions on Biomedical Engineering*, Vol. **41**, No. 11, pp. 1039-1052.

Haykin, S. (1994), *Neural Networks*, Macmillan College Publishing Company.

Hebb, D. O. (1949) *The Organization of Behaviou: A Neuropsychological Theory*. New York: Wiley.

Herzog, W., Guimaraes, A.C.S., Zhang, Y.T., (1994) EMG. In *Biomechanics of the Musculo-skeletal system* (ed. B.M. Nigg and W. Herzog). pp. 308-336. New York: John Wiley and Sons.

Herzog, W. and Leonard, T.R. (1991)Validation of optimization models that estimate the forces exerted by synergistic muscles. *J. Biomech.* **24(S1)**, pp. 31-39.

Herzog, W., Leonard, T.R. and Guimaraes, A.C.S (1993) Force in gastrocnemius, soleus and plantaris tendons of the freely moving cat. *J.Biomechanics* **26**, pp. 945-953.

Hill, A.V. (1938) The heat of shortening and the dynamic constants of muscle. *Proc. R. Soc.* **B-126**, pp 136-195.

Hill, A.V. (1949) The abrupt transition from rest to activity in muscle. *Pro. R. Soc. (Biol.)* **B-136**, pp. 399-420

Hof, A.L. and van den Berg, J. (1977) Linearity between the weighted sum of the EMG's of the human triceps surae and the total torque. *J.Biomechanics* **10**, 529-539.

Hof, A.L. and van den Berg, J. (1981_a) EMG to Force Processing I: An Electrical Analog of the Hill Muscle Model. *J. Biomech.* **14(11)**, pp. 747-758.

Hof, A.L. and van den Berg, J. (1981_b) EMG to Force Processing II: estimation of parameters of the Hill muscle model for the human triceps surae by means of a calfergometer. *J. Biomech.* **14(11)**, pp. 759-770.

Hof, A.L. and van den Berg, J. (1981_c) EMG to Force Processing III: estimation of model parameters for the human triceps surae muscle and assessment of the accuracy by means of a torque plate. *J. Biomech.* **14(11)**, pp. 771-785.

Hof, A.L. and van den Berg, J. (1981_d) EMG to Force Processing IV: Eccentric-concentric contractions on a spring-flywheel set up, *J. Biomech.* **14(11)**, pp. 787-792.

Hopfield, J. J. (1982) Neural network and physical systems with emergent collective computational abilities. *Proceedings of the National Academy of Sciences of the U. S. A.* **79**, pp. 2554-2558.

Johnson, J.C. (1978) Comparison of analysis techniques for electromyographic data. *Avia: space envir. Med.* **49**, pp. 14-18.

Kentie, M. A., van der Schee, E. J., Greshins, J. L. and Smout, A. J. P. M. (1981) Adaptive filtering of canine electrogastrographic signals. II. Filter performance. *Med. Biol. Eng. Comput.* **19**, pp. 765-769.

Khanna, T. (1990). *Foundations of neural networks.* Reading, MA: Addison-Wesley.

Komi, P.V. and Viitasalo, J.H.T. (1976) Signal characteristics of EMG at different levels of tension. *Acta physiol. scand.* **96**, pp 267-276.

Kawato, M., Furukawa, K. and Suzuki, R. (1987) A hierarchical neural-network model for control and learning of voluntary movement. *Biol. Cybernet.* **57**, pp. 169-185.

Kramer, H., Kuchler, G. and Brauer, D. (1972) Investigations of the potential distribution of activated skeletal muscles in man by means of surface electrodes. *Electromyography* **12**, pp. 19-27.

Krnjevic, K., Miledi R. (1958a) Motor units in the rat diaphragm. *J. Physiol* (Lond). **40**, pp. 427-439

Lippold, O.C.J. (1952) The relation between integrated action potentials in a human muscle and its isometric tension, *J.Physiol.* Vol. **117(4)**, pp. 492-499.

McCullooch, W. S. and Pittts, W. (1943) A logical calculus of the ideas immanent in nervous activity. *Bulletin of Mathematical Biophsics.* **5**, pp. 115-133.

Milner-Brown, H.S. and Stein, R.B. (1975) The Relation between the surface electromyogram and muscular force. *J. Physiol.* **246**, pp. 549-569.

Moritani, T. and deVries, H.A. (1978) Re-examination of the relationship between the surface integrated electromyogram and force of isometric contraction. *Am. J. Phys. Med.* **57 (6)**, pp. 263-277.

Massone, L. and Bizzi, E. (1989) Generation of limb trajectories with a sequential network. *International Joint Conference on Neural Networks*, Vol. 2 pp. 345-349. IEEE Press, New York.

Norman, R. W., R. J. Gregor, and J. J. Dowling. (1988) The prediction of cat tendon force from EMG in dynamic muscular contractions. *Proceedings of the 5th Biennial Conference of the* Canadian Society for Biomechanics, Ottawa, Ontario, Spodyin Publishers, London, Ontario, *Canada*, pp. 120-121.

Olney, S.J. and Winter, D.A. (1985) Predictions of Knee and Ankle Moments of Force in Walking from EMG and Kinematic Data. *J. Biomech.* **18(1)**, pp.9-20.

Paton W.D.M., Wand D.R. (1967) The margin of safety of neuromuscular transmission. *J.Physiol.*(Lond) Vol. **191**, pp. 59-90.

Prilutsky, B.I., Herzog, W., and Allinger, T.L. (1994) Force-sharing between cat soleus and gastrocnemius muscles during walking: explanations based on electrical activity, properties, and kinematics. *J. Biomech.* **27**, pp.1223-1235

Rumelhart, D.E., G.E. Hinton, and R.J. Williams (1986) Learning representations by error propagation. *In Parallel Distributed Processing: Explorations in the Microstructure of cognition* (D.E. Rumelhart and J.L.McClelland, eds.), Vol. I, Chapter 8, Cambridge, MA: MIT Press.

Savelberg, H.C.M. and Herzog, W. (1995)Artificial Networks used for the prediction of muscle forces from EMG-patterns. *Proc. Int. Soc. Biomechanics XV* (eds. Hakkinen, K., Keskinen, K.L., Komi, P.V., and Mero, A.) Jyvaskyla. Finland, pp. 810-811.

Sherif, M. H., Gregor, R. J., Liu, L. M., Roy, R. R. and Hager, C. L. (1983) Correlation of myoelectric activity and muscle force during selected cat treadmill locomotion. *J. Biomech.* **16**,pp.691-701.

van den Bogert, A.J., Hartman, W., Schamhardt, H.C., and Sauren, A.A.H.J. (1988) In Vivo Relationship Between Force, EMG, and Length Change in Deep Digital Flexor Muscle of Horse. *Biomechanics XI-A* (eds. Hollander, A.P., Huijing,P.A.,and van Ingen Schenau, G.J.). Free University, Amsterdam. pp. 68-74.

van Ruijven, L.J.and Weijs, W.A. (1990) A New Model for Calculating Muscle Forces from Electromyograms. *Eur. J. Appl. Physiol.* **61**, pp. 479-485.

Vredenbregt, J. and Rau, G.(1973) Surface eletromyography in relation to force, muscle length and endurance. *New Developments in Electromyography and Clinical Neurophysiology* (Edited by Desmedt, J. E.) Vol. **1**, pp. 607-622.,Karger, Basel.

Walmsley, B., Hodgson, J. A., and Burke, R. E. (1978) Forces produced by Medial Gastrocnemius and Soleus Muscles During Locomotion in Freely Moving Cats. *J. Neurophysiol.* **41(5)**, pp. 1203-1216.

Wells, D. M. and Vaughan, C. L. (1989) A 3D transformation of a rigid link system using back propagation. *International Joint Conference on Neural Networks*, Vol. 2 pp. 630. IEEE Press, New York.

Yelderman, M., Widrow, B., Cioffi, J. M., Hesler, E. and Leddy, J. A. (1983) ECG enhancement by adaptive cancellation of electrosurgical interference. *IEEE Trans. Biomed. Engn.* **30**, pp. 392-398.

Zhang, Y. T., Frank, C. B., Rangayyan, R. M., Bell, G. D. and Ladly, K. O. (1991) Step size optimization of non-stationary adaptive filtering for knee sound analysis. *Med. Biol. Eng. Comput.* **29** (Supplement, part 2), pp. 836.

Zipser, D. and Andersen, R. A. (1988) A back-propagation programmed network that simulates response properties of a subset of posterior parietal neurons. *Nature* **331**, pp. 679-684.